2014

Partitioning of fuel bound nitrogen in biomass gasification

Karl Monroe Broer
Iowa State University

Partitioning of fuel bound nitrogen in biomass gasification

by

Karl M. Broer

A dissertation submitted to the graduate faculty

in partial fulfillment of the requirements for the degree of

DOCTOR OF PHILOSOPHY

Co-majors: Mechanical Engineering; Biorenewable Resources & Technology

Program of Study Committee:
Robert C. Brown, Major Professor
Theodore John Heindel
Terrence Meyer
D. Raj Raman
Brent H. Shanks

Iowa State University

Ames, Iowa

2014

DEDICATION

While pursuing the degree Doctor of Philosophy in Mechanical engineering, I learned that the emotional and spiritual support that one receives from family and good friends is just as important as technical support. This document is dedicated to those who listened to my troubles, picked me up when I fell down, and lent their assistance when it was needed most:

1.) My immediate and extended family

2.) My friends, particularly Donni Anderson, Claire Basset, Mariah Bell, Anne Falbowski, John Little, Heather McCann-Young, Mariko Peterson, Kristen Pudenz, Jonathan Roberts, Sarah Schroeder, Kevin Stillman, Josh Riley, and Melissa Wickham

3.) The co-workers that I worked closely alongside, particularly Tannon Daugaard, Andrew Larson, Lysle Whitmer, and Patrick Woolcock

4.) The roommates that I had during grad school, including Brent Brewer, Catie Brewer, Jay Duncan, Simon Nielsen, Hannah Raatz, Michael Romey, and Curt Sporrer

TABLE OF CONTENTS

LIST OF FIGURES

Page

LIST OF TABLES

Page

NOMENCLATURE

BECCS	Bioenergy carbon capture and storage
CAD	Computer aided drafting
%CC	Percent carbon conversion
C_b	Carbon content of biomass
C_c	Carbon content of char
char-N	Char bound nitrogen
daf	Dry, ash-free basis
DDGS	Dried distiller's grains with solubles
DI	Deionized (water)
ER	Equivalence ratio
ESP	Electrostatic precipitator
FBN	Fuel bound nitrogen
FTIR	Fourier transform infrared spectroscopy
GC	Gas chromatograph
GHG	Greenhouse gas
HDPE	High-density polyethylene
HHV	Higher heating value
IC	Ion chromatograph
ID	Inner diameter
IDLH	Immediately dangerous to life and health
IPCC	Intergovernmental panel on climate change
mGC	Micro gas chromatograph

$\dot{m}_{O_2\ actual}$	Actual mass flowrate of pure oxygen gas
$\dot{m}_{O_2\ stoich}$	Stoichiometric mass flowrate of pure oxygen gas
NCD	Nitrogen chemiluminescence detector
NIOSH	National Institute for Occupational Safety and Health
NO_X	Nitrogen oxides
SLPM	Standard liters per minute
SPME	Solid phase micro-extraction
tar-N	Tar bound nitrogen
TGA	Thermogravimetric analyzer
$\dot{V}_{He}$	Volumetric flowrate of helium
$\dot{V}_{syngas}$	Volumetric flowrate of syngas
X_{He}	Percent vol/vol concentration of helium
XRF	X-ray fluorescence

ACKNOWLEDGEMENTS

I would like to first and foremost thank my committee chair, Prof. Robert C. Brown for his patience, guidance, support, and helpful advice throughout my time as a graduate student.

I would also like to thank my other committee members, Prof. Heindel, Prof. Meyer, Prof. Raman, and Prof. Shanks for the feedback and discussion that they provided during my qualifiers, preliminary examination, and personal meetings.

I am grateful for the generous funding provided by the Phillips 66 Company, the United States Department of Energy, and Iowa State University's Bioeconomy Institute that enabled me to carry out my research work.

The pilot scale gasification experiments that I conducted were of relatively large scale, and began with an empty room. It would not have been possible to complete the design and construction process without a team of colleagues committed toward the success of the project. I would like to thank Doug Bull for designing the feed system and providing guidance on the design of the gasifier, Dr. Samuel Jones for project management guidance, and Andrew Suby for technical advice on commissioning, automatic control, and safety. I am also grateful for engineering support provided by Lysle Whitmer and Andrew Friend, and the CAD expertise provided by Andrew Larson.

Construction of the pilot scale gasifier also allowed me to work with and learn a great deal from the experienced and highly qualified personnel representing the contractors and vendors that supplied the equipment necessary for conducting gasification research. I would like to thank Gary Ballard, Brian Bettini, John Dawley,

Sean DeGeest, Rick Ennis, Ken Gielow, James Graefe, Dan Hampton, Doug Owens, and Mike Schmidt for useful conversations and advice. I would also like to thank Badger Mining Corporation and ILC Resources for generously donating high quality silica sand and crushed limestone for use as reactor bed material.

Once experimental work was underway, equipment retrofits, routine maintenance, and material preparation were provided by Jordan Funkhouser, Adam Bohl, Memo Hinckley, Brandon Huth, Clark Ennis, Dan Hunting, Alex Haag, Nate Hamlett, and Benjamin Deininger. Recognition is also deserved by Jacob Broer and Audrey Wallace for patiently analyzing great numbers of biomass, char, and tar samples.

I am indebted to Dustin Dalluge, Patrick Woolcock, and Tannon Daugaard for offering assistance in operating laboratory equipment, and Patrick Johnston for providing assistance, training, and analytical expertise with the ion chromatograph, micro gas chromatograph, and elemental analyzer.

It was also a pleasure to work with Ryan Smith, who efficiently organized funding, labor, and logistics to support my experimental work. Marjorie Rover and Andrew Suby also provided important support to my research efforts by insuring that my colleagues and I had access to state-of-the-art, clean, well-organized, well-equipped, and most importantly, safe laboratory facilities in which to perform our research.

Special thanks finally go to Maxwell Morris for important statistical guidance and coaching, and to Mark Wright for computer programming assistance.

Over the course of my undergraduate and graduate education, I appreciated the opportunity to work alongside many other talented, friendly, supportive, and

helpful students, many of who are now graduated, including but not limited to Catie Brewer, Bernardo del Campo, David Chipman, Nicholas Creager, Preston Gable, Kwang Ho Kim, Patrick Meehan, Pedro Ortiz, Yanwen Shen, Chamila Thilakaratne, Kaige Wang, and Yanan Zhang.

I began my career in biomass gasification as an undergraduate research assistant. I would finally like to thank each of my early supervisors - Young Do, Nate Nelson, Jerod Smeenk, David Starks, and Kevin Timmer for staking confidence in my abilities, serving as mentors, and patiently teaching me important skills that I am still proud of today.

ABSTRACT

Gasification of biomass can produce process heat, electricity, liquid fuels, and chemicals without the use of fossil fuels. Most biomass feedstocks contain small amounts of fuel bound nitrogen (FBN) which converts during gasification to mainly hydrogen cyanide (HCN), ammonia (NH_3), char bound nitrogen (char-N), tar bound nitrogen (tar-N), and diatomic nitrogen (N_2). Of these five products, HCN and NH_3 are most problematic. They lead to NO_X air pollution when the syngas is combusted. They also poison the catalysts used for conversion of syngas to fuels or chemicals.

Yields of NH_3 and HCN from FBN vary broadly in response to both feedstock properties and gasification conditions. Efforts to predict their yields via kinetic modeling have been hindered by lack of reliable experimental data, as nitrogen products are relatively difficult to measure. The differing physical and chemical properties dictate that separate analysis equipment and procedures are required for each one. There is even disagreement regarding whether char-N, tar-N, and HCN are significant products of FBN.

To study FBN evolution, switchgrass was gasified in a 25 kg/h pilot scale fluidized bed gasifier. Equivalence ratio (ER) was varied from 0.21 to 0.38 while measurements of NH_3 and HCN were taken. Switchgrass gasification experiments were also conducted with a smaller 100 g/h gasifier. Temperature and ER were varied independently from 650 to 850°C and zero to 0.4. Measurements of NH_3, HCN, char-N, and tar-N were taken. N_2 was found by difference.

For all tests conducted, HCN yields remained on the same order of magnitude as NH_3 yields. The methods of researchers reporting near-zero HCN yields were

replicated, and their results were found to be the result of flawed sampling methodologies.

Large amounts of nitrogen were found in char and tar. As temperature and ER were increased, char and tar conversion also increased, leading to increased release of nitrogen to gas phase. This tended to increase yields of NH_3 and HCN. These results suggest that the performance of kinetic models could be improved by including char-N, tar-N, and reactions for their conversion to gaseous nitrogen products.

CHAPTER 1

INTRODUCTION

The Intergovernmental Panel on Climate Change (IPCC) [1] estimated that as of 2010, global carbon dioxide (CO_2) emissions from anthropogenic sources reached 37 Gt of CO_2 emissions per year. To put this extremely large number into perspective, one can reference the surface area of the earth [2], assume standard temperature and pressure, and find that this CO_2 would have enough volume to cover the entire earth's surface with a layer about 4 cm thick. In addition to CO_2, an additional 12 Gt of equivalent CO_2 emissions were produced in 2010 as other greenhouse gases (GHGs) such as methane and nitrous oxide [1]. The sheer size of these emissions is impressive considering that they are completely generated by human societies. Although production of significant anthropogenic GHG emissions began at the start of the industrial revolution, emissions over the last few decades have increased at an especially steep rate. The IPCC [1] estimates that humanity has released roughly half of the GHG emissions in its entire history in the last 40 years. These ever increasing annual emissions of CO_2 and other GHGs are beginning to significantly affect the biosphere, leading to global warming and other types of climate change. These changes are expected to affect humanity and the biosphere in numerous ways, many of which are negative. Alarmingly, the exact severity and details of all of the impacts are difficult to accurately predict, due to the tremendous scale on which they are occurring, and the diversity of the effects.

IPCC [3] estimated that the maximum safe level of global warming lies at about a 1.5-2.0°C increase in the global mean surface temperature of the earth. Scenarios were presented by the IPCC to demonstrate roadmaps for successfully limiting climate

change to a 2.0°C increase or less. Most scenarios that achieve this level of mitigation demand that anthropogenic GHG emissions be steadily decreased toward nearly complete cessation by 2100. Negative annual emissions (net removal of GHGs from the atmosphere) are even recommended toward the end of the 21st century for some scenarios that considered the possibility of overshooting safe atmospheric CO_2 levels, and then returning to safe levels by 2100. An overshoot scenario appears likely if dramatic reductions in GHG emissions are not achieved before midway through the century.

Much of the emissions responsible for global climate change originate from the combustion of fossil fuels (accounting for 60% in 2010) [4]. Upon combustion, the carbon in these fuels is converted to CO_2, which generally goes directly into the atmosphere. An obvious approach to mitigating global climate change is to deploy energy technologies at significant scale that utilize alternative energy sources that do not release carbon from ancient geological formations into the atmosphere. The term "decarbonization" is sometimes used to describe this migration of energy production from conventional fossil fuels to alternatives that emit little or no CO_2.

One means of decarbonizing energy production is to use biomass as an energy source in place of fossil fuels. Whereas CO_2 emissions from fossil fuels come from carbon that has been stored in geological deposits for millions of years, the CO_2 emissions resulting from biomass derived fuels come from CO_2 that was recently absorbed from the atmosphere by plants. The use of biomass as an energy resource also has side benefits that extend beyond global climate change mitigation. Fossil fuel resources are non-renewable, and they are often concentrated in politically unstable regions of the world. In contrast, biomass can be employed as an energy source in any

region of the world with soil and climate suitable for supporting plant growth. Biomass resources are more politically secure than fossil fuel resources because they are inherently diffuse, renewable, and widely available.

Many of the obstacles that lie in the way of widespread use of biomass as an energy resource are related to its physical properties. Most biomass resources are relatively low density solids, making transport and handling difficult. Other characteristics such as moisture content, particle size, particle shape, ash content, and elemental makeup vary widely. Often the biomass resources that can be obtained at the lowest prices are also the ones whose properties make them the most challenging to process. For these reasons, a biomass energy process that is able to accommodate such variations is advantageous.

Gasification can accommodate biomass and waste feedstocks with a broad range of physical properties. A few examples reported in literature include wood products of various qualities [5-7], tree bark [5], railroad ties [8], cacao shells [8], olive pomace [9, 10], dried distiller's grains with solubles (DDGS) [11], sewage sludge [12, 13], and polyethylene [10]. Gasification is distinguished from many other biomass processing technologies by its high temperatures, as feedstocks are typically heated to at least 600°C [14]. For most industrial scale operations, a small amount of air or pure oxygen is provided in order to partially oxidize the fuel as gasification proceeds to maintain the necessary processing temperature. Gasification transforms the biomass feedstock into a flammable mixture of gases including carbon monoxide (CO), hydrogen (H_2), methane (CH_4), CO_2, and steam [15]. The mixture of gases is collectively referred to as syngas[1].

[1] Though the term "syngas" was originally used to refer to a mixture of strictly hydrogen gas (H_2) and carbon monoxide (CO), it is also widely used to describe the gaseous product formed from any type of gasification process. Syngas will be referred to here with the broader meaning in mind [18].

Once produced, syngas is free of many of the original challenges associated with biomass materials. Syngas is gaseous, homogenous, and suitable for several different types of energy applications. Syngas can be directly combusted to produce process heat and electrical power, or it can also be used to make liquid fuels or renewable chemicals via chemical reaction pathways, many of which are outlined by Spath and Dayton [16].

It may become important to have technology available for removing CO_2 from the atmosphere in the event that levels of GHGs in the atmosphere go beyond acceptable levels. Removal of CO_2 from the atmosphere via artificial processes has been proposed by some as a solution for bringing atmospheric CO_2 levels back down again. Cost and energy analyses for such an artificial process indicate however, that it is quite unfeasible compared to focusing instead on decarbonizing our energy production, increasing energy efficiency, and sequestering carbon via changes in forestry and agricultural practices [17]. In contrast to artificial processes, plants are able harness solar energy to fix carbon from the atmosphere. This fixed carbon can be gasified to produce a concentrated stream of CO_2, which requires less energy to recover for sequestration. The recovered CO_2 could then be diverted from return to the atmosphere by injecting it into suitable rock formations for long term storage. This type of scheme, called bioenergy carbon capture and storage (BECCS), has been endorsed by the IPCC [1]. BECCS processes may become important for reducing climate change, as they represent one of only a few practical methods for removing CO_2 from the atmosphere.

Some of the largest technological obstacles to the broad deployment of biomass gasification are related to the need to remove contaminants from the syngas before it is used to produce fuels, chemicals, or electricity. Raw syngas as it emerges from a biomass gasifier typically contains char and ash particulate, tar vapors, sulfur compounds,

chlorides, and nitrogen species [18]. These contaminants lead to a variety of problems in downstream syngas applications including corrosion, catalyst poisoning and coking, pipeline fouling, and air pollution [5, 19, 20].

Of these contaminants, the nitrogen compounds in syngas are detrimental to nearly every application of syngas. The most problematic ones are ammonia (NH_3) and hydrogen cyanide (HCN). Both are precursors to NO_X formation when syngas is combusted for heat and power applications [5]. They also poison catalysts used to upgrade syngas into fuels and chemicals [16, 21]. Nitrogen can also be found in syngas within the char and tar products (char-N and tar-N), and as diatomic nitrogen (N_2). These forms are less problematic. Char and tar generally must be removed from the syngas to satisfy other syngas cleanliness requirements [19]. Diatomic nitrogen gas is quite inert, and is often already found in the syngas in much larger amounts, due to the use of air as a gasifying agent.

The origin of the nitrogen species in syngas is fuel bound nitrogen (FBN) in the feedstocks. Most biomass feedstocks contain small amounts of nitrogen, originating mainly from proteins, but also from nitrates, ammonium, chlorophyll, and nucleic acids. Nitrogen generally comprises a relatively small portion of the overall makeup of the biomass (0.05 to 2 wt% for most fuels) [22]. Despite this, FBN has a large impact on syngas quality, given the stringent nature of pollution regulations concerning NO_X, and the potency of NH_3 and HCN in regards to interfering with catalysis [16].

Measurements of nitrogen compounds in syngas are generally more difficult and less frequently conducted compared to permanent gas composition and tar, char, and water content. With the exception of N_2, it is normally not necessary to measure nitrogen species in order to complete a full mass balance, as their mass fraction is

usually smaller than measurement error. The relatively small concentrations of the nitrogen species also makes them difficult to detect. Except in extreme circumstances, NH_3 and HCN concentrations in syngas can be expected to fall below 1%. The diversity of the physical properties of the nitrogen bearing compounds (gases, solids, and condensable vapors) also makes them more difficult to study since separate, and very different analytical techniques must be used for each one. Nitrogen compounds are normally only measured in studies which take interest in each one specifically due to the technical difficulty, unique procedures, and unique equipment associated with measuring each one.

Of the five main forms of nitrogen in syngas (NH_3, HCN, char-N, tar-N, and N_2), NH_3 has been measured most frequently [6-8, 10, 13, 20, 23-27]. The most common method of measuring NH_3 in syngas is by bubbling the syngas through an acidic capture solution such as dilute sulfuric acid (H_2SO_4) or hydrochloric acid (HCl). Upon exposure to the acidic solution, the NH_3 dissolves into the aqueous phase as ammonium (NH_4^+). Analysis of the aqueous solution is then conducted off-line. By measuring the volume of syngas bubbled through the solution, the concentration of NH_3 in the syngas can be accurately determined. Useful descriptions of the methodology for conducting measurements of NH_3 have been published by Xu et al. [28].

It can be laborious to prepare, process, and analyze NH_3 captured in aqueous solutions, but wet chemical methods have some notable advantages. They have excellent sensitivity. Relatively low concentrations of NH_3 in the syngas can be detected by simply bubbling a larger volume of syngas through the liquid. Once the NH_3 is captured in aqueous form, it is detected with relative ease via ion selective probe [13, 29], titration [25, 30, 31], or ion chromatograph [32]. The wet chemical technique is also robust and

tolerates relatively dirty, unconditioned gas streams. Steam in the syngas poses no problems as it can simply condense into the solutions. Some char and tar can also be tolerated, since they can be filtered out while preparing the samples for analysis.

Hydrogen cyanide has also been measured via wet chemical techniques much like those used for NH_3, except with basic capture solutions instead of acidic ones. The most popular capture solution is dilute sodium hydroxide (NaOH). The wet chemical technique for measuring HCN has the same robustness advantages as that used to capture NH_3. Modest amounts of char and tar in the syngas are tolerated. Once HCN has been collected into the capture solutions, they can be analyzed by ion selective probe or by ion chromatography. High quality information about the procedures and methodology for collecting HCN for measurement, along with techniques for measuring other types of syngas contaminants have been published by Kurkela et al. [31] and Ståhlberg et al. [33].

In addition to the wet chemical method, it is also possible to measure HCN via Fourier transform infrared spectroscopy (FTIR) [6, 7] and gas chromatography in combination with a nitrogen chemiluminescence detector (NCD) [34]. These methods are advantageous because they allow direct measurement of HCN in the gas phase, avoiding propagation of error that can arise from the multiple analytical steps associated with wet chemical methods. Direct measurement can also improve statistical power since more frequent sampling of the gas can be conducted. In contrast, wet chemical techniques are often too slow and laborious to allow collection of more than a few samples. Nevertheless direct measurement of HCN can require sophisticated and expensive analytical instrumentation. Rigorous gas stream cleanup of tar and char must be conducted to avoid damaging instruments. Calibration of gas analysis instruments

for HCN presents a serious safety concern since calibration gases toxic to humans are required. The U.S. National Institute for Occupational Safety and Health (NIOSH) has assigned HCN an "Immediately Dangerous to Life and Health" (IDLH) concentration of only 50 ppm [35]. While a calibration standard containing cyanide ion (CN^-) is also required for analysis of aqueous samples, small amounts of aqueous sodium cyanide standard required can be handled with relative ease and safety. Despite the attractive aspects of direct measurement, most measurements of HCN in syngas are made via the wet chemical technique due to its relative safety, high sensitivity, and robustness.

Despite the similarity of the wet chemical techniques for HCN and NH_3, HCN measurements from continuous gasification of biomass have been less frequently performed than NH_3 measurements. The results published by some authors suggest that yields of HCN from FBN are negligible (0.22% yield from FBN or less) [24, 26, 36]. These three frequently cited studies have encouraged some authors to neglect taking HCN measurements. Other authors report that yields of HCN can be one to two orders of magnitude higher [6, 7, 13, 23, 31], inferring that HCN is significant, and that monitoring of its concentrations is warranted.

Measurements of tar-N yields in the literature for continuous biomass gasification are even rarer than HCN measurements. The few that are available also disagree about whether tar-N is a significant nitrogen product. Yu et al. [36] employed a solid phase extraction technique, and reported yields of tar-N from two woody feedstocks and two herbaceous feedstocks to be low (0.37 to 1.3% of FBN). Kurkela et al. [31] also reported low tar-N yields for straw gasification (0.8 to 1.8% of FBN). These two sets of results seem low enough to neglect tar-N when considering the complete profile of nitrogen products, but the results of a more recent study of sewage sludge gasification

dispute this. Aznar et al. [25] used a gas chromatograph equipped with a flame ionization detector and a mass spectrometer to analyze tar for nitrogen compounds, and reported tar-N yields of 5.9 to 20.6% of FBN.

Measurement of char-N is relatively simple compared to the complex procedures needed to measure other nitrogen species. Most researchers have used elemental analysis similar to that used to obtain ultimate analysis of biomass samples. Despite the ease of measuring char-N, accurate measurements of char-N are still not widely available. The reason for this may be that authors focused on NH_3 and HCN, as they are the most detrimental nitrogen species. Other authors may not have had access to the necessary elemental analysis equipment. Finally, some gasification studies focused on nitrogen partitioning chose operating conditions which produced very little char, leading to very little char-N [7]. As with the published HCN and tar-N results, it is disputed whether char-N is a significant form of nitrogen in syngas. Char-N yields reported by Zhou et al. [26] and Yu et al. [36] were below 10%, but other yields such as those reported by Vriesman et al. [24] were higher (14.0 to 21.0%). The char-N yield results of Abelha et al. [23] were especially high, in the range of 12% to 32%.

The final major nitrogen product from the FBN is diatomic nitrogen (N_2). In contrast to the other four major forms of nitrogen in syngas, micro gas chromatograph (mGC) technology suitable for detecting N_2 concentrations is widely available, and frequently has online monitoring capability. Despite this ease of detection, there are difficulties in measuring N_2 arising from FBN. Many gasification experiments are conducted with air, which is 79% nitrogen gas, and leads to around 50% N_2 in the syngas. This makes it impossible to measure the N_2 that would have originated from FBN for air blown gasification, since the amount of N_2 generated from the FBN would

be about two orders of magnitude less than that from the air. In order to solve this problem, special arrangements must be made to use gasifying agents such as pure oxygen and high purity inert gases other than N_2. Accurate measurement of N_2 arising from FBN is further complicated by the possibility of air contamination from leaks and from air in the interstitial spaces of the biomass fuel. These contamination problems are lessened somewhat for gasification of fuels which are very rich in FBN, since leaks and interstitial nitrogen become less significant. Zhou et al. [26] and Aznar et al. [25] successfully measured N_2 generated from fuels with very high nitrogen content of 2.51 and 7.55 wt% nitrogen, respectively.

In addition to the five most important products of FBN, a few studies have also found that small amounts of FBN may also convert to nitric oxide (NO) and isocyanic acid (HNCO). Significant conversion of FBN in miscanthus to HNCO was reported by de Jong et al. [37] for slow heating rates to gasification temperatures in a thermogravimetric analyzer equipped with a Fourier transform infrared detector (TG-FTIR). Significant NO *yields*, but low NO *concentrations* were reported by Zhou et al. [26] and Van Huynh and Kong [20]. Both groups of authors utilized wood fuels with extremely low nitrogen content (0.03% and 0.05% respectively). Other studies seem to provide compelling evidence against the significance of NO and HNCO. Leppälahti and Kurkela [30] injected NO gas into a fluidized bed gasifier processing peat fuel, and were unable to detect any NO present in the final syngas product, suggesting that NO quickly evolves into other species. de Jong et al. [6] were unable to detect NO or HNCO via FTIR when they conducted pilot scale gasification of miscanthus. It seems likely that NO and HNCO play some role in the mechanisms of nitrogen evolution in gasification, as they

are often included in reaction networks of nitrogen species [8, 25], but they are seldom detected as final products of continuous gasification reactors.

Researchers have attempted to predict yields of nitrogen species, particularly NH_3 and HCN, in models of biomass gasification. Several models have been created based on kinetic theory [6, 7, 38, 39], with the intention of being able to predict NH_3 and HCN yields across relatively broad gasification conditions. These models have been successful in predicting NH_3 over small ranges of operating conditions and for selected fuels, but they demonstrate serious shortfalls when applied to wider operating ranges and more diverse feedstocks. Efforts have also been made to predict HCN yields [6, 39], but validation of these predictions has been very minimal due to a paucity of reliable HCN data.

In contrast to NH_3 and HCN, which are gaseous species, it is much more difficult to model evolution of the char and tar, even without consideration of their possible nitrogen content. Models generally contain only a few char and tar reactions, which are very simple compared to the reactions typically used to describe homogeneous gas phase reactions of gasification [6, 7, 38, 39]. There is much less agreement on the mechanisms and rate parameters for the reactions in which tar and char participate. This uncertainty arises from the dramatic differences in char and tar properties that result from differences in biomass fuel properties and gasification conditions. These issues make it difficult to consider any possible release of nitrogen species from the char and tar as they are converted to gaseous form.

These difficulties have often deterred modelers from considering the possibility that significant amounts of nitrogen might be bound in the char and tar. Among the four kinetic models presented by Chen et al. [38], Liu and Gibbs [39], and de Jong et al. [6,

7], tar-N was neglected by all four studies. Yields of char-N were predicted in very simple ways in the models by Chen et al. [38] (assumed yields) and Liu and Gibbs [39] (empirical volatile release model), and was neglected by de Jong et al. [6, 7]. Experimental literature does not always support the effectiveness of neglecting char-N and tar-N in modeling efforts [23-25].

Most studies of nitrogen species feature measurements of only one, two, or three forms of nitrogen. This is inadequate for supporting modeling work, particularly if char-N and tar-N constitute significant fractions of the FBN, as this possibility has been mostly ignored in available models. Experimental studies are needed which feature measurements of all of the major forms of nitrogen created during biomass gasification (HCN, NH_3, char-N, tar-N, and N_2). Documentation of the responses exhibited by all five of these nitrogen products within the same study in response to fundamental gasifier operating variables is an important first step toward understanding the complete picture of nitrogen partitioning. Special focus is particularly needed regarding HCN, char-N, and tar-N results. These three species have been infrequently reported, and there is conflicting evidence regarding their relative importance.

Project Objectives

Objective 1

Design, construct, and commission a 25 kg/h fluidized bed gasifier. Simulate the behavior of a very large industrial scale gasifier being operated with steam/oxygen fluidizing agents. Quantify syngas quality, including permanent gas makeup, char, tar and water content. Quantify yields of NH_3 and HCN from FBN.

Objective 2

Simulate the HCN measurement techniques of Vriesman et al. [24], Yu et al. [36], and Zhou et al. [26]. Investigate the possibility of unintentional removal of HCN upstream of where measurements were taken.

Objective 3

Investigate the mechanisms of nitrogen evolution during biomass gasification by gasifying switchgrass at an ER of zero while varying temperature. Document the response of nitrogen partitioning by measuring all major nitrogen bearing products. Compare results to assumptions that were made by authors of kinetic models for predicting nitrogen partitioning.

Objective 4

Investigate the mechanisms of nitrogen evolution during biomass gasification by gasifying switchgrass at a constant temperature while varying ER. Document the response of nitrogen partitioning by monitoring all major nitrogen bearing products. Compare results to findings of the previous study where temperature was varied under equivalent conditions.

Dissertation Outline

This document is organized into six main chapters. Chapter 1 described the motivation behind research in biomass utilization, gasification, and the evolution of nitrogen in a gasification environment. Chapters 2-5 constitute the body of the

dissertation, and take the form of four scientific articles written to document pursuit of the four project objectives. Chapter 6 summarizes the findings of the four studies, and makes recommendations for future work.

CHAPTER 2

STEAM/OXYGEN GASIFICATION SYSTEM FOR THE PRODUCTION OF CLEAN SYNGAS FROM SWITCHGRASS

A paper published in *Fuel*, 2015, 140, 282-292

Karl M. Broer[1], Patrick J. Woolcock[2], Patrick A. Johnston[3], Robert C. Brown[4]

Introduction

Biomass gasification can convert a wide range of biomass feedstocks into syngas for the production of process heat, electricity, fuels, or chemicals that would otherwise be derived from fossil fuels [16]. Though the term "syngas" was originally defined as a mixture strictly limited to hydrogen gas (H_2) and carbon monoxide (CO) [14], it has been more widely applied to refer to the gaseous product of any kind of gasification process. We will we use the term syngas here in this broader meaning. Most biomass gasifiers are air-blown and produce syngas that contains roughly 50% nitrogen gas (N_2) [14]. This high inert gas content means that the syngas also has relatively low energy content (a higher heating value (HHV) of around 5.5 MJ/N-m^3 [22], compared to 38 MJ/N-m^3 [39] for natural gas). The N_2 diluent also makes downstream syngas cleanup and utilization more costly as the equipment must be sized to handle greater volumes of gas. These shortcomings can be remedied by using pure oxygen, oxygen-enriched air, or

[1] Primary researcher and author
[2] Conducted and reported on syngas cleanup system performance
[3] Provided technical support with gas analytical equipment
[4] Provided document editing assistance, serving as author for correspondence, and major professor

oxygen/steam mixtures as gasification agents. These strategies produce syngas with far less inert gas content and much higher energy content per unit volume. Steam is frequently used because it promotes H_2 production via the water-gas shift reaction, and can help control temperature in the gasifier [22].

Steam and oxygen blown gasification studies are relatively rare due to the extra equipment and operational complexity that is required compared to air gasification. Gasification studies employing steam and oxygen-enriched air, which tend to have operating characteristics lying between air gasification and steam and oxygen gasification, are more common. Examples of both types of studies are listed in Table 1. Among the few studies that have been conducted, experimental work related to varying reactor temperature, ratios between the constituents of the fluidizing gas, feedstock type, and bed material has been conducted. While all studies have measured the permanent gas composition of the syngas, data related to char, tar, and water content, sulfur species, and especially nitrogen compounds are sparser.

Table 1. A summary of oxygen/steam and enriched air/steam biomass gasification studies (EA – Enriched Air, BFB – Bubbling Fluidized Bed, CFB – Circulating Fluidized Bed, ER – Equivalence Ratio, T – Temperature, OC – Oxygen Concentration of fluidizing agents, SBR – Steam to Biomass Ratio, BM – bed material, CBR – Coal/Biomass Ratio)

Reference	Fluidizing Agents	Gasifier Type	Biomass Type	Variables Studied	Data Reported									
					Perm. Gases	Tar	Tar Makeup	Char	Water	Gas Yield	Sulfur	NH_3	HCN	NO
Gil et al. [41]	H_2O/O_2	BFB	Pine Chips	ER, T, OC	X	X	X	X	X	X				
Meng et al. [11]	H_2O/O_2	CFB	Agrol, Willow, DDGS	ER, T, SBR, BM	X	X	X			X	X			
Pinto et al. [10, 42]	H_2O/O_2	BFB	Pine, Bagasse, Plastic, Coal	CBR	X	X				X	X	X		
Campoy et al. [43]	H_2O/EA	BFB	Wood Pellets	ER, SBR	X					X				
Siedlecki and de Jong [44]	H_2O/EA	CFB	Wood, Miscanthus, Straw	BM	X	X	X		X	X				
Turn et al. [45]	H_2O/EA	BFB	Sawdust	ER, T, SBR	X					X				
Van Huynh and Kong [20]	H_2O/EA	BFB	Wood, Seed Corn	OC	X	X			X			X		X

In order to study steam/oxygen blown gasification relevant to bioenergy applications, a 25 kg/h gasification reactor and downstream syngas cleaning equipment was constructed at Iowa State University. The effect of equivalence ratio (ER) on syngas composition and quality was determined, and the performance of a new syngas cleanup system was tested. Many constituents of the syngas were measured including permanent gas, C_2 hydrocarbons, water, heavy tar, light tar, char, hydrogen sulfide (H_2S), carbonyl sulfide (COS), carbon disulfide (CS_2), ammonia (NH_3), and hydrogen cyanide (HCN).

A novel gas cleaning system was designed to remove char, tar, sulfur, and NH_3. After using cyclonic separation to remove most particulate from the syngas, the following unit operations were employed:

1. An oil scrubber for tar and residual particulate removal
2. A packed-bed adsorption system for sulfur removal
3. A water-based absorption scrubber for NH_3 removal

Materials and Methods

Preparation and analysis of biomass

Switchgrass was harvested by Chariton Valley RC&D, Inc. near Centerville, Iowa, USA and baled into 1.8 m diameter round bales. After transport to Iowa State University, the bales were disintegrated and coarsely chopped using a Vermeer BP-8000 whole bale grinder. The material was dried using an Advanced Trailer & Equipment

trailer style drier and then ground again using an Art's Way hammer mill equipped with a 6.35 mm (0.25 in) screen.

Moisture content was determined by drying the biomass for 72 hours at 95°C in a Fisher Scientific IsoTemp Oven. Proximate analysis was conducted using a Mettler Toledo TGA/DSC 1 Thermo-Gravimetric Analyzer, and determined volatile content, fixed carbon, and ash content. Analysis of carbon, hydrogen, and nitrogen content was conducted using an Elementar vario MICRO cube analyzer. Analysis for ten different ash elements was conducted by using an X-ray fluorescence (XRF) spectrophotometer (PHILIPS PW2404) equipped with a rhodium target X-ray tube and a 4 kW generator. Oxygen content was found by difference. The combined results of these four analyses are found in Table 2.

Feed system

The gasification reactor was equipped with a custom lock hopper feed system to allow feeding of solid biomass into the pressurized gasification reactor. The feed system was constructed from carbon steel pipe with an inner diameter of 390 mm. It was designed to handle fibrous and low-density particles up to 6 mm in size. Two knife gate valves were used to admit biomass into the pressurized environment. Nitrogen gas (N_2) was used to pressurize and blanket the batches of biomass entering the hopper. Biomass was fed into the reactor at 10.3-12.6 kg/h via a two-stage auger feeding system consisting of a slow moving variable speed metering auger followed by a faster moving constant speed injection auger for stoking the fluidized bed. A small amount of N_2 (10

SLPM) was introduced into the metering auger to cool the auger housing and blanket the biomass with inert gas.

Table 2. Switchgrass fuel proximate and ultimate analyses (uncertainty reflects 95% confidence interval).

Proximate Analysis	**(wt%, as received)**
Moisture	8.26 ± 0.08
Volatiles	75.5 ± 1.2
Fixed Carbon	13.3 ± 0.5
Ash	5.8 ± 0.8
Ultimate Analysis	**(wt%, dry basis)**
C	46.7 ± 1.0
H	4.99 ± 0.08
N	0.86 ± 0.10
Al	0.03 ± 0.01
Ca	0.35 ± 0.10
Cl	1.49 ± 0.14
K	2.55 ± 0.11
Fe	0.01 ± 0.01
Mg	0.20 ± 0.02
Na	0.03 ± 0.00
P	0.09 ± 0.02
S	0.06 ± 0.03
Si	1.67 ± 0.54
O (by difference)	41.0

Gasifier

An illustration and a photograph of the gasifier and feed system are shown in Figure 1 and Figure 2, respectively. The gasifier was specially designed to allow pressurized gasification under essentially adiabatic conditions between 650 and 900°C. The pressure vessel was constructed from 489 mm ID carbon steel pipe of 3050 mm length. As shown in Figure 3, the pipe was lined with 19 mm of BTU-BLOCK microporous insulation followed by 137 mm of castable Resco EZ-cubed LO-ERODE

refractory, resulting in an internal diameter of 178 mm. Each layer served a distinct purpose. The microporous insulation kept the steel pipe from exceeding permissible temperature limits for pressure vessels, and minimized heat loss from the reactor. The castable refractory served as an erosion barrier against the scouring action of fluidized sand in the reactor, and supported six electric cartridge heaters near the perimeter of the fluidized bed. The guard heaters were equipped with integral thermocouples and controlled automatically to maintain the temperature of the refractory slightly above the gasification temperature. This ensured that heat loss from the gasifying biomass was close to zero. Each cartridge heater had a maximum output of 4 kW, for a total of 24 kW of heating capacity. Two dimensional heat transfer simulations of the reactor cross section indicated that maintaining the thermocouples inside the cartridge heaters at 100°C above the gasification temperature would achieve essentially adiabatic gasification. After warm-up of the gasifier, about 8 kW of power was needed to satisfy temperature requirements while steady-state operation was underway. This was consistent with the approximate heat loss rate predicted by the heat transfer simulation. The temperature profile of the fluidized bed itself was monitored via five evenly spaced thermocouple probes protruding into the center of the reactor.

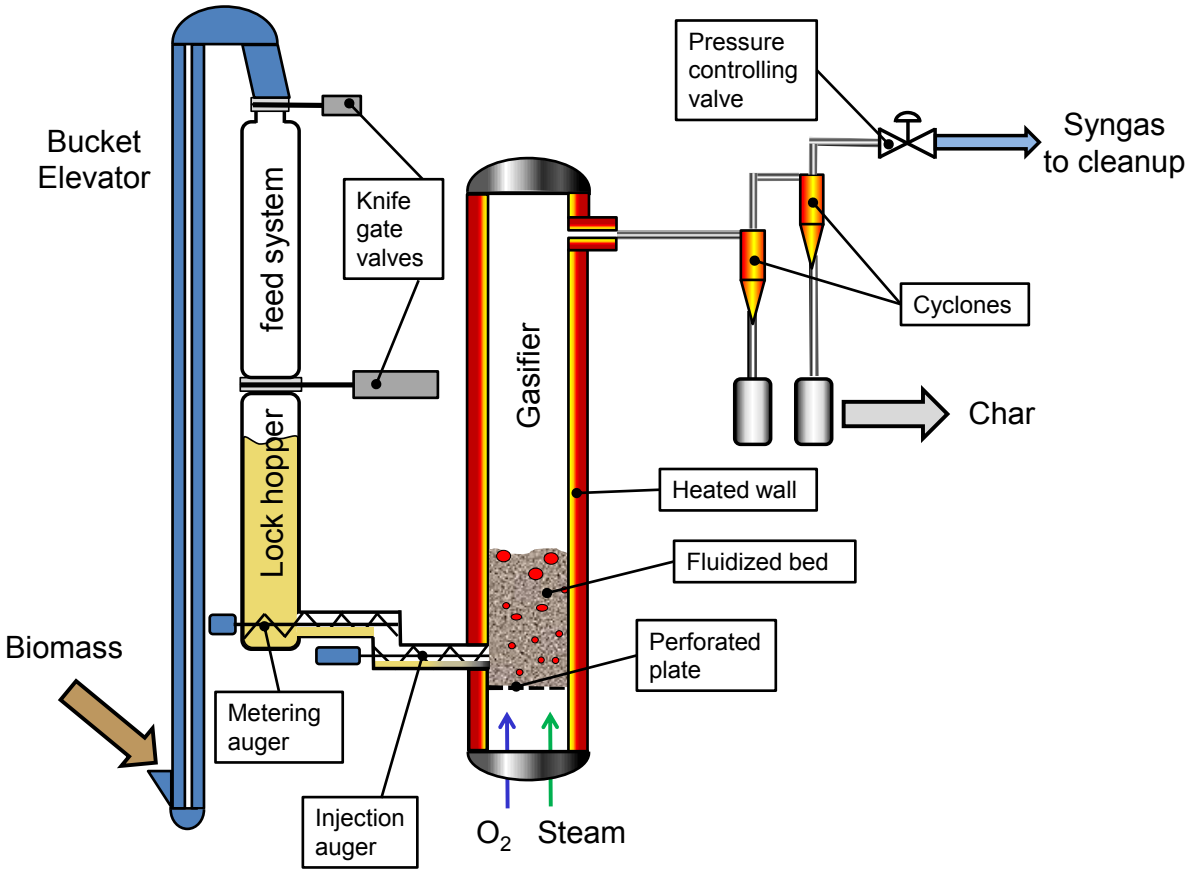

Figure 1. The new feed system and fluidized bed gasifier at Iowa State University.

Figure 2. A photo of: (1) The pressurized feed system and (2) the 25 kg/h fluidized bed gasifier.

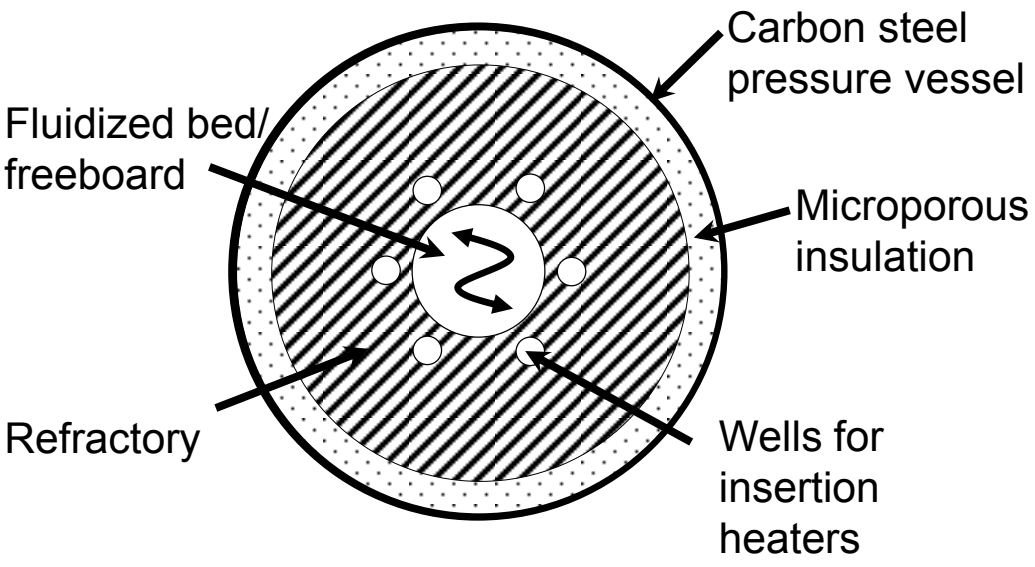

Figure 3. The gasification reactor consisted of a carbon steel pressure vessel lined with first a layer of microporous insulation, followed by a layer of refractory. Six wells were included in the refractory for accommodating insertion heaters.

Upon exiting the reactor, syngas was passed through two gas cyclones in series that were designed according to Stairmand High Efficiency geometry [46]. An automatically actuated valve was used to control gasifier operating pressure by throttling syngas flow, and was located after the cyclones to mitigate char erosion of valve internals. The reactor, feed system, cyclones, and cyclone catches were all designed to be operated at pressures up to 1 bar gauge.

Syngas cleanup system

Three unit operations for cleaning the syngas of fine particulate, tar, sulfur species, and NH_3 were carried out downstream of the pressure control valve, and are illustrated in Figure 4. A photograph is included in Figure 5.

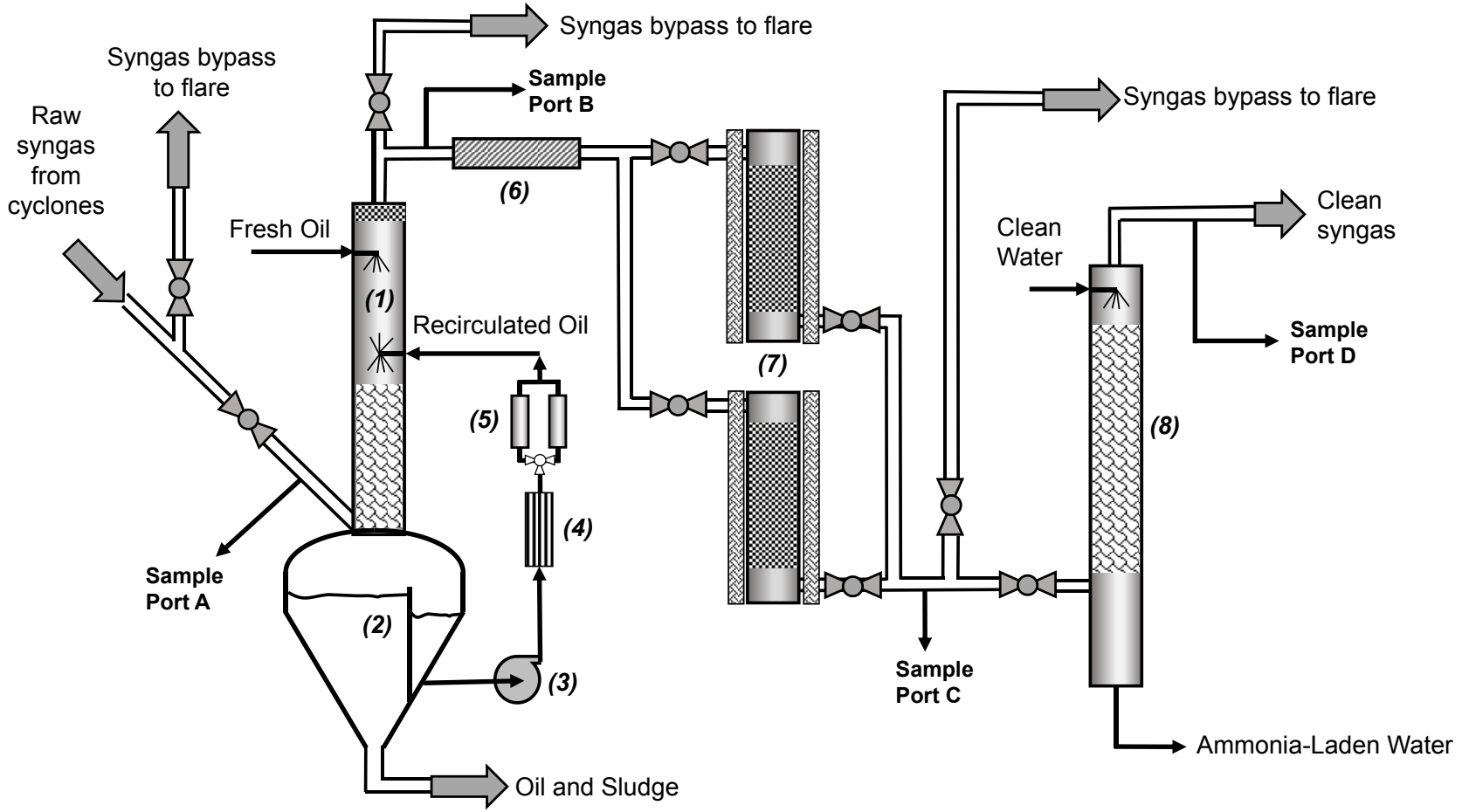

Figure 4. The gas cleaning system consisted of: (1) Oil scrubbing column for removing fine char and tars, (2) oil decanter tank for allowing collected solids to settle out of oil, (3) oil circulation pump, (4) oil cooling heat exchanger, (5) oil filter, (6) electrical syngas circulation heater, (7) packed bed sulfur adsorbent canisters, and (8) water scrubber for ammonia removal.

Figure 5. A photo of: (1) The oil scrubbing column, (2) packed bed sulfur adsorbent canisters, and (3) water scrubber for ammonia removal. Vessels are shown with all insulation and heat tracing/jacketing removed.

Scrubbing of tar and fine particulate was conducted using Xceltherm 600 oil in a 150 mm ID and 2000 mm tall pressure vessel. Spray nozzles were strategically oriented in the column for effective removal of tar via condensation and aerosol collection [47]. A full cone spray pattern nozzle was located in the middle of the column, and pointed downwards to distribute 200 kg/h of recirculated oil to continuously wet a bed of structured packing 1000 mm tall. This lower half of the scrubber served as the primary heat exchange portion of the column, designed to reduce the incoming gas temperature by 150-250°C, depending on the inlet temperature. Additional spray streams were then used for the purpose of removing condensed tar aerosols via impingement. A 100 kg/h

stream of recirculated oil was sprayed in immediately above the middle of the column, and divided between three hollow cone spray nozzles pointed in an upwards swirl pattern. A photograph of this configuration was documented previously by Woolcock [47]. A third and final 20 kg/h stream of fresh makeup oil was sprayed straight downwards in a hollow cone pattern near the top of the scrubber. The final 300-450 mm of column space above the fine misting nozzle served as a disengagement zone, and included a 200 mm tall mist eliminator at the very top. The temperature of the tar scrubber was maintained above the dew point of the syngas (generally between 85 and 100°C) to prevent water condensation, avoiding a two-phase spent oil stream that would have been difficult to treat. To study tar scrubbing performance, syngas tar concentration and makeup was measured both upstream and downstream of the oil scrubber at sampling ports A and B (shown in Figure 4).

The oil scrubber column system included a filtration system and recycle unit to minimize the amount of oil required. A decanting vessel located immediately below the scrubbing tower provided the oil approximately 45 minutes of residence time to allow char and agglomerated tar to settle out of the oil. These compounds were periodically discharged to a holding tank located below the vessel. Fresh oil entering the column at the upper misting nozzle served as makeup oil. All oil streams on the scrubbing system were equipped with Coriolis mass flow meters, and the waste oil tank was mounted on a scale to enable calculation of mass balances.

After the oil scrubber, the syngas was reheated to approximately 400°C using a 7.5 kW Chromalox circulation heater, which was necessary for efficient operation of the sulfur sorbent system. Hydrogen sulfide (H_2S) was removed via solid phase adsorption

using two parallel packed bed reactors configured in a lead-lag fashion, with the inactive reactor undergoing regeneration or reloading while the other was in service. Typical operational time was 4-12 h per scrubber vessel, depending on the sulfur concentration in the raw syngas (several hundred to nearly one thousand ppm H_2S). Performance of the sulfur scrubbers was monitored via gas sampling at ports B and C in Figure 4.

Commercially available zinc-oxide based sorbents Actisorb S2 and S6 (Süd-Chemie, Munich, Germany) were utilized as scrubbing media. The 130 mm diameter and 1220 mm long reactors were maintained at 400°C via automatically controlled Watlow ceramic electrical heaters. Three sets of separately controlled heaters were used for each packed bed. The temperature gradients across the packed beds and their inlet and outlet concentrations of H_2S (at gas sampling ports B and C in Figure 4) were monitored to determine breakthrough of the adsorption front, upon which the columns were switched.

Saturated sulfur sorbent canisters were either allowed to cool for removal and reloading with fresh sorbent, or were regenerated in place using small amounts of air mixed with nitrogen. Regeneration required special care due to the highly exothermic oxidation reaction that transformed the sulfided metal sorbents back into their oxidized forms. Regeneration air was diluted with nitrogen in order to reduce the concentration of oxygen to a few percent of the gas flow, and temperatures were monitored constantly to avoid any dangerous temperature excursions.

Ammonia and other water-soluble contaminants were removed from the syngas via a water scrubber, the third unit operation of the cleanup system. The scrubbing column was 150 mm in diameter and 2000 mm tall. At the top of the column, 115 kg/h

of water was sprayed onto a 1750 mm tall bed of random packing material consisting of 5/8 inch size stainless steel Pall Rings. The bottom of the column contained level sensors and a discharge drain to maintain a small pool of water at the bottom of the column. Syngas flow proceeded from bottom to top of the scrubber, counter to the flow of water. Syngas exiting the scrubber was 50-60°C. Performance of the water scrubber was monitored via gas sampling ports C and D in Figure 4.

Gasifier operating conditions

The fluidized bed material consisted of 12.8 kg of 40/70 silica sand obtained from Badger Mining Corporation (409 South Church St., Berlin, WI USA) blended with 3.2 kg of Uni-Cal 'L' crushed limestone from ILC Resources (3301 106th Circle, Urbandale, IA USA). The limestone was included in order to absorb the low melting point alkali metals commonly found in herbaceous feedstocks, as discussed by Turn et al. [48] and Basu [49]. The bed was refreshed before each experiment.

For all tests the composition of the fluidizing agent was 50 wt% oxygen and 50 wt% steam. Equivalence ratio (ER) was varied from 0.21 to 0.38 by simultaneously adjusting the rates of fluidizing agent and biomass feed into the reactor. For continuous flow gasification studies, ER is defined according to Equation 1, where $\dot{m}_{O_2\ actual}$ is the mass flowrate of oxygen supplied to the reactor and $\dot{m}_{O_2\ stoich}$ is the stoichiometric amount of oxygen needed to achieve complete oxidation of the biomass. The order in which different ER levels were tested was randomized. The reactor was operated at 0.28 bar gauge pressure for all gasification runs. The total mass throughput (biomass, steam, and oxygen) was held constant throughout all tests at 18.3 kg/h. Despite the constant

mass flow, gas residence time of the reactor varied from 4.2-5.6 s between tests due to changes in syngas yield, makeup, and temperature. The bed fluidization velocity, assuming that the volatiles released from the biomass during gasification did not contribute toward the fluidization, was between 2.4-3.4 times the minimum fluidization velocity. The minimum fluidization velocity was determined by conducting fluidization tests using air and the electrically pre-heated bed, prior to introduction of feedstock.

$$ER = \frac{\dot{m}_{O_2\ actual}}{\dot{m}_{O_2\ stoich}} \qquad \text{Eq 1}$$

Gas sampling

After achieving steady state gasification conditions, gas sampling was conducted for 70-180 minutes. Exact length of data collection time depended on the combined quantity of nitrogen and tar measurements taken. Upon conclusion of data collection, the reactor was shut down. Sampling of raw syngas prior to gas cleaning was conducted by extracting a 1-2 SLPM slipstream via isokinetic sampling at gas sampling port A (Figure 4) where syngas temperature was typically 450°C. A detailed illustration of the sampling line setup is shown in Figure 6. An L-shaped probe was used to extract the slipstream from the main syngas pipeline. The appropriate isokinetic sampling rate was determined beforehand based on the syngas pipeline diameter, the sampling probe diameter, and an approximation of the syngas yield for each set of operating conditions tested. There were over twenty pipe diameters of straight syngas pipeline upstream, and eight pipe diameters downstream of the isokinetic probe to insure established flow conditions. Immediately following extraction, the slipstream was drawn through a 25 X

90 mm ceramic thimble filter canister held at 450°C to trap particulate for gravimetric measurement. The gas was then passed through a dry tar condenser fabricated from a household pressure cooker in a similar manner to the apparatus utilized by Xu et al. [28]. The dry tar condenser was held at temperatures between 100 and 115°C. For the purposes of this paper, the tars collected and measured in this manner will be referred to as "heavy tars." For three select tests, measurements of light tars in the raw syngas were also made immediately downstream of the dry tar condenser via a novel Solid Phase Micro-Extraction (SPME) technique (Figure 6). The details of the SPME technique are described elsewhere [47, 50].

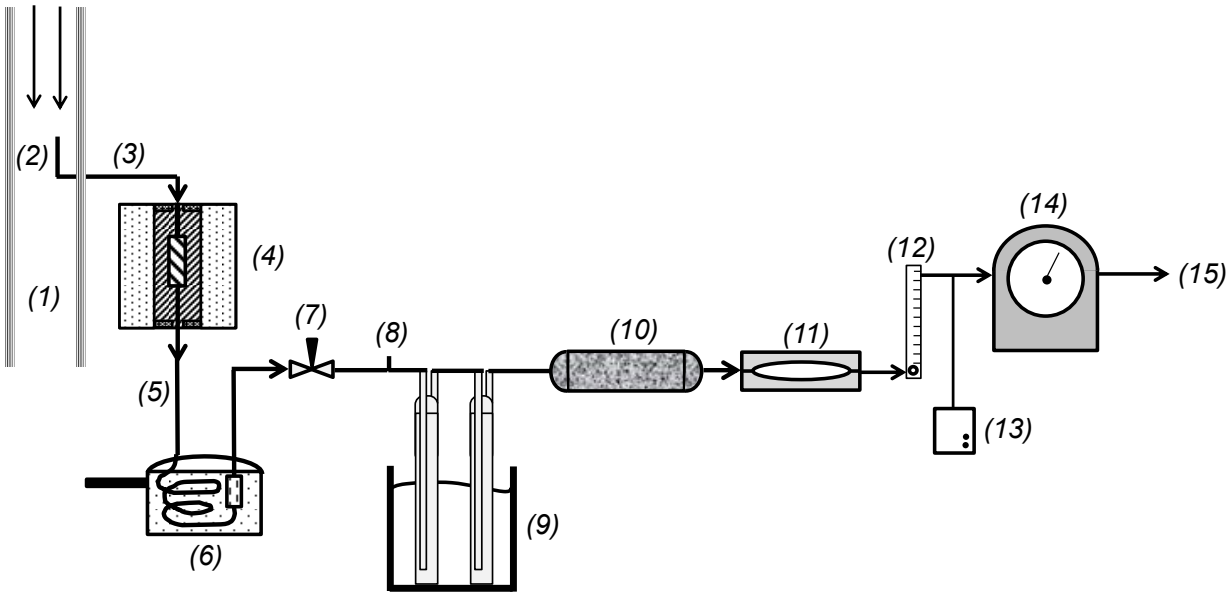

Figure 6. Sample line setup for measurement of char, heavy tar, light tar, water, and permanent gas composition of the syngas: (1) 53 mm inner-diameter (ID) raw syngas pipeline, (2) isokinetic sampling probe located at sampling port A, (3) 8 mm ID stainless steel tubing heat traced to 450°C, (4) quartz thimble filter inside tube furnace at 450°C, (5) 8 mm ID tubing at 450°C, (6) tar collection pressure cooker at 100-115°C, (7) stainless steel needle valve and 8 mm ID tubing heated to 120°C, (8) tubing tee and septum for SPME sampling of light tars, (9) two 500 mL glass impingers in a water-ice bath for water collection and wet chemical measurements of ammonia and hydrogen cyanide, (10) desiccant canister for final water aerosol removal, (11) diaphragm vacuum pump, (12) rotameter with integral control valve, (13) Varian CP-4900 micro gas chromatograph, (14) drum-type total flow gas meter, and (15) to exhaust.

After measurement of tars, the slipstream was bubbled through a pair of 500 mL glass impingers configured in series. Each impinger was filled with 200 mL of collection solution for measuring nitrogen species. Two pairs of impingers were used during each experimental run. The first pair was installed for 30 minutes of collection time after which they were removed and replaced with a second pair for a second 30 minute collection time. One pair of impingers was filled with 5% hydrochloric acid for measuring NH_3. The other pair was filled with 100 mM sodium hydroxide for measuring HCN. The order in which the two nitrogen species were collected during each test run was randomized. All impingers were weighed before and after they were used to measure water condensed from the syngas. After collection, the solution from each impinger was transferred into a high quality HDPE sample bottle with a tightly fitting lid. Samples were held at 5°C until analysis.

After the impingers, the slipstream was passed through a desiccant canister to remove any remaining moisture. The stream was then analyzed with a Varian CP-4900 micro gas chromatograph (mGC) to measure N_2, carbon monoxide (CO), carbon dioxide (CO_2), hydrogen (H_2), methane (CH_4), ethane (C_2H_6), ethylene (C_2H_4), acetylene (C_2H_2), and helium (He). The flow rate of the sampling line was controlled via a rotameter/valve combination. The total volume of dry syngas sampled was measured using a drum-type total flow gas meter at the end of the sampling line. While gasification was underway, a small He tracer of a known flow rate was injected into the main syngas pipeline just upstream of the gas cyclones. The concentration of He in the syngas measured by the mGC could then be used to determine the total volumetric flow rate of syngas ($\dot{V}_{syngas}$)

from the volumetric flowrate of He tracer ($\dot{V}_{He}$) and the measured concentration of He (X_{He}) via Equation 2.

$$\dot{V}_{syngas} = \dot{V}_{He}\left(\frac{1}{X_{He}} - 1\right) \quad \text{Eq 2}$$

An Agilent 7890 gas chromatograph (GC) (Santa Clara, CA USA) with Chemstation version B.04.03 software was use to evaluate the performance of the gas cleanup system. The GC was configured with a Wasson-ECE Instrumentation (Fort Collins, CO USA) custom online gas sampling system, which was connected to sampling ports B, C, and D (see Figure 4) via sampling lines that were heat traced and maintained at 250°C. The GC was equipped with five different detectors for online analysis. An Agilent 355 Sulfur Chemiluminescence Detector (SCD) was used to determine H_2S, COS, and C_2S. An Agilent 255 Nitrogen Chemiluminescence Detector (NCD) was used to quantify NH_3 concentrations. Two Agilent Thermal Conductivity Detectors (TCD) were used to quantify light hydrocarbons and NH_3 at high concentrations (>1000 ppm). The use of three sampling locations and the broad capabilities of this GC system enabled gas composition before and after each gas cleaning stage to be monitored during experiments.

Analysis of NH_3 and HCN

The solutions from the acidic impingers, containing NH_3 as ammonium ion (NH_4^+), were vacuum filtered through 110 mm diameter Whatman 42 filter paper and diluted to 500 mL using deionized water. They were then placed into new HDPE bottles

with tight fitting lids, and transported to MVTL Laboratories, Inc. (Nevada, IA USA) and analyzed for NH_4^+ content via distillation followed by titration in accordance with National Environmental Methods Index Standard Method 4500-NH_3 B,C [51].

The samples from the basic impingers were diluted to 500 mL using 100 mM sodium hydroxide (NaOH). The samples were then agitated, filtered using 0.45 μm glass micro-fiber syringe tip filters, and then dispensed into 1500 μL sample vials for cyanide ion analysis using a Dionex ICS-3000 ion chromatograph (IC). Samples were brought into detection range of the IC by conducting dilutions with 100 mM NaOH as needed. Dilutions were conducted with Eppendorf Multipipette Repeaters equipped with tip sizes carefully chosen to maximize precision. All reagents used for aqueous sample operations were prepared using 18.2 MΩ deionized water.

Equilibrium modeling

Thermodynamic equilibrium calculations were conducted using the Aspen Plus software package with the inputs being based on the gasification conditions explored in this study. A constant temperature and pressure assumption was employed. Temperatures were specified according to those observed during experimental test runs. Pressure was specified at 0.28 bar for all equilibria calculated. Biomass, steam, and oxygen inputs were also matched to the experimental conditions tested. Nitrogen purge and He tracer gases were omitted from the calculations. The composition of the biomass was simplified to include only the carbon, oxygen, hydrogen, and nitrogen content.

Results

Gasifier performance

Eight test runs were conducted in order to evaluate gasifier performance. Each test run yielded one measurement of char, heavy tar, water, NH_3, and HCN. Between 10 and 30 sets of permanent gas data were collected for each test run, depending on data collection time available. The permanent gas data reported represent the average of these measurements. Due to assorted technical difficulties, one tar, one HCN, and one NH_3 data point were not recovered.

Gasification temperature increased almost linearly with equivalence ratio (ER) up to ER of 0.32 (see Figure 7), as would be expected for adiabatic gasification [15]. Padban [52] found a similar linear relationship for an air blown reactor of similar throughput. For operation above ER=0.32, the temperature became constant at about 900°C. This occurred because the operating limits of the cartridge heaters embedded in the refractory wall had been reached. For process temperatures above 880°C, it was no longer possible to trim the set point of the cartridge heaters to 100°C above the process temperature as their operating limit was 980°C. This resulted in increased heat loss to the surroundings, departing from the near-adiabatic conditions that were otherwise achieved.

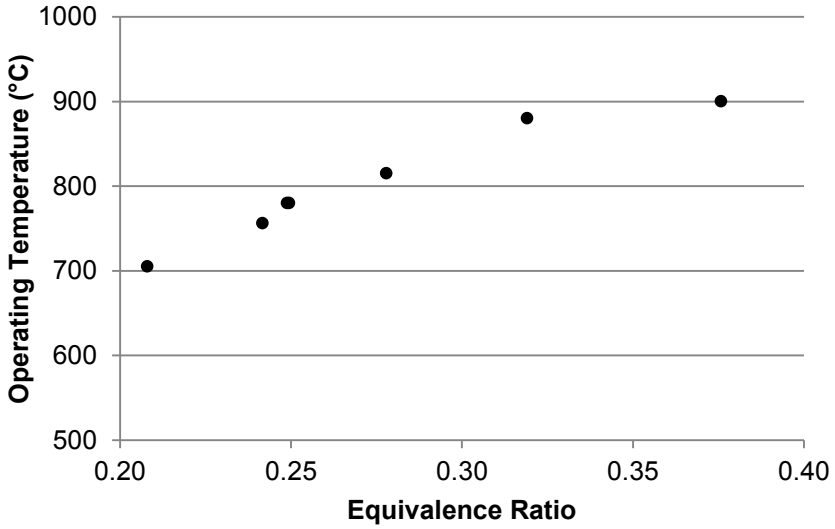

Figure 7. The effect of ER on adiabatic reactor temperature. Fluidizing agent was 50 wt% O_2, balanced with steam. Temperature measurements were taken from a thermocouple inserted into the fluidized bed, 110 mm above the perforated plate.

Bed agglomeration was another limit to operating above 900°C. Agglomeration occurred at this temperature after only four hours of fuel feed (representing only 30 minutes of steady state operation). This 900°C limit corresponds to a maximum possible ER of only 0.33. Different maximum ERs could be expected for other fuels and gasification conditions. For fuels with different ash concentration and makeup, agglomeration problems might present themselves at different temperatures due to changes in ash accumulation rates in the bed and the melting point of the ash eutectic.

The effect of ER on permanent gas composition is shown in Figure 8. The percent concentrations are stated on a dry "inert free" basis, since the He content of the syngas originates only from the tracer and essentially all of the N_2 comes from the feed system purge. In practice, the N_2 content varied from 2-10% vol/vol dry basis, and He content varied from 1.0-2.5% vol/vol dry basis. The thermodynamic equilibrium concentrations of each of the permanent gases have been superimposed onto the plots for comparison.

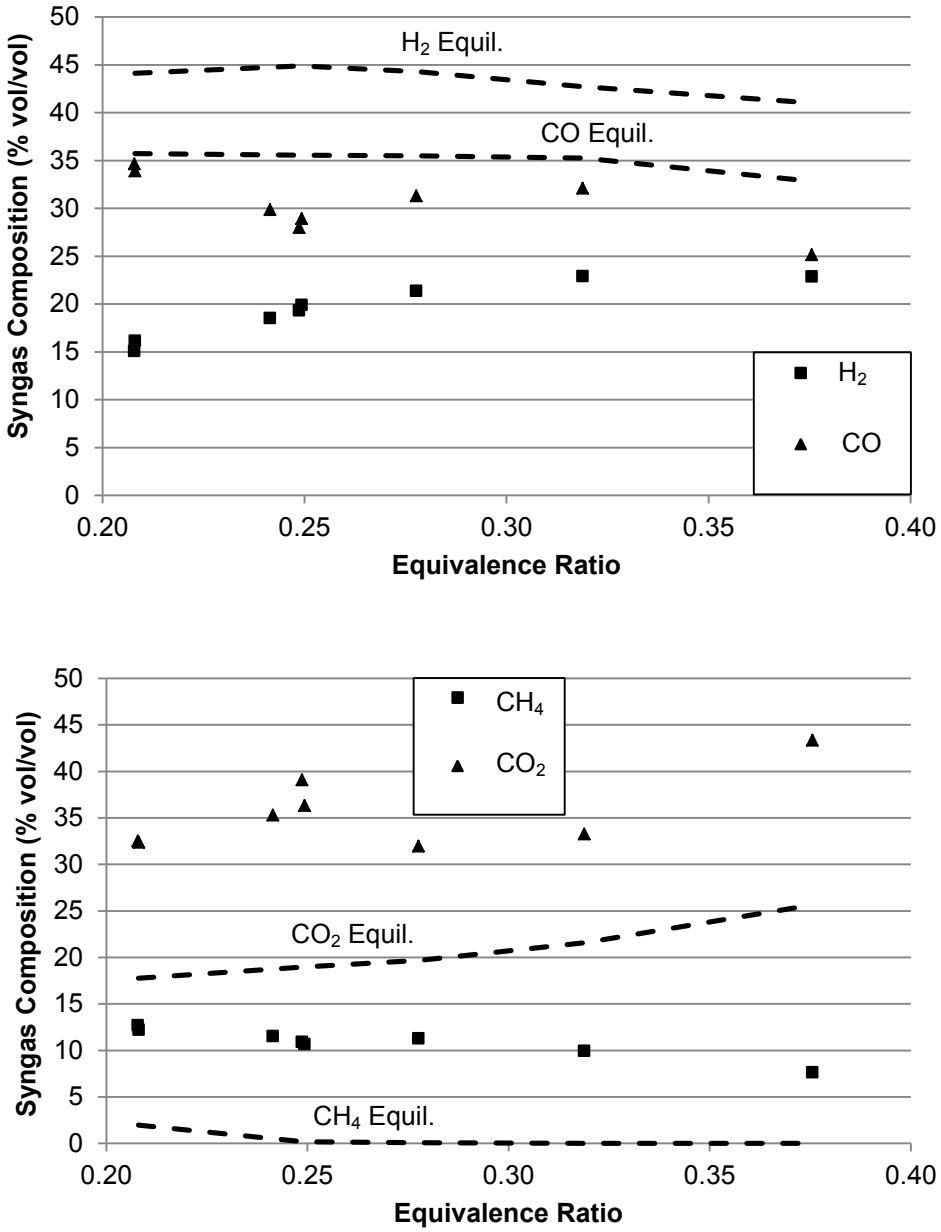

Figure 8. The effect of ER on H_2, CO, CO_2, and CH_4 concentrations. Fluidizing agent was 50 wt% O_2, balanced with steam. Values are reported on a % vol/vol dry, inert-free basis. The results from thermodynamic equilibrium modeling for the same reactor conditions are included for comparison.

Thermodynamic equilibrium calculations predicted that CH_4 should only be present when ER is less than 0.25; however, significant amounts of methane were measured for all ER levels tested. The experimental results demonstrated a continual

steady decline in CH_4, indicating a slow approach toward equilibrium as ER (and reactor temperature) increased. Though CO_2 remained far away from predicted equilibrium concentrations for all ER levels tested, the increasing trend in CO_2 was predicted by the trend of the equilibrium CO_2 concentration results. The experimental results demonstrated a steady increase in H_2, and generally declining CO concentration as ER increased. Both species remained far away from equilibrium predictions for all ER levels tested. A likely reaction pathway for converting the methane to other species is the methanation reaction (Equation 3) [22]. The back reaction of the methanation reaction is endothermic; thus, increasing gasification temperature and steam availability would be expected to reduce CH_4 and increase H_2.

$$CO + 3H_2 \leftrightarrow CH_4 + H_2O \qquad \text{Eq 3}$$

One would also expect CO concentration to increase as CH_4 is consumed by the methanation reaction; however, our results demonstrated a downward trend in CO concentration. This is likely due to destruction of CO via the water-gas shift reaction (Equation 4) [22]. The water-gas shift reaction is exothermic, and would be slowed by increasing gasification temperature that accompanies increasing ER; however, the increasing steam flow to the reactor would encourage the destruction of CO and production of H_2.

$$CO + H_2O \leftrightarrow CO_2 + H_2 \qquad \text{Eq 4}$$

The experimental results of Meng et al. [11] and Siedlecki and de Jong [44] displayed the same upward trend in H_2.

The effect of ER on C_2 hydrocarbons is shown in Figure 9. Ethylene was generally the most prevalent C_2 hydrocarbon, although small amounts of C_2H_6 and C_2H_2 were also present. The trend of C_2H_4 is most significant, declining steeply from 4.2% to only 0.7% as ER was increased. This decline represents an approach to equilibrium conditions, as no significant amounts of C_2 hydrocarbons were predicted by the equilibrium calculations. Reactions similar to methanation are probably responsible for the downward trends, since they would be similarly endothermic and accelerated by increased temperatures and steam presence.

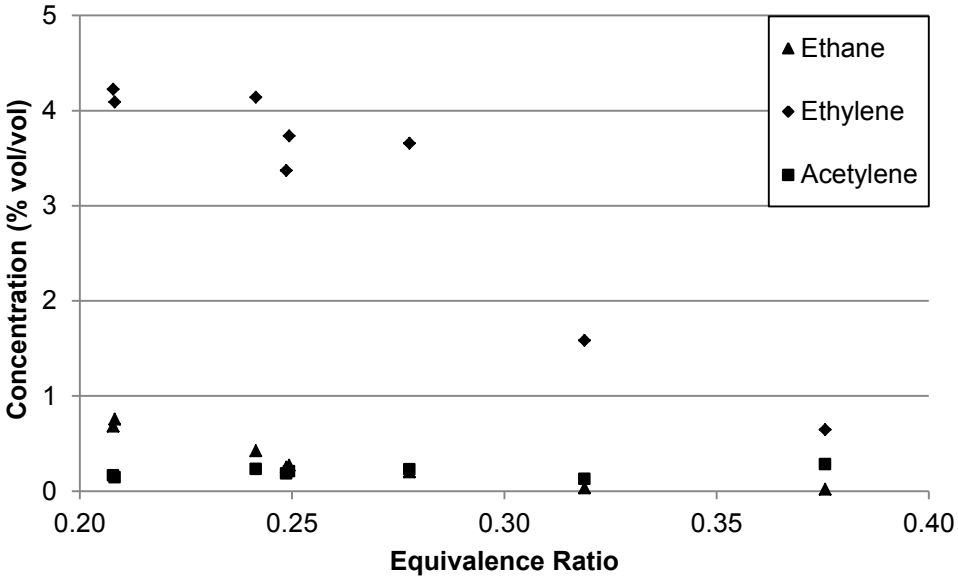

Figure 9. The effect of ER on concentrations of C_2 hydrocarbons. Fluidizing agent was 50 wt% O_2, balanced with steam. Values are reported on a % vol/vol dry, inert-free basis. The results from thermodynamic equilibrium modeling demonstrated essentially no production of C_2 hydrocarbons.

The effect of ER on heavy tar is demonstrated in Figure 10. Heavy tar content decreased steadily from 43 to 17 g/N-m^3 with increasing ER. This range is comparable

to values reported by Gil et al. [41] for similar operating conditions. The decline in tar concentration with increasing ER is consistent with an approach to equilibrium for which no tar is expected among gasification products. Endothermic tar cracking and steam reforming reactions are responsible for destruction of tar [53].

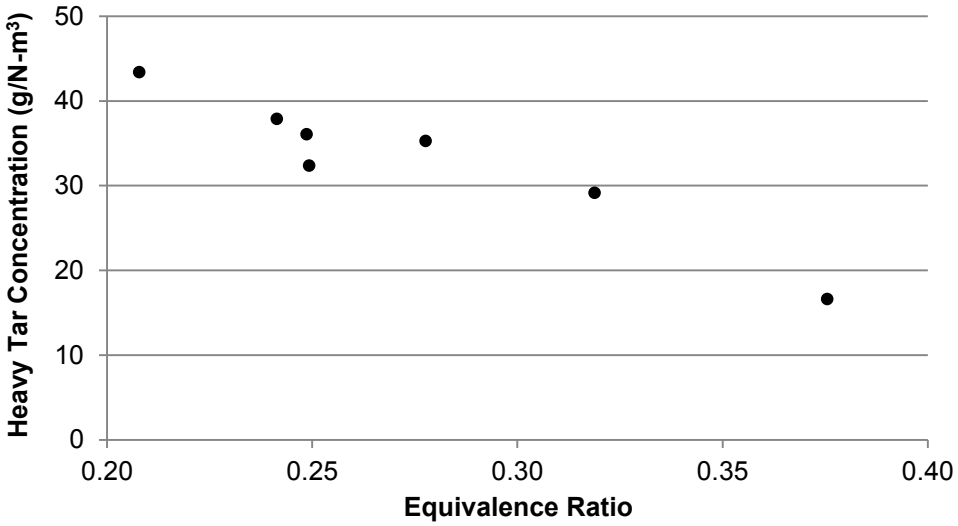

Figure 10. The effect of ER on heavy tar concentration. Fluidizing agent was 50 wt% O_2, balanced with steam. Values are reported on a dry, inert-free basis. The results from thermodynamic equilibrium modeling for the same reactor conditions demonstrated essentially no tar production.

The effect of ER on water content of the syngas is shown in Figure 11. The thermodynamic equilibrium concentration of water for the same conditions is superimposed onto the plot for comparison. Interestingly, the experimental trend in water content decreased as ER was increased from 0.21, reached a minimum near ER=0.26, and then increased again for higher ERs. This minimum was not predicted by the equilibrium modeling results, which show H_2O content increasing steadily as ER is increased, mostly due to increased amounts of steam coming in as fluidizing agent. The downward trend of the steam content from an ER of 0.21-0.25 is probably caused by the participation of steam in several reactions including methanation [22], water-gas shift

[22], and reforming of C_2 hydrocarbons and tars [53]. These endothermic steam consuming reactions might be expected to first increase with ER (and temperature), but then slow as the supply of hydrocarbon reactants is depleted, as is the case at high ER, accounting for the trend in water content.

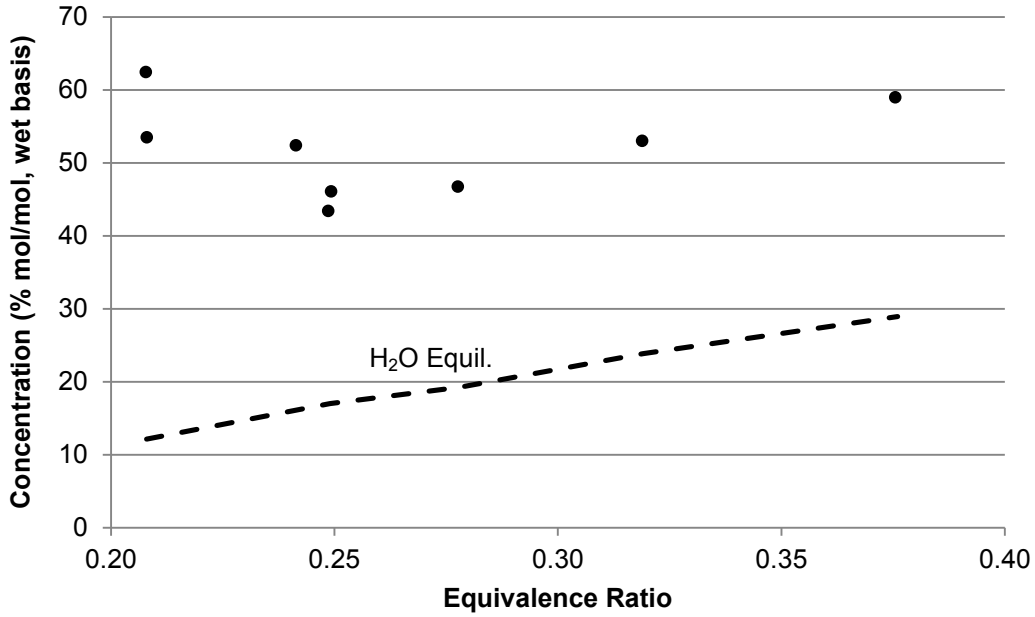

Figure 11. The effect of ER on the water content of the syngas. Fluidizing agent was 50 wt% O_2, balanced with steam. Values are reported on a % vol/vol wet, inert-free basis. The results from thermodynamic equilibrium modeling for the same reactor conditions are included for comparison.

The effect of ER on char content of the raw syngas is shown in Figure 12. In general, char content decreased with ER. This reflects conditions more closely approaching equilibrium as temperatures increased, as equilibrium predicted zero solid carbon. This result is in accord with expectations for higher levels of O_2 and H_2O in the gasifier and higher reactor temperature [22]. Surprising, the char concentration increased dramatically at the highest ER (0.38). This unexpected result may reflect

increasing elutriation of char due to increased attrition in the fluidized bed in combination with the higher superficial gas flow velocity through the reactor. It may also simply be an artifact of the decreased run time for this particular gasification trial, which was terminated after only 30 minutes of steady state operation due to bed agglomeration. Further experiments at high ER would be required to resolve this question.

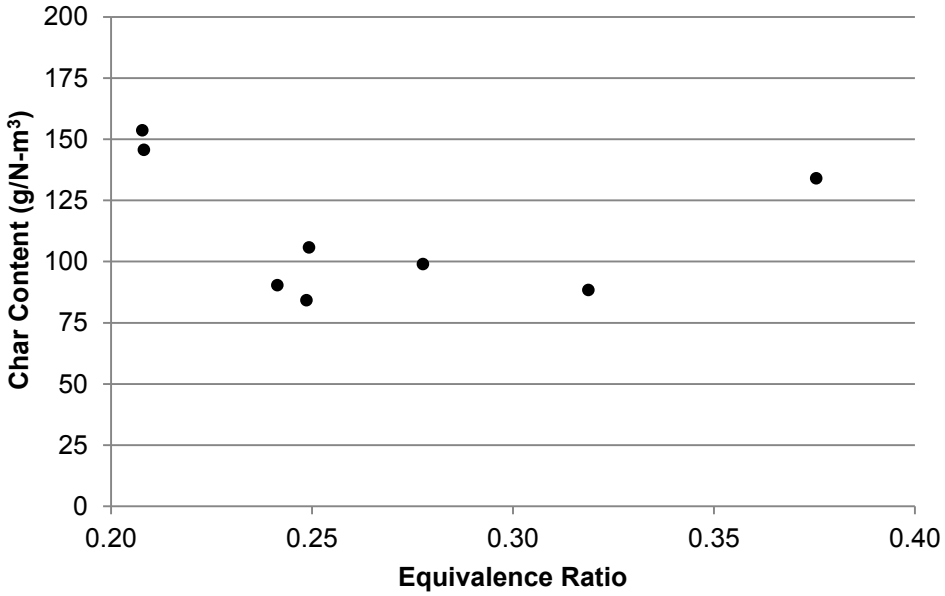

Figure 12. The effect of ER on the syngas char content. Fluidizing agent was 50 wt% O_2, balanced with steam. Values are reported on a dry, inert-free basis. The results from thermodynamic equilibrium modeling for the same reactor conditions demonstrated essentially no solid carbon production.

Equilibrium calculations predicted that molecular nitrogen (N_2) should be the only significant product of the FBN, amounting to about 0.45% vol/vol dry basis concentration for all ER levels. Despite this, significant amounts of NH_3 and HCN were measured for all ER levels tested. The effect of ER on the yield of NH_3 and HCN as a percentage of fuel bound nitrogen (FBN) in the biomass is illustrated in Figure 13. The yield of NH_3 declined from about 50% to 32% of FBN as ER increased from 0.21 to 0.32,

which corresponds to dry-basis concentrations in the syngas of 10,000 ppm and 5800 ppm, respectively. These concentrations are far higher than predicted for thermodynamic equilibrium, which indicates that the yield of NH_3 should be less than 0.17% (15 ppm concentration) for ER between 0.21 and 0.38.

This trend cannot be directly compared to previous gasification studies, which have not studied the response of nitrogenous species to ER for oxygen/steam environments. Most air-blown gasification studies using fluidized bed reactors have documented increasing concentrations of NH_3 as ER and/or temperature are increased [13, 24, 29, 52, 54]. We hypothesize that these generally upward trends are due to increased release of NH_3 from tar and char as carbon conversion increased, which is the subject of a future study. For the conditions explored in the present study, it appears that increases in ER and temperature accelerated NH_3 to N_2 conversion pathways more strongly than NH_3 release pathways. These reactions are predicted by homogeneous gas reaction kinetics; a detailed overview of these mechanisms has been presented by Leppälahti and Koljonen [55].

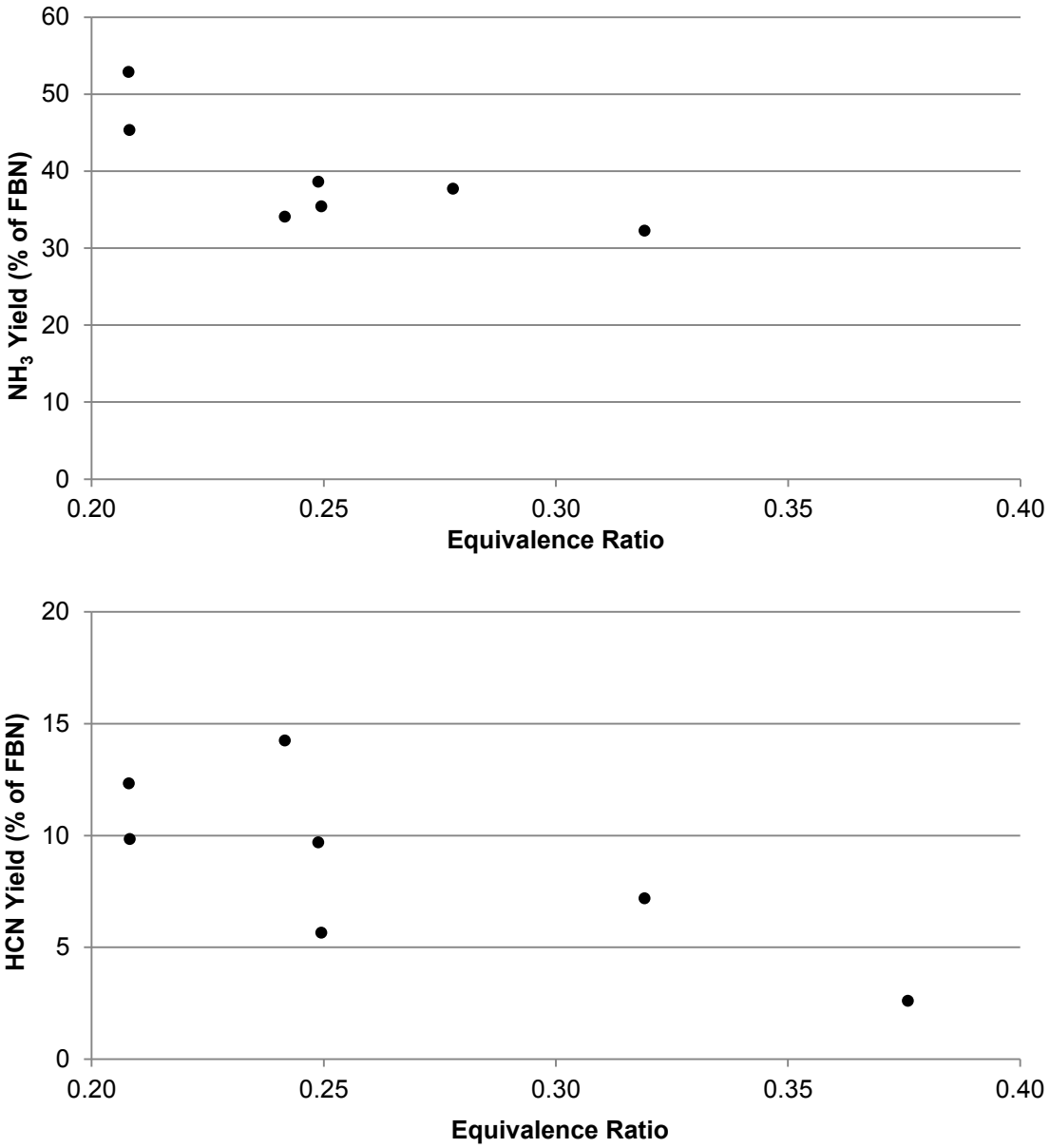

Figure 13. The effect of ER on the yields of NH_3 and HCN (as a percentage of the FBN). Fluidizing agent was 50 wt% O_2, balanced with steam.

The yield of HCN declined from 14% to 2.6% as ER was increased, corresponding to concentrations of 2500-440 ppm. The data showed large variations for the replicated runs at ER of 0.25. During the course of the study, it was discovered that aqueous cyanide samples are prone to aging, with significant declines in cyanide ion

concentrations over the course of several weeks of sample storage. Other researchers have previously noted this phenomenon [56]. In fact, the lowest measured HCN yield in the present study (one of the replications at ER of 0.25) was not analyzed until after nine weeks of storage in contrast to shorter delays for the other six samples. Even without assuming that this lowest HCN yield is an underestimate, an ANOVA statistical analysis on the linear regression of HCN yield data indicated a p-value of 0.045, indicating a likely inverse correlation between HCN yield and ER.

All of the HCN yields measured in the present study were higher by one to two orders of magnitude compared to three previous studies of HCN in biomass-derived syngas [24, 26, 36]. In contrast, three other studies have found HCN yields comparable to ours. Kurkela et al. [31] conducted straw gasification and found HCN yields of 4-14% of FBN. de Jong et al. [6, 7] conducted wood pellet and miscanthus gasification and found yields of 0-14%. We think this discrepancy is the result of inadequate sampling methodology used in the studies that reported much lower HCN yields, all of which used acidic impingers for trapping NH_3 upstream of HCN impingers. This series sampling overlooked the possibility that the NH_3 impinger absorbed both NH_3 and HCN. The importance of using separate sampling trains for these two forms of inorganic nitrogen in the syngas is the subject of a future paper.

Hydrogen cyanide concentrations of up to 2500 ppm in the syngas for switchgrass gasification have important safety implications. Concentrations as low as 50 ppm are considered immediately hazardous to human health [35]. The nitrogen content of the switchgrass featured in the present study is 0.91%, which is modest compared to

other potential gasification feedstocks such as distillers grains (5.52%) [11], sewage sludge (7.06%) [8], and verge grass (lawn clippings) (2.47%) [8].

The effect of ER on several other gasification performance parameters, including carbon conversion, gas yield, syngas energy content, and cold gas efficiency are shown in Table 3. Gas yields varied from 0.82 to 1.01 N-m^3/kg dry ash-free (daf) biomass, and generally increased with ER. The higher heating value (HHV) of the dry syngas varied from 8.8 to 13.2 MJ/N-m^3, with the greatest heating values occurring at the lowest ERs. Cold gas efficiency varied from 42-64% with the highest efficiency occurring at ERs between 0.24 and 0.28. Percent carbon conversion (%CC) was computed from the quantity of carbon fed to the reactor in the biomass (C_b) and the quantity of carbon in the produced char, C_c via Equation 5. Carbon conversion varied from 74-89% with no clear relationship to ER evident. Mass balance closures for the eight runs were 91-117%.

$$\%CC = \left(\frac{C_b - C_c}{C_b}\right) * 100\% \qquad \text{Eq 5}$$

Table 3. Other gasifier performance parameters that were measured. Fluidizing agent was 50 wt% O_2, balanced with steam. Data are reported on a dry inert-free basis.

Equivalence Ratio	Dry gas yield (N-m^3/kg daf)	HHV syngas (MJ/N-m^3)	Cold gas efficiency (%)	Carbon Conversion (%)
0.21	0.82	12.8	53	77
0.24	0.92	13.0	64	81
0.25	1.01	11.5	58	89
0.25	0.86	13.1	56	83
0.28	0.92	12.6	59	82
0.32	0.93	10.6	50	74
0.38	0.96	8.8	42	76
0.21	0.85	13.2	56	74

The gasification reactor was operated for approximately 200 hours for its initial commissioning and collection of the data reported in the present study. The reactor bed was disassembled upon conclusion of testing for inspection. There were no signs of refractory erosion, and very little refractory cracking had occurred.

Cleanup system performance

Particulate removal efficiency of the pair of gas cyclones was determined by comparing the amounts of char trapped in each of the two cyclone catches with the char concentration measured by isokinetic sampling at port A (Figure 4). The combined removal efficiency of the two cyclones varied from 91% to 97% for the tests conducted for this study. This is comparable to the generally recognized efficiency for well-designed gas cyclones [19].

The performance of the oil scrubber is shown in Table 4. It was found that nearly all of the heavy tars were removed by the tar scrubber, resulting in 60-80% overall tar removal efficiency. The novel SPME tar measurement method demonstrated that most of the unremoved tar was benzene. Smaller amounts of toluene, styrene, and indene were also found. Traces of the heavier naphthalenes were occasionally observed during unintentional deviations in the operating conditions of the tar scrubber.

Table 4. Tar removal performance of the oil scrubber during three select gasification tests.

Equivalence Ratio	Reactor Temperature (°C)	Raw syngas tar (g/N-m^3)			Total tar after oil scrubbing (g/N-m^3)	Tar Removal (%)
		Heavy	Light	Total		
0.21	705	43.4	12.7	56.1	8.8	84%
0.28	815	35.3	8.7	44.0	11.9	74%
0.32	880	29.1	13.7	42.8	8.5	80%

Operating the tar scrubber at lower temperature would likely have improved tar removal efficiency by increasing the number of light tars collected. In practice, this would have also condensed water in the oil, which is undesirable from the standpoint of recovering and disposing of the tars. More elaborate multi-stage tar removal systems have been developed, such as described by Zwart et al. [57], capable of removing up to 99% of light tars such as phenolic monomers and single-ring aromatic hydrocarbons, along with almost complete removal of heavy tar compounds. These systems are highly complex though, requiring three or more unit operations and multiple types of scrubbing liquids. The additional complexity may not be justified for all applications of syngas.

The performance of the sulfur and ammonia removal systems is reported in Table 5. All concentrations here are given on a wet syngas basis and including added gas since data on inputs of steam, N_2, and He were unavailable at the time these experiments were performed. The sulfur scrubbers performed very well, removing more than 99.9% of H_2S, and dropping the concentration of all sulfur species below 1 ppm. This compares well with other solid phase adsorption processes used commercially. For example, copper and zinc based materials remove more than 99% of sulfur compounds [19]. The sorbent system also removed COS and CS_2. As shown in Table 5, COS was reduced from 20-49 ppm to 0.3-0.6 ppm (97-99 % removal) and CS_2 was reduced from 0.2-1 ppm to less than 0.01 ppm (greater than 95 % removal). The sulfur removal system typically was operated for only a few hours at a time, because these tests were performed in conjunction with relatively short shakedown trials of the tar scrubbing system.

Table 5. Major sulfur compounds and NH_3 removal efficiency (wet basis, inerts included).

Compound	Before cleaning stage (ppm)	After cleaning stage (ppm)
H_2S	170-320	0.02-0.2
COS	20-49	0.3-0.6
CS_2	0.2-1	<0.01
NH_3	1270-2270	<0.9

The NH_3 scrubber was also very efficient, removing NH_3 by 99.9%, resulting in a final gas concentration of less than 1 ppm. This was consistent with previous studies, which showed that merely condensing water from syngas can remove up to 90% of NH_3 [12].

Conclusions

The use of electrical cartridge heaters embedded in ceramic insulation surrounding the fluidized bed of a 25 kg/h biomass gasifier was able to simulate adiabatic steam/oxygen gasification for temperatures as high 900°C. This allowed switchgrass to be gasified at ERs between 0.21 and 0.32. At higher ERs, the cartridge heaters were unable to operate at sufficiently high temperatures to produce a temperature barrier against heat loss from the gasifying biomass. Agglomeration of bed material also limited temperature and ER to about 900°C and 0.33 respectively, despite the use of limestone in the bed to ameliorate this phenomenon. The observed behavior of non-condensable gases suggested that methanation and the water-gas shift reaction became increasingly active as ER increased. This study is among the first to report NH_3 and HCN yields from FBN for oxygen and steam blown gasification of biomass. The yields of both were found to decrease with increasing ER. HCN was produced at concentrations that were as much as an order of magnitude larger than reported in

several previous studies of biomass gasification. This has important implications for syngas clean-up and safe operation of gasifiers using feedstocks with high FBN content.

The gas cleanup system was effective in reducing the level of contaminants in syngas although none of the unit operations had been optimized. The oil scrubber effectively removed all the heavy tars, resulting in overall tar removal efficiency as high as 80%. Light tars consisting of mostly phenolic monomers and single-ring aromatic compounds are difficult to remove without operating below the dew point of water, which can complicate recovery of tar for disposal. Both the sulfur and nitrogen scrubbing systems removed over 99.9% of these contaminants.

CHAPTER 3

RESOLVING INCONSISTENCIES IN MEASUREMENTS OF HYDROGEN CYANIDE IN SYNGAS

A paper published in *Fuel*, 2015, 140, 97-101

Karl M. Broer[1], Patrick A. Johnston[2], Alex Haag[3], Robert C. Brown[4]

Introduction

Nitrogen compounds in biomass-derived syngas are considered minor constituents in terms of their concentrations, but play an outsized role in determining the quality of syngas. Ammonia (NH_3) and hydrogen cyanide (HCN) represent NO_X precursors when syngas is burned [20], and they can poison catalysts during chemical synthesis [58].

Methods of measuring HCN

The most common method of measuring HCN in syngas is the wet chemical technique, which entails bubbling syngas through a basic solution, usually dilute sodium hydroxide (NaOH). Upon exposure to the base, HCN dissolves into the aqueous phase as cyanide ion (CN^-). Analysis of the aqueous solution is then conducted off-line. By

[1] Primary researcher and author
[2] Provided technical support with analytical equipment
[3] Provided laboratory and data preparation assistance
[4] Provided document editing assistance, serving as author for correspondence, and major professor

measuring the volume of syngas bubbled through the solution, the concentration of HCN in the syngas can be accurately determined.

Though laborious, the wet chemical technique has excellent sensitivity. Relatively low concentrations of HCN in the syngas can be detected by simply bubbling a larger volume of syngas through the liquid. Once the HCN is captured in aqueous form as CN^-, it is easily detected via an ion chromatograph (IC). This wet chemical technique is robust and tolerates relatively dirty gas streams. Steam in the syngas poses no problems as it can simply condense into the solutions. Some char and tar can also be tolerated. The char and part of the tar are insoluble in the collection solution and can be filtered out while preparing the samples for analysis.

It is also possible to measure HCN in syngas using Fourier transform infrared spectroscopy (FTIR) [6, 7] and gas chromatography in combination with a nitrogen chemiluminescence detector (NCD) [34]. These methods are advantageous because they allow direct measurement of HCN in the gas phase, avoiding the propagation of error that can arise from the multiple analytical steps associated with wet chemical methods. Direct measurement can also improve statistical power since more frequent sampling of the gas can be conducted. In contrast, wet chemical techniques are often too slow and laborious to allow collection of more than a few samples. Nevertheless, direct measurement of HCN can require sophisticated and expensive analytical instrumentation. Rigorous gas stream cleanup of tar and char must be conducted to avoid damaging instruments. Calibration of gas analysis instruments for HCN also presents a serious safety concern since calibration gases toxic to humans are required. The U.S. National Institute for Occupational Safety and Health (NIOSH) has designated

HCN as “Immediately Dangerous to Life and Health” (IDLH) at concentrations of only 50 ppm [35]. In comparison, the IDLH of carbon monoxide (CO) is 1200 ppm [59]. A calibration standard containing cyanide ion (CN^-) is also required for analysis of aqueous samples, but the small amounts of aqueous sodium cyanide standard required can be handled with relative ease and safety. Despite the attractive aspects of direct measurement, most measurements of HCN in syngas are made via the wet chemical technique due to its safety, high sensitivity, and robustness.

Approaches to sampling NH_3 and HCN

When syngas is burned, the NH_3 and HCN are both precursors to NO_X formation. It is very common to measure both in thermochemical studies of nitrogen compounds. NH_3 and HCN are both captured in aqueous solutions, although NH_3 requires an acidic solution and HCN requires a basic solution. Either two complete sampling trains are required, or NH_3 and HCN must be collected in turns. Collection in turns is commonly done to avoid the complexity of operating two sampling trains, but this doubles run time for experiments. Another disadvantage of collection in turns is that the syngas quality can drift between the two collection sessions.

Vriesman et. al [24] attempted simultaneous measurement of NH_3 and HCN in syngas from the gasification of miscanthus using one sampling train with NH_3 and HCN impingers arranged in series. The acidic impingers for trapping NH_3 were placed upstream of the basic impingers used to trap HCN. The raw syngas was lightly conditioned by removing particulate via hot ceramic filters before entering the impinger trains. There is no mention of tar removal upstream of the impingers.

Yu et al. [36] also performed simultaneous sample collection of NH_3 and HCN in their gasification study of three different biomass feedstocks. Like Vriesman et al. [24], acidic impingers were used to capture NH_3 followed by basic ones to capture HCN. Although no provisions for removing char and tar upstream of the impingers are described, the temperature of the slipstream line (200-250°C) was probably cool enough that some heavy tars dropped out prior to reaching the impingers. A relatively high gasification temperature was employed as well (900°C), which would have minimized char and tar yield.

The series configuration employed by these two groups simplified and accelerated the process of collecting nitrogen samples, but also allowed the possibility of HCN being unintentionally collected by the acidic solution used to capture NH_3. If this occurred, it would lead to underestimation of the true HCN concentration.

A third study by Zhou et al. [26] also employed acidic and basic impingers in series to capture NH_3 and HCN, respectively, along with extensive gas cleaning before the impingers. After removing particulate matter via a high temperature sintered metal filter, tars were removed via an acetone rinse. The syngas was then cooled using a heat exchanger before collection of NH_3 and HCN in impingers. The acetone scrubbing undoubtedly resulted in cleaner, tar-free nitrogen samples, but also introduced additional risk that HCN might have been removed by the acetone wash or by water condensation in the heat exchanger.

Evidence of unintentional removal of HCN

Evidence of unintentional removal of HCN in the studies by Vriesman et al. [24], Yu et al. [36], and Zhou et al. [26] is found by comparing their results to five similar gasification studies that measured HCN in isolation from acidic solutions and polar solvents (Table 6). From Table 6, it is clear that studies using acidic solutions prior to HCN sampling consistently reported much lower yields of HCN. The highest HCN yield reported in the three studies that used acidic impingers ahead of HCN sampling (Vriesman et al. [24], Yu et al. [36], and Zhou et al. [26]) was only 0.22%. In contrast, the three studies that avoided use of acidic impingers or solvent scrubbers ahead of HCN sampling (Kurkela et al. [31] and Abelha et al. [13, 23]) reported HCN yields that were one to two orders of magnitude higher. de Jong et al. [6, 7] used a third approach that directly measured HCN concentrations in syngas via FTIR and found HCN yields as high as 14%, far exceeding the yields reported when acidic impingers preceded HCN sampling.

Under reporting of HCN has been noted by Tan and Li [56]. Although they had previously used acidic and basic impingers in series [60], their more recent work acknowledged that HCN was sufficiently soluble in the acidic solutions to seriously underestimate HCN yield. No further information was given regarding the severity of this problem. Inspection of the HCN yields reported in their earlier work [60] varied from 1-22%, which does not obviously support or refute their concern about sampling errors.

Table 6. The following studies featured fluidized gasification of woody or herbaceous feedstocks, and measured HCN using different variants of wet chemical collection techniques or direct measurements using FTIR spectroscopy. Dramatically different results were obtained between studies collecting NH_3 and HCN in series and studies measuring them separately.

Reference	Feedstock(s)	Temperature (°C)	ER	HCN Yield (% of FBN)	Summary of collection setup
Vriesman et al. [24]	Miscanthus	700-800	0-0.25	0.01-0.06	NH_3 and HCN collection in series
Yu et al. [36]	Reed canary grass, miscanthus, willow	900	NA	0.10-0.22	NH_3 and HCN collection in series
Zhou et al. [26]	*Leucaena*	750-950	0.25	0.07-0.11	Acetone scrubber, then NH_3 and HCN collection in series
Kurkela et al. [31]	Wheat straw	670-885	0.25-0.35	4.5-14.2	NH_3 and HCN collection in parallel or in turns
Abelha et al. [13, 23]	Thistle, Eucalyptus, Sawdust	700-900	0	3-47	Tar and water condensation, then NH_3 and HCN collection in turns. Analysis of water condensates[1]
de Jong et al. [6, 7]	Wood, Miscanthus	NA	0.26-0.52	0-14	Direct measurement (FTIR spectroscopy)

[1] The setup used by Abelha et al. [13, 23] to condition the sampled syngas differed from the other authors in that both tar and water were condensed upstream of the HCN collection solutions. To address the possibility of HCN collecting in the condensate, Abhela et al. [13, 23] analyzed both the condensate and the impinger solutions, and added the results together.

We have performed a series of experiments to better understand the discrepancies in HCN measurements reported in the literature for gasification studies. We hypothesize that acidic and acetone impingers upstream of HCN sampling can dramatically reduce the amount of HCN reported for the gasification of nitrogenous feedstocks.

Materials and Methods

Feed system and reactor

A fluidized bed gasification reactor with an inner diameter of 38 mm and a height of 380 mm was used to generate syngas at nearly atmospheric pressure to study HCN collection techniques. The reactor included a volumetric feed system equipped with a two-auger system. The first auger was used to accurately dispense fuel and the second was operated at high rotational speed to stoke the fluidized bed. A small stream of inert gas purged the feed system to keep the injection auger and its contents cool. Switchgrass fuel was utilized for this study, which was prepared by drying followed by grinding and sieving the material to 212-500 μm in size. Ash content was measured using a Mettler Toledo TGA/DSC 1 Thermo-Gravimetric Analyzer. Analysis of carbon, hydrogen, and nitrogen content was conducted with an Elementar vario MICRO cube analyzer. Oxygen content was found by difference. Moisture content was determined by heating samples for 72 hours at 95°C in a Fisher Scientific IsoTemp Oven. The analysis results are shown in Table 7.

Table 7. Switchgrass fuel elemental analysis, moisture content, and ash content (uncertainty reflects 95% confidence interval). Elemental and ash content are on an as prepared basis.

C	44.6 ± 0.85
H	5.15 ± 0.11
N	0.48 ± 0.02
O (by difference)	44.0
Ash	5.8 ± 0.8
Moisture	4.89 ± 0.08

A perforated plate and heated plenum below the fluidized bed preheated and distributed incoming fluidizing gas. The plenum, bed, and freeboard of the reactor were enclosed in Watlow ceramic fiber heaters that provided both temperature-controlled heating and insulation. The fluidized bed consisted of 20 g of limestone obtained from ILC Resources (3301 106th Circle, Urbandale, IA USA) and 80 g of silica sand obtained from Badger Mining Corporation (409 South Church St., Berlin, WI USA). The bed material was replaced for each experiment. Both bed materials were sieved to 150-180 μm size. Upon exiting the fluidized bed reactor, the syngas passed through a pair of high efficiency gas cyclones in series, removing about 98% of all particulate. Syngas was maintained at 450°C until after the cyclones to prevent tar condensation. An illustration of the gasification system is shown in Figure 14.

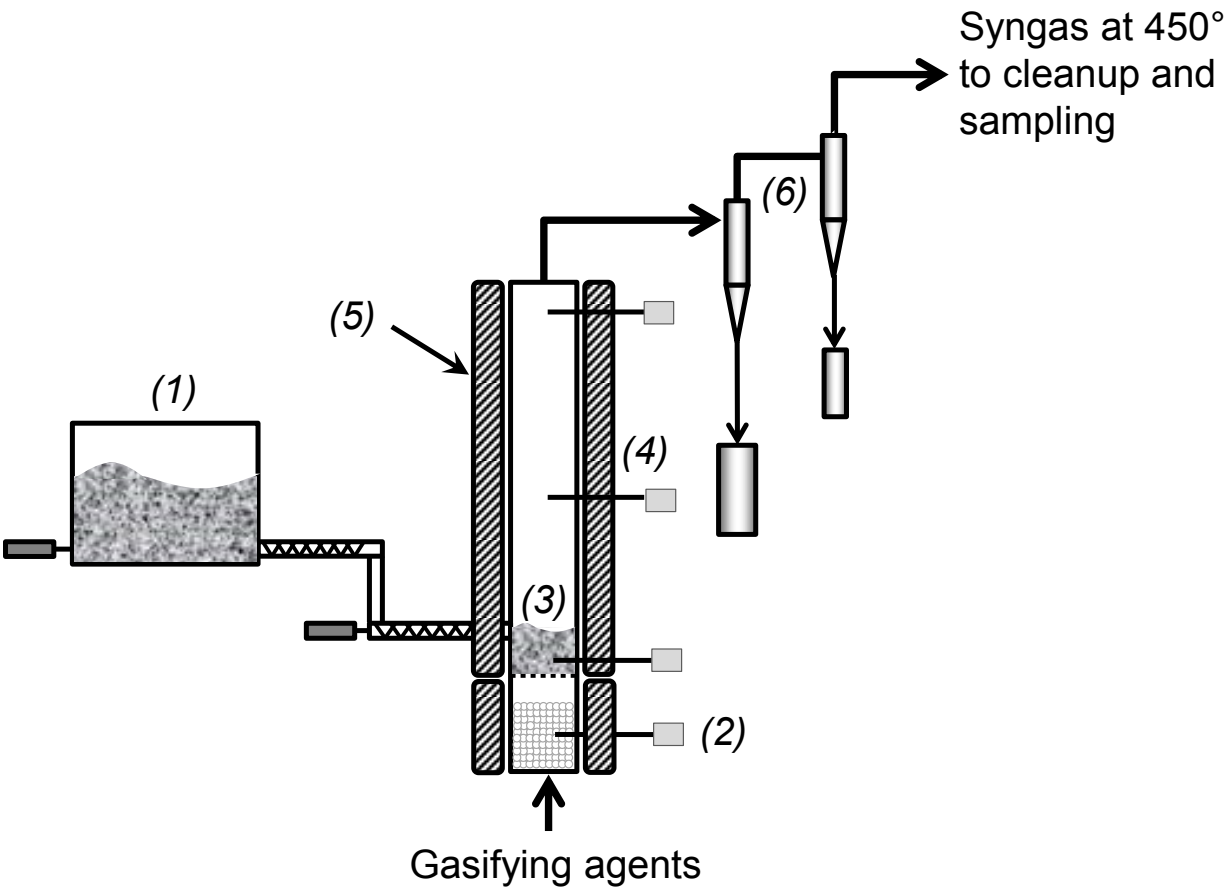

Figure 14. Reactor experimental setup consisted of: (1) variable rate feed system equipped with two augers, (2) plenum thermocouple probe and heated plenum packed with steel spheres, (3) fluidized bed comprised of silica sand and crushed limestone, (4) reactor body with three thermocouple probes, the middle for reactor temperature control, the other two for temperature monitoring, (5) Watlow ceramic heaters encasing the reactor to maintain temperature, and (6) two gas cyclones.

Gas cleanup and sampling

Following cyclonic removal of particulate matter, the syngas stream (1.6-1.8 SLPM) entered the gas clean-up and sampling system shown in Figure 15. Tar was removed from the syngas via an electrostatic precipitator (ESP). The outer wall of the ESP was maintained at 110°C by evenly applied heat tracing that was covered with insulation. A thermocouple affixed to the ESP wall was used for input to the temperature control system. The wall temperature was chosen to allow the syngas to

cool enough to condense all but the lightest tar compounds, but not water. Most of the syngas tar collected in the lower half of the ESP, with the walls of the upper half being nearly tar-free after each run, indicating high tar removal efficiency. Syngas exited the top of the ESP through a Tygon tube with an inner diameter of 13 mm and a length of 380 mm. The hose interfaced with an HCN sampling train consisting of four or five 500 mL glass impingers in series. The hose entering the first impinger was positioned to assure all condensate was collected in the impingers. The impingers were kept in a water ice bath prior to, during, and after use in order to absorb heat, condense water vapor, and facilitate dissolution of HCN. Downstream of the impingers, a desiccant canister and coalescing filter removed small amounts of aerosols escaping the impingers. After these traps, the dry syngas flowrate was measured by a Ritter drum-type total flow gas meter. A Varian CP-4900 micro gas chromatograph was used after the gas meter to monitor non-condensable gases.

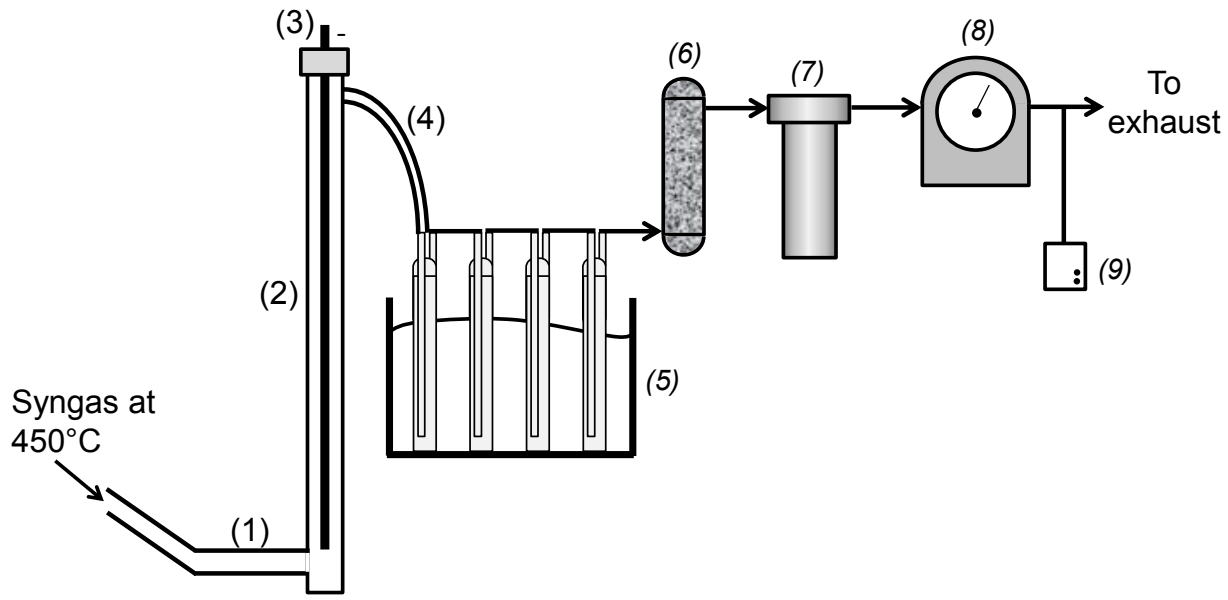

Figure 15. Setup for testing HCN measurement techniques: (1) 22 mm ID stainless steel tubing at 150°C, (2) 36 mm ID electrostatic precipitator (ESP) case, electrically grounded, and heat traced to 110°C, (3) ESP electrode mounted in an insulator, and operated at a negative voltage of 15-17 kV, (4) 13 mm ID Tygon tubing at room temperature, curving steeply downward to allow water condensation to run into impingers, (5) either four or five 500 mL glass impingers in series in a water-ice bath, with each containing 200 mL of collection solution, (6) desiccant canister for water aerosol removal, (7) coalescing filter canister for final gas cleaning, (8) Ritter drum-type total flow gas meter, and (9) Varian CP-4900 micro gas chromatograph.

Experimental procedure

Two gasification test runs were conducted for this study. Prior to each run, the gasification reactor, ESP, and all temperature controlled lines were electrically preheated for at least one hour before feeding biomass into the reactor to achieve stable temperatures. After preheating, the final operating conditions were set, and gasification was allowed to occur for 20 minutes to achieve stable operation after which sampling for HCN commenced. The operating conditions used for each of the two test runs are summarized in Table 8.

Table 8. A summary of the fluidized bed operating conditions used to create syngas for testing HCN measurement techniques. Fluidization ratio was computed from the ratio of actual gas superficial velocity (neglecting biomass volatiles) to the minimum fluidization velocity. Minimum fluidization velocity was determined from fluidization tests performed after the reactor had been electrically preheated, but before biomass feeding commenced.

	Acidic Impinger	Acetone Impinger
Fuel Type	Switchgrass	Switchgrass
Fuel Feed Rate	115 g/h	115 g/h
Equivalence Ratio	0	0.25
Reactor Temperature	780°C	780°C
Bed Makeup	20g limestone 80g silica sand	20g limestone 80g silica sand
Bed Particle Size	150-180 μm	150-180 μm
Fluidization Ratio	3.2	3.2
Feeder Purge	0.10 SLPM CO_2	0.10 SLPM N_2
Bed Fluidizing Agents	1.0 SLPM CO_2	0.63 SLPM N_2 0.41 SLPM O_2
Syngas Flowrate	1.6 SLPM	1.8 SLPM

The first run investigated the effect of using an acidic impinger upstream of HCN measurements. Once the gasifier reached steady state, two 30-minute HCN collection sessions were carried out, one designated as “control” and one as “acidic impinger.” For the control session, four impingers each filled with 200 mL of 100 mM NaOH solution were used. For the acidic impinger session, five impingers were employed. The first impinger was filled with 200 mL of 100 mM H_2SO_4, and the other four impingers were filled with 200 mL of 100 mM NaOH.

The second gasification run investigated the effect of acetone scrubbing upstream of HCN sampling. For the control session HCN was collected using four impingers, each filled with 200 mL of 100 mM NaOH. For the acetone impinger session, five impingers

were used, the first filled with 200 mL of acetone, and the following four each filled with 200 mL of 100 mM NaOH.

After HCN collection was complete, the impingers were immediately sealed with parafilm and stored on ice for 30-60 minutes until disassembly could be carried out. Following disassembly, the contents of each impinger was transferred to separate HDPE sample bottles with tight fitting lids. The impinger bottle and stopper containing H_2SO_4 solution was washed into its sample bottle using small amounts of 18.2 MΩ DI water. All other impinger bottles and stoppers were rinsed into their respective sample bottles using 100 mM NaOH. The H_2SO_4 sample was then diluted up to 500 mL using 18.2 MΩ DI water and a volumetric flask. All other samples were diluted to 500 mL using 100 mM NaOH. The samples were then kept at 0-5°C until analysis.

Aqueous sample analysis

Each sample was agitated prior to extracting approximately 5 mL and filtering it using a Whatman 0.45 µm syringe tip filter. The filtrate was then used to prepare 1500 µL samples for analysis. Dilutions were conducted according to the anticipated CN^- concentration in order to satisfy the detection range of the analytic equipment. For example, a 10-fold dilution would have been conducted by dispensing 150 µL of filtered sample and 1350 µL of NaOH solution into the analysis vial. An Eppendorf Multipipette and disposable tips of assorted sizes were used to dispense and dilute samples. Tip sizes were selected carefully in order to maximize accuracy. Three analysis vials were prepared in an identical fashion from each 500 mL sample in order to replicate vial

preparation. The samples collected in acetone and H_2SO_4 were handled in the same way as the samples collected in NaOH.

Once vial preparation was complete, the analysis vials were agitated and loaded into a Dionex ICS-3000 ion chromatograph (IC) with an auto-sampler. In advance of analysis, the IC was calibrated from 1.0 to 10 ppm using standards prepared from certified 1000 ppm aqueous CN^- solution. Each sample vial was sampled by the IC three times, for a total of nine measurements per original collection impinger. The order in which each vial was analyzed was randomized. If vials were found to be out of the calibration range, new vials were prepared from the 500 mL sample bottles and re-analyzed using revised dilution ratios until results inside the calibration range were obtained. Sample bottles with low anticipated concentrations of HCN (less than 10 ppm) were filtered and dispensed straight into IC vials undiluted. Samples containing less than 1 ppm of CN^- fell below detection range. These samples could be neglected since concentrations this low correspond to less than 0.5 mg of collected CN^-, which is negligible compared to the approximately 20-60 mg of CN^- typically collected in the experiments.

The result for each test represented the mean of nine IC readings. The error bars in the graphed data signify 95% confidence intervals about the mean based on a two-tailed test using the Student-t distribution for eight degrees of freedom.

Results and Discussion

The results of the test on the effect of an acidic impinger upstream of the basic impingers are shown in Figure 16. For the control session, 18 mg of CN^- was found in the

first impinger and 1.6 mg in the second. Amounts collected in the third and fourth impinger were below detection range, and are not depicted. For the acidic impinger session, the amount of CN^- in the first basic impinger dropped to 1.4 mg, and the second basic impinger fell below detection range. When the solution in the acidic impinger was analyzed, 21 mg of CN^- was found. This amount is statistically equal to the difference in CN^- found in the basic impingers for the control and acidic impinger sessions. This result confirms that inclusion of acidic impingers to collect NH_3 upstream of basic impingers to collect HCN will underreport HCN. In fact, a single acidic impinger captured 93% of the HCN, resulting in gross underreporting of HCN. Unfortunately, most researchers have used two or more acidic impingers to assure that all NH_3 is collected. Our results suggest that such setups would result in underestimation of true HCN concentrations by approximately two orders of magnitude.

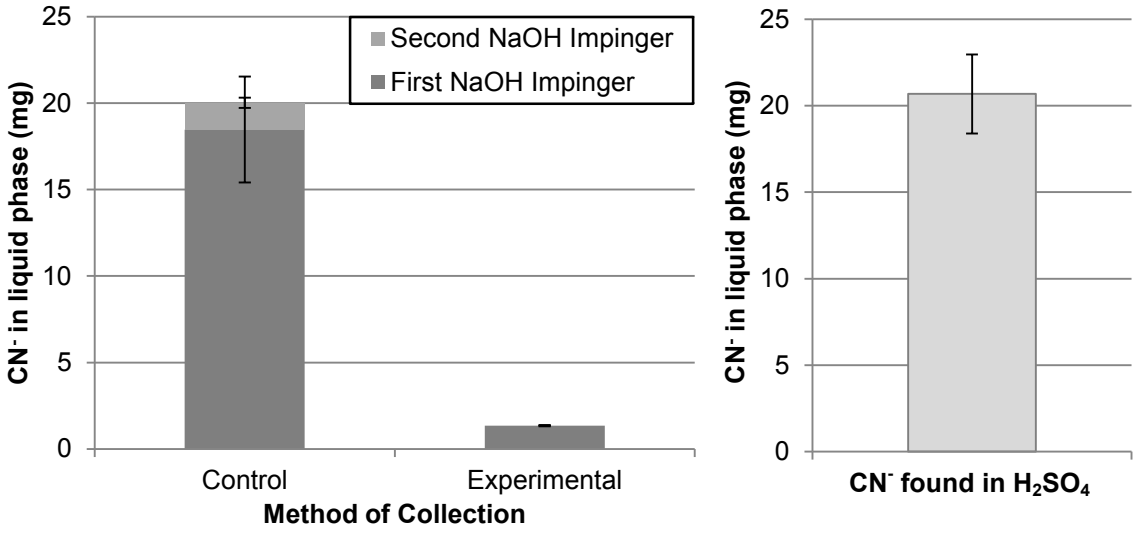

Figure 16. When an H_2SO_4 impinger was added upstream of the series of 100 mM NaOH impingers, the total dissolved HCN concentration dropped 93% compared to the control. Dissolved HCN dropped from 19 mg to 1.4 mg in the first impinger, and from 1.6 mg to undetectable levels in the second NaOH impinger. Analysis of the H_2SO_4 itself found 21 mg, confirming that the missing HCN had been trapped by the H_2SO_4.

The results of the test on the effect of an acetone impinger upstream of the basic impingers are shown in Figure 17. The control session (no acetone impinger) resulted in 58 mg of CN^- being trapped in the first impinger and 5.5 mg in the second. The amount of CN^- in the third and fourth impingers was below detection limits and is not depicted. For the acetone impinger session, the concentration of CN^- in the first basic impinger was only 1.2 ppm. The concentrations of CN^- in the three remaining basic impingers were below the detection range. The acetone impinger collected 61 mg of CN^-, which is statistically equal to the difference in CN^- found in the basic impingers for the control and acetone impinger sessions. A single acetone impinger captured over 99% of the HCN in the syngas, resulting in dramatic under reporting of HCN from analysis of the basic impingers.

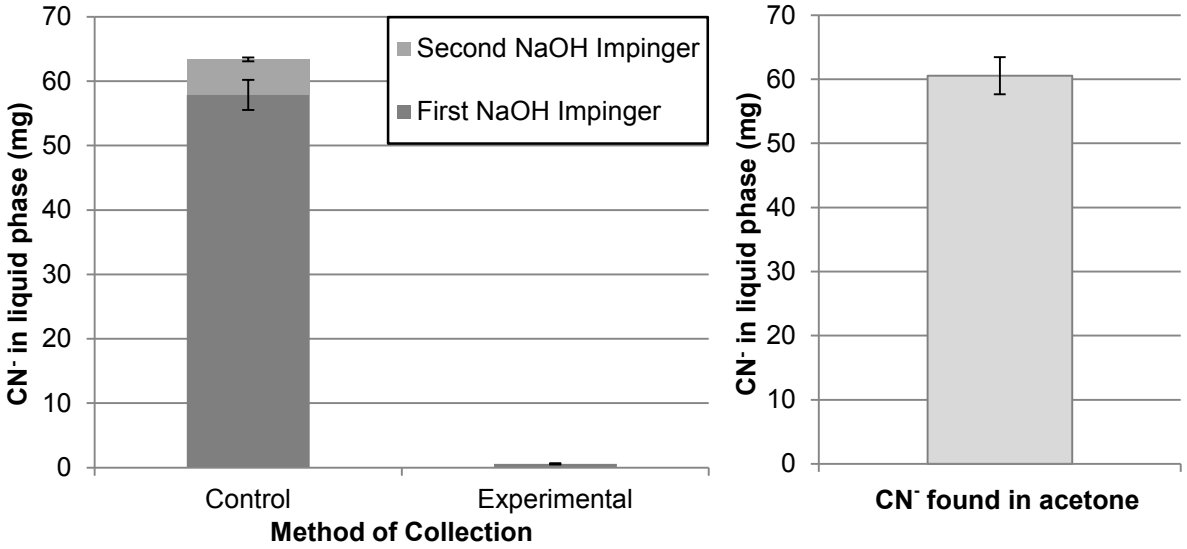

Figure 17. When an acetone impinger was added upstream of the series of 100 mM NaOH impingers, the total dissolved HCN concentration dropped 99%. Dissolved HCN dropped from 58 mg to 0.58 mg in the first impinger, and from 5.5 mg to undetectable levels in the second NaOH impinger. Analysis of the acetone itself found 61 mg, confirming that the missing HCN was captured by the acetone.

Since both basic and acidic impingers were able to remove HCN with comparable efficiency, this raises the possibility that condensation of water from syngas at any pH will remove significant amounts of HCN. Condensation results in liquid water being in close proximity to the syngas, on both pipe surfaces and as water aerosols, providing large surface areas for HCN to migrate into the condensate. Some evidence of this possibility is found in the published literature. Pinto et al. [12] found that 90% of the NH_3 in syngas was removed from syngas simply by condensing the water in syngas. The precautions taken by Abelha et al. [13, 23] to include water condensed upstream of the basic impingers in their analysis of HCN demonstrates that they were conscious of this possibility. Accordingly, the temperatures of all char filters, tar condensers, and syngas sampling lines upstream of HCN collection should be kept above the water dew point of the syngas in order to avoid condensation and potential loss of HCN. The results of any HCN study where syngas is allowed to come into contact with water upstream of HCN collection should be interpreted with caution.

Conclusions

Previous studies of gasification have been plagued by inconsistencies in measuring the concentrations of HCN in syngas, which often vary by orders of magnitude. This inconsistency has hampered investigations into the fate of FBN during gasification. The present study traces the problem to contacting syngas with solvents prior to intentional removal of HCN. This can occur in acidic solutions used to remove NH_3, or acetone solutions used to remove tar. To eliminate this problem, we recommend avoiding placement of NH_3 collecting impingers upstream of where HCN is to be

sampled. This type of configuration can be avoided by collecting NH_3 and HCN in turns, or by collecting the two species using separate sampling lines. Hydrogen cyanide can also be unintentionally removed when polar solvents are used to remove tar ahead of HCN sampling. To avoid this problem, a solvent-free tar removal method should be employed. Meticulous attention should also be given to temperature control to avoid water condensation in sample lines, tar condensers, and any other components upstream of HCN sampling.

CHAPTER 4

PARTITIONING OF NITROGEN DURING BIOMASS GASIFICATION: PART 1. THE EFFECT OF TEMPERATURE

In preparation for submission to *Applied Energy*

Karl M. Broer[1], Robert C. Brown[2]

Introduction

Gasification is attractive for its ability to transform carbonaceous solids into a variety of energy products including process heat, electrical power, and liquid transportation fuels. Gasification is attractive compared to other common biomass conversion technologies in that it can efficiently utilize lignin and mixed wastes which are usually inaccessible to biological based processes.

Most biomass feedstocks contain small amounts of nitrogen originating mostly from protein, but also from nitrates, ammonium, chlorophyll, and nucleic acids. Nitrogen generally comprises a relatively small portion of the overall makeup of the biomass (0.05 to 2 wt% for most fuels) [22]. Despite this, fuel bound nitrogen (FBN) has a large impact on syngas quality. Upon gasification, FBN transforms mainly into diatomic nitrogen (N_2), ammonia (NH_3), hydrogen cyanide (HCN), char bound nitrogen (char-N), and tar bound nitrogen (tar-N). NH_3 and HCN are the most problematic of these five forms. Both are precursors to NO_X formation during

[1] Primary researcher and author
[2] Provided document editing assistance, serving as author for correspondence, and major professor

combustion of syngas for heat and power applications [5]. They also poison catalysts used to upgrade syngas into fuels and chemicals [16, 21].

Herbaceous feedstock products such as miscanthus, switchgrass, wheat straw, and corn stover can easily contain over 0.5 wt% nitrogen, which is enough to generate NH_3 and HCN in concentrations on the order of 5000 ppm and 1000 ppm, respectively [61]. Much larger concentrations can be expected from gasification of some waste feedstocks such as grass clippings, (2.47%) [8] sewage sludge, (3.7-7.4%) [8, 12, 13], and *leucaena* (2.51%) [26]. When these fuels are gasified, dry basis concentrations of NH_3 in the syngas can easily exceed 10,000 ppm [8, 12]. Most studies have found the yield of NH_3 to increase with gasification temperature. Rosen et al. [62] conducted birch gasification in air and found that NH_3 yield on the basis of FBN increased from 0-13% to 32-57% as gasification temperature increased from 700°C to 900°C. Small increases in NH_3 yield were also observed by Vriesman et al. [24] as gasification temperature increased from 700°C to 800°C.

Availability of data on HCN is sparse for continuous gasification of biomass. The data that are available suggest that HCN yields are generally less than NH_3 yields, but certainly not insignificant [6, 7, 31]. A few research results even report HCN yields that are higher than NH_3 yields, such as the study by Abhela et al. [13] where sawdust was gasified at 700-900°C and an ER of zero in a 300 g/h fluidized bed reactor. HCN yields from FBN increased rapidly with temperature, reaching 47% at 900°C. Such yields are remarkable high, and would translate to around 20,000 ppm dry basis HCN for air gasification of a high nitrogen content feedstock. HCN yields on the order of 1-15% of the FBN are more typical, but the results of Abhela et al. [13] and others [6, 7, 31] support the contention that HCN is usually a significant

nitrogen product in syngas. Despite this, the difficulty of measuring HCN has made some authors unaware of its importance [63]. The technically challenging and laborious techniques for measuring it have resulted in accurate continuous gasification HCN measurements being available for only a relatively narrow range of fuels and operating conditions.

Researchers have attempted to predict concentrations of some of the nitrogen bearing products of gasification through models based on chemical kinetics [6, 7, 38, 39]. Most published models have been successful in predicting NH_3 over small ranges of operating conditions and for selected fuels, but they demonstrate serious shortfalls when applied to wider operating ranges and more diverse feedstocks. Modeling efforts to predict HCN, char-N, and tar-N are rare, due to the conventional view that they play minor roles in gasification.

One of the most challenging aspects of chemical kinetic modeling is determining the initial conditions for gas-phase and gas-solid reactions after biomass devolatilization. This is particularly difficult for the nitrogen bearing compounds. In most kinetic modeling approaches, the model does not consider nitrogen species as they occur in the biomass, since their chemical structures are complex, heterogeneous, and not thoroughly understood. Instead the primary gaseous products of pyrolysis are taken as the initial composition of the reacting mixture. Initial amounts of these species are typically found either by assumption or via devolatilization experiments conducted in the absence of oxygen. Chen et al. [38], Liu and Gibbs [39], and an early study by de Jong et al. [7] all employed this approach to kinetic modeling. A later study by de Jong et al. [6] incorporated an analytical model of devolatilization based on experiments in a thermogravimetric

analyzer coupled with a Fourier Transform Infrared Spectrometer (TG-FTIR). Although this second approach offered better predictions of light gaseous nitrogen species for subsequent (secondary) gas phase reactions, char-N and tar-N were still excluded from the model.

After determining devolatilization products, the models either used global (Chen et al. [38] and Liu and Gibbs [39]) or fundamental (de Jong et al. [6, 7]) combustion reaction networks to model homogenous reactions of the low molecular weight gas phase species. These reaction networks tend to be well developed, and include many different species. It is relatively easy to apply homogenous reactions to a modeling effort. Combustion studies providing kinetic rate parameters for global and fundamental reactions of simple carbon, oxygen, hydrogen, and nitrogen species have been widely published, and both types of reactions are frequently recruited for modeling gasification reactions [64, 65].

In contrast to the low molecular weight species, it is much more difficult to model evolution of the char and tar. Models generally contain relatively few char and tar reactions compared to the homogeneous gas chemistry. There is also much less agreement on the proper mechanisms and rate parameters for the reactions in which tar and char participate. Tar is typically dealt with by referencing literature to determine how much tar might be produced by primary pyrolysis, and then assuming that it undergoes a single step secondary cracking reaction which converts it to a few common carbon, oxygen, and hydrogen bearing species. To model char gasification, the char yield from primary pyrolysis is used as an initial condition, and then char destruction rates are modeled via char combustion and gasification reactions. These reactions are usually assumed to be mass transfer limited, and

therefore depend on char particle properties. Models sometimes also include reactions catalyzed by the char, which follow similarly complex mass transfer limited rate equations. In summary, uncertainties about the exact properties of the char and tar make it difficult to model the reactions in which they participate.

These difficulties have often deterred modelers from considering the possibility that significant amounts of nitrogen might be bound in the char and tar. Among the four kinetic models presented by Chen et al. [38], Liu and Gibbs [39], and de Jong et al. [6, 7], tar-N was neglected by all four studies, and char-N was considered by only Chen et al. [38] and Liu and Gibbs [39]. Experimental literature does not always support the effectiveness of neglecting char-N and tar-N. Char-N yields reported by Zhou et al. [26] and Yu et al. [36] were below 10%, but other yields such as those reported by Vriesman et al. [24] were higher (14.0-21.0%). The char-N yield results of Abelha et al. [23] for cardoon gasification are the highest, and report char-N yields of 12% and 32%. The results of Abhela et al. [23] may be particularly relevant toward indicating initial char-N yield in the volatiles because the residence time was short (approximately 2 s), and the reactor was operated in the absence of oxygen (ER=0). These conditions would tend to produce char-N results more representative of the devolatilization products than the other studies since the lack of O_2 and residence time would have minimized char oxidation and gasification reactions.

Measurements of tar-N yields in the literature are rarer. The few that are available give conflicting evidence of whether tar-N produced by devolatilization is significant or not. Yu et al. [36] reported yields of tar-N from two woody feedstocks and two herbaceous feedstocks to be low (0.37-1.3% of FBN). Kurkela et al. [31] also

reported low tar-N yields for straw gasification (0.8-1.8% of FBN). While these results seem low enough to neglect tar-N in modeling reactions of FBN, the gasification conditions in these studies would have encouraged significant conversion of tars via secondary reactions after devolatilization. It is possible that much of the original tar-N from primary pyrolysis has already been converted into gaseous species such as HCN and NH_3. If this were the case, tar-N could be an important constituent of the volatiles used for the initial conditions for models, and an important participant in nitrogen reactions. A more recent study by Aznar et al. [25] hints that this may be the case. Aznar et al. [25] gasified sewage sludge with a relatively short residence time (approximately 2 s) at an ER of zero and found tar-N yields of 5.9-20.6%. Caution should be taken in assuming that these yields would also occur for wood and energy crop feedstocks, since sewage sludge also has extremely high ash and volatile content, perhaps leading to unusual nitrogen partitioning behavior. A more interesting possible explanation would be that the short residence time and absence of oxygen applied by Aznar et al. [25] are leading to the products being a more accurate reflection of the devolatilization products compared to other gasification studies. Experimental work is needed to verify if similar results could be produced for equivalent short residence time studies with an ER of zero for biomass resources with more moderate properties. If char-N and tar-N are significant sources of nitrogen-bearing products of devolatilization, it would be important for kinetic models to account for them in the initial conditions and provide reactions to model their subsequent evolution.

A few studies have also found that FBN may convert to nitric oxide (NO) and isocyanic acid (HNCO). Significant conversion of FBN in miscanthus to HNCO was

found by de Jong et al. [37] for slow heating rate high temperature devolatilization of miscanthus using TG-FTIR. Significant NO *yields*, but low NO *concentrations* were reported by Van Huynh and Kong [20] and Zhou et al. [26]. Both groups of authors utilized wood fuels with extremely low nitrogen content (0.03% and 0.05% respectively). Other studies appear to completely refute the significance of NO and HNCO. Leppälahti and Kurkela [30] experimented with injecting bottled NO gas into a fluidized bed gasifier processing peat fuel, and were unable to detect any NO present in the final syngas product, suggesting that NO quickly evolves onwards into other species. de Jong et al. [6] were unable to detect NO or HNCO via FTIR when they conducted pilot scale gasification of miscanthus. Further study is needed to learn about what role these compounds may play in the evolution of FBN during gasification, but analyzing for their presence was beyond the resources of the present study.

Materials and Methods

Switchgrass was harvested by Chariton Valley RC&D, Inc. near Centerville, Iowa, USA, baled into 1.83 m diameter round bales, and transported to Iowa State University. The bales were disintegrated and coarsely chopped using a Vermeer BP-8000 whole bale grinder. The material was ground with an Art's Way hammer mill and 6.4 mm screen, and then ground again using a Retsch SM 2000 knife mill with a 1000 μm screen. The material was sieved, retaining particles 212-500 μm in diameter. Several biomass analyses were then conducted on the retained biomass. Wet basis moisture content was determined by oven drying for 72 hours at 95°C in a

Fisher Scientific IsoTemp Oven. Ash content was determined using a Mettler Toledo TGA/DSC 1 Thermo-Gravimetric Analyzer. Ultimate analysis was conducted using an Elementar vario MICRO cube analyzer. The results of these analyses are found in Table 9. Amino acid profile analysis was obtained from the Agricultural Experiment Station Chemical Laboratories at the University of Missouri (Columbia, MO, USA), and is shown in Table 10.

Table 9. Switchgrass ultimate analysis, ash, and moisture content after feedstock preparation. Feedstock moisture is included in the elemental analysis. Uncertainties reflect a 95% confidence interval.

C	45.98 ± 0.52
H	5.21 ± 0.07
N	0.49 ± 0.02
O (by difference)	44.8
Ash	3.5 ± 0.4
Moisture	4.63 ± 0.21

Table 10. Complete amino acid profile of the switchgrass measured after feedstock preparation (wt%, as received).

Taurine	0.10
Hydroxyproline	0.03
Aspartic Acid	0.24
Threonine	0.13
Serine	0.12
Glutamic Acid	0.27
Proline	0.13
Lanthionine	0.00
Glycine	0.15
Alanine	0.17
Cysteine	0.03
Valine	0.17
Methionine	0.03
Isoleucine	0.11
Leucine	0.20
Tyrosine	0.05
Phenylalanine	0.14
Hydroxylysine	0.02
Ornithine	0.00
Lysine	0.11
Histidine	0.04
Arginine	0.10
Tryptophan	< 0.04

Gasification tests were performed in a reactor consisting of a stainless steel pipe with an internal diameter of 38 mm and height of 340 mm. As illustrated in Figure 18, the reactor body was encased in Watlow ceramic heaters, and temperature controlled via a thermocouple probe located at the center of the reactor. The reactor was operated at atmospheric pressure for all tests. The reactor contained a fixed bed consisting of 100 g of 425-600 μm diameter silica sand obtained from Badger Mining Corporation (409 South Church St., Berlin, WI USA). The sand was refreshed before each experiment. The reactor was fed via a two auger feed system consisting of first a slow moving, variable speed metering auger calibrated to feed fuel at 100 g/h, and then a faster moving injection auger designed to sweep fuel

quickly into the reactor. The tip of the injection auger was even with the top of the sand bed. Fuel in the feed hopper was weighed before and after each run in order to more exactly determine feed rates for mass balance purposes. Below the fixed sand bed was a perforated plate and gas distribution plenum of the same diameter as the reactor. The plenum was enclosed in Watlow ceramic electrical heaters and temperature controlled via a separate control loop and thermocouple. The plenum and reactor were operated at the same temperature for all tests. Steel spheres were packed into the 170 mm long plenum to facilitate heat transfer to incoming gases.

Syngas exited the reactor and was immediately passed through a pair of gas cyclones with a collective char removal efficiency of greater than 99%. The syngas then passed to the gas analysis system illustrated in Figure 19. An electrostatic precipitator 940 mm tall and 36 mm in diameter was used to remove and measure heavy tar. Typical operating voltage for the ESP was 14 kV. The syngas exited at the top of the ESP via a 13 mm inner diameter by 380 mm long Tygon hose connected to a set of three 500 mL glass impingers installed in series. The hose was positioned to slope steeply downward into the impingers to allow aqueous condensates to run down into the impingers. The impingers contained either 200 mL of 100 mM sodium hydroxide (for collecting HCN) or 5% hydrochloric acid (for collecting NH_3) in each bottle. The impingers were immersed in a water-ice bath to absorb heat from the syngas, facilitate water condensation, and maximize collection efficiency of the nitrogen species. A desiccant canister and coalescing filter were then used downstream of the impingers to act as final guard filters. After all filtration was complete, the gas stream was sent through a Ritter rotating drum-type gas flowmeter to measure gas yields, followed by a Varian CP-4900 micro gas chromatograph

(mGC). The mGC measured permanent gas composition every four minutes throughout all tests. The mGC results were mainly used to verify that steady state operation had been reached, and to determine syngas average molecular weight for mass balance purposes.

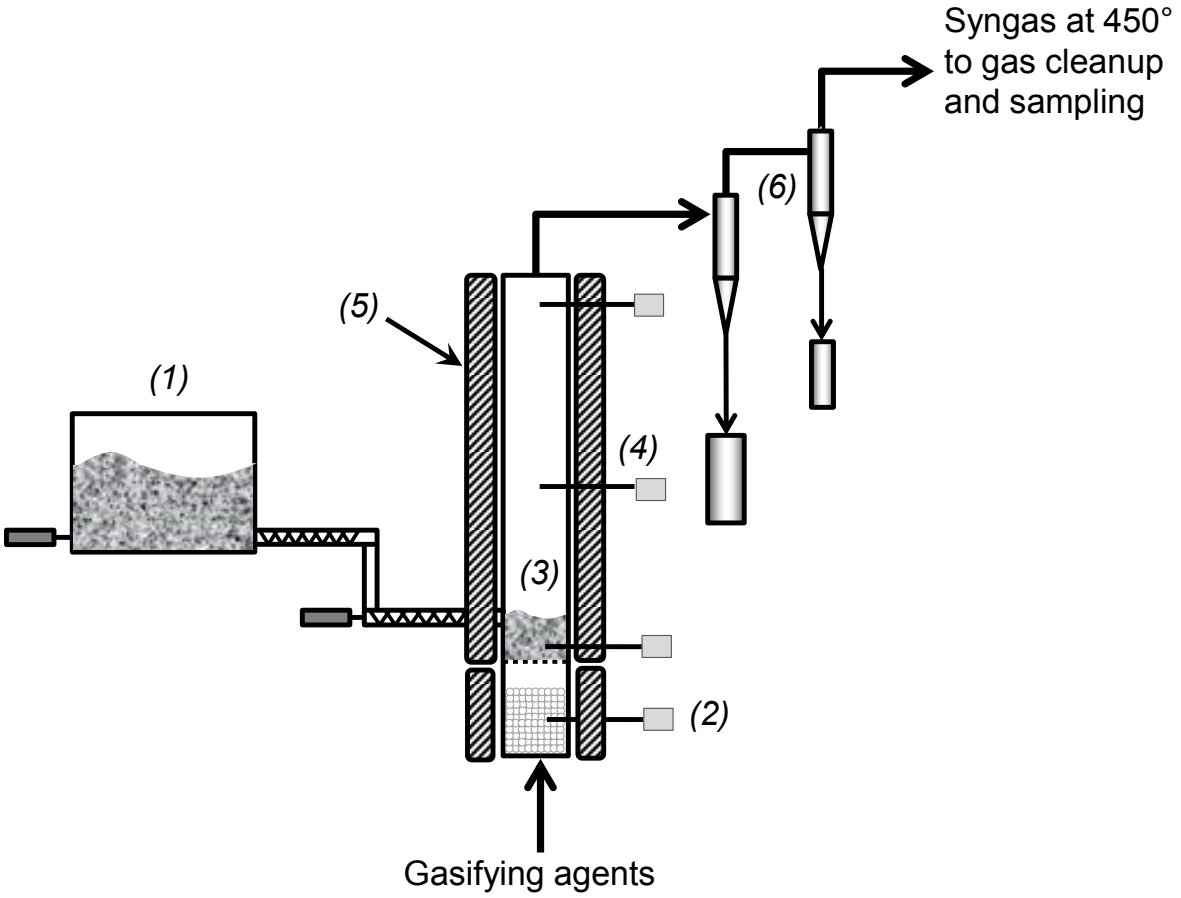

Figure 18. Gasification reactor consisting of: (1) Volumetric feed system calibrated for 100 g/h switchgrass feed rate, (2) thermocouple probe and temperature controlled plenum packed with steel spheres, (3) 100 g of silica sand fixed bed, (4) three thermocouple probes, the middle one for reactor temperature control, the upper and lower for temperature monitoring, (5) Watlow ceramic heaters encasing the reactor to maintain temperature, (6) two gas cyclones heat traced and insulated to 450° for particulate removal.

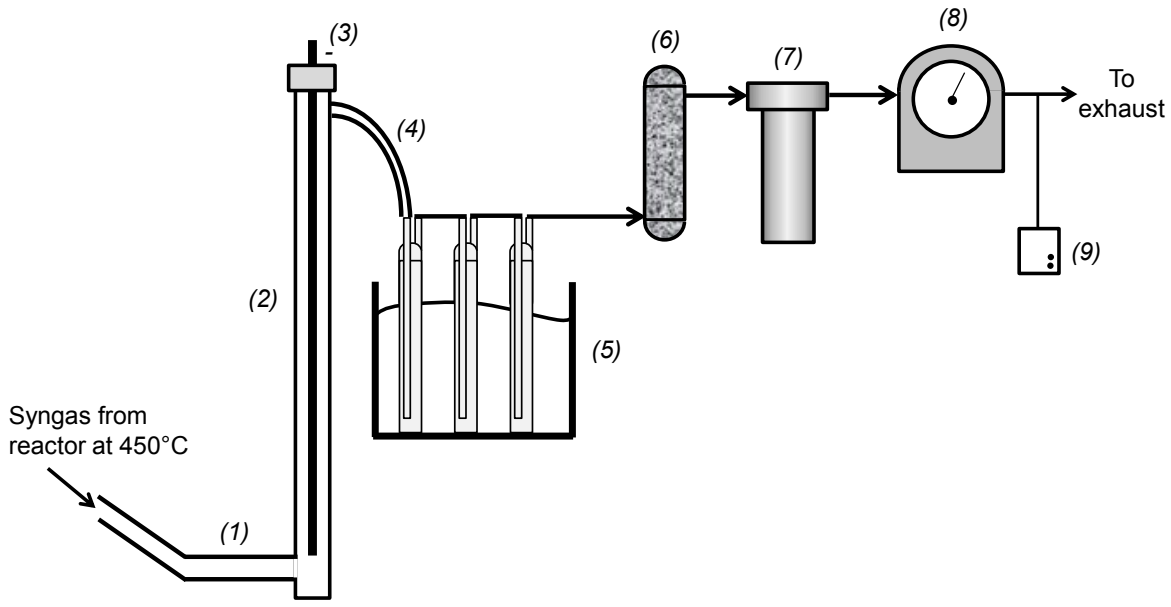

Figure 19. Apparatus for collecting tar, NH_3, and HCN samples: (1) 22 mm ID stainless steel tubing at 150°C, (2) 36 mm ID electrostatic precipitator (ESP) case, electrically grounded, and heat traced to 110°C, (3) ESP electrode mounted in an insulator, and charged to a negative voltage of 14 kV, (4) 13 mm ID Tygon tubing at room temperature, curving steeply downward to allow water condensation to run into impingers, (5) three 500 mL glass impingers in series in water-ice bath, with each containing 200 mL of collection solution, (6) desiccant canister for water aerosol removal, (7) coalescing filter canister for final gas cleaning, (8) Ritter drum-type total flow gas meter, and (9) Varian CP-4900 micro gas chromatograph.

All syngas pipelines were temperature controlled to specific set points via computer controlled electrical heat tracing and insulation. The syngas pipelines from the reactor to the second cyclone were kept at 450°C to prevent inadvertent tar collection until just upstream of location (1) in Figure 19. The entry duct just upstream of the ESP at location (1) in Figure 19 was held at 150°C to allow tar condensation to begin. The ESP body was heat traced and insulated to 110°C to collect as much tar as possible without collecting water. The Tygon hose at location (3) in Figure 19 had neither tracing nor insulation to allow further gas cooling just ahead of the impingers. All gas lines after the impingers were at room temperature. Tars collected upstream of the hose at location (3) had condensation points above 110°C, and will be referred to as “heavy tars” for the purposes of this study. All

remaining tar had condensation points less than 110°C, and will be referred to as "light tars."

Carbon dioxide gas was used as a gasifying agent and feed system purge. Nitrogen gas of 99% purity was used instead on one occasion to check for any obvious effects from gasifying agent. No significant differences were noted for any measured parameter, so the data from this run is included among the others. High purity CO_2 (99.999%) was chosen in an attempt to directly measure the N_2 generated from the FBN; however, in practice it was found that significant amounts of N_2 was trapped in the void space of the biomass in the feed hopper. This interstitial N_2 tended to bleed slowly into the reactor along with the biomass fuel, making it impossible to directly measure N_2 generated from FBN. For the purposes of this study, it was assumed that char-N, tar-N, NH_3, HCN, and N_2 represented all significant nitrogenous products, allowing N_2 generation to be determined by difference.

Reactor temperature was varied between tests for this study, with the different setpoints being 650, 700, 750, 800, and 850°C. Nine test runs were performed. Tests were conducted in random order except where circumstances prevented from doing so.

The flowrates of inert gas to the reactor were set to achieve constant gas residence time for all tests despite the different temperatures of operation. A schedule of the flowrates to the reactor for the different temperatures of operation, and the resulting residence times are shown in Table 11. In cases where multiple runs were conducted at a given temperature level, the average residence time among them is given. The residence time for the tests was designed to be relatively short (1.0 – 1.2

s), and no oxygen (O_2) was used for any of the tests to allow the gasification results to emphasize devolatilization by minimizing secondary gasification reactions. The short residence time minimized the amount of time available for tar cracking and homogenous reactions between gases to occur. The lack of oxygen (O_2) minimized conversion of char after devolatilization by preventing the carbon-oxygen reaction (Equation 6) from occurring [22]. Though CO_2, H_2O, and H_2 can also react with char and convert it to gaseous form [22], these reactions occur at much slower rates [66].

$$C + \frac{1}{2}O_2 \rightarrow CO \qquad \text{Eq 6}$$

Table 11. The flowrate of inert gas used was adjusted between runs to keep reactor residence times uniform between tests in lieu of temperature driven changes in syngas density and yield.

Operating Temperature (°C)	Hopper Purge (SLPM)	Bed (SLPM)	Residence Time (s)
650	1.20	3.40	1.0
700	1.10	3.20	1.2
750	1.00	3.00	1.1
800	0.95	2.80	1.1
850	0.90	2.60	1.0

The gasification reactor was preheated for at least one hour via the external electrical heaters until the control temperature had reached steady state. After preheating was complete, the flow of gasifying agents and biomass fuel was turned on for the experiment, and operated for about 85 min. The first 20 minutes of fuel feed was conducted without impingers to allow steady-state to be reached before samples were collected. The order in which HCN and NH_3 were collected for measurement was randomly chosen for each test. Upon completion of the startup phase, the first set of impingers, either for NH_3 or HCN collection, was inserted and

allowed to bubble for exactly 30 minutes. This set was then replaced with the impingers for collection of the other nitrogen species, also performed for 30 minutes.

Each set of glass impingers was weighed before and after sample collection in order to monitor syngas water content. Some light tar tended to collect in the impingers, as was indicated by mild discoloration of their solutions. The mass of light tars was assumed to be insignificant compared to the water collected, as the water yield was generally about one order of magnitude greater than the total heavy tar yield. The desiccant and coalescing canisters immediately after the impingers were also weighed prior to and after each test in order that any weight gains could also be credited toward syngas water content. Gas meter readings were taken before and after the installation of each impinger set to monitor gas production rates and enable mass balance calculations.

Upon completion of a test, the contents of each impinger were transferred to 500 mL HDPE sample bottles with tightly fitting lids. The three acidic impingers containing NH_3 in ammonium form (NH_4^+) were washed into their bottles using 18.2 MΩ deionized (DI) water. The three basic impingers containing HCN in cyanide ion form (CN^-) were washed into their sample bottles using 100 mM NaOH. The sample bottles were stored at 0-5°C until further processing and analysis could be conducted.

The three acidic samples were vacuum filtered using ceramic vacuum funnels and 110 mm diameter Whatman 42 filter paper. DI water was used to wash the filter paper, vacuum funnel, and vacuum flask after filtering each sample. Each sample was then diluted to 500 mL using DI water and volumetric flasks. The filtered and diluted samples were then transferred into new HDPE sample bottles. The samples

were transported to MVTL (1201 W Lincoln Hwy, Nevada, IA USA), and analyzed via distillation followed by titration using the National Environmental Methods Index Standard Method 4500-NH_3 B,C [51]. Final NH_3 analysis was typically completed within one week, and never more than two weeks after collection.

The three basic samples containing dissolved HCN as CN^- were diluted to 500 mL using volumetric flasks and 100 mM NaOH. Small amounts (ca. 5 mL) of each 500 mL sample were filtered using 0.45 µm syringe tip filters. The filtrate was then dispensed into 1500 µL vials for analysis, and analyzed with a Dionx ICS-3000 ion chromatograph (IC). The IC was calibrated for 1 to 10 ppm CN^- using a standard solution. Dilutions were conducted for each sample vial, and designed in order to keep the analyzed amounts within the calibration range. Any samples found to be out of the range were re-diluted and re-analyzed as needed. Sample solutions from the first impinger of a series were generally diluted by 10- to 20-fold. Solutions from the second impinger contained far less CN^-, and were generally diluted by only 2-fold. Cyanide ion concentration in the third and final impinger was low enough to allow undiluted analysis. An Eppendorf Multipipette equipped with disposable tips of assorted sizes was used for sample dispensing and dilutions. All dilution operations were carried out with the smallest possible tip sizes to maximize precision. The sample solutions from each impinger were prepared in triplicate into three vials to replicate the pipetting process. After vial preparation, each vial was agitated and then analyzed by the IC three times, for a total of nine readings per original impinger sample. The final data reported were derived from the mean of these nine readings. Analysis was typically conducted within 72 hours of sample collection.

Char collected by the gas cyclones from each run was measured gravimetrically. After weighing, the char from both catches was transferred into air-tight plastic bags for storage until analysis could be conducted. All char samples were analyzed for nitrogen content using an Elementar vario MICRO cube analyzer with at least three readings taken per sample. The sand bed in the reactor was removed after each test and weighed. Gains in bed mass were credited toward the total amount of char generated. A large amount of char tended to collect in the reactor due to the ER of zero and relatively low superficial gas velocity. Upon conclusion of each run, thirty to seventy percent of the char produced was found inside the reactor, nearly all other char was collected by the first cyclone, and less than 1% was recovered by the second cyclone, suggesting that essentially all char was accounted for.

To assure complete gravimetric determination of condensed tar, all piping and ESP parts starting at location (1) on Figure 19 and proceeding to the Tygon hose at the top of the ESP (location 4) were pre-weighed clean before each test run, and then disassembled and weighed afterwards. All disassembled piping and ESP parts were washed with acetone. The acetone washing process allowed most, but not all of the tars to be recovered from the parts, due to the high surface area and irregular shape of some of the parts. To compensate for the small amounts of tar that were left behind, the parts were weighed again after acetone cleaning to quantitate the efficiency of the cleaning process, allowing accounting for minor amounts of unrecovered tar.

The acetone-tar mixture was poured into clean pre-weighed HDPE bottles, and dried in a vacuum oven at 27-34 kPa and 35°C. The HDPE bottles were removed

and weighed again once drying was complete. The difference between the final weight and the clean sample bottle weight was found and designated the “tar residue mass.” The nitrogen content of each tar residue was then determined using an Elementar vario MICRO cube analyzer. Two replicate measurements were taken for each tar residue. Additional measurements were taken when the initial two measurements differed significantly. These results were then used to calculate the mass of elemental nitrogen contained in each tar residue sample. This amount of nitrogen was then corrected upwards according to the fraction of tars successfully recovered from the parts in the acetone washing process. The final result was used to report the total amount of nitrogen in the tar from each run. After tar recovery was complete, all parts were re-washed using industrial soap and hot water. The tars that collected on the pipe at location (1) in Figure 19 were very heavy, and resisted water washing. To solve this problem, this particular part was instead cleaned by oven baking at 650°C for two hours.

Final results were obtained for the percent yield of NH_3, HCN, char-N, and tar-N as compared to the molar quantity of FBN that was fed into the reactor during each test. Regression lines were fitted to data for trends that were noted. Statistical ANOVA was performed for each relationship to verify the statistical significance of the trends. 95% confidence interval bands were assigned to all regression lines to demonstrate precision. Conclusions of statistical significance of observed slopes and curvatures of trends are based on critical p-values of 0.05.

Results and Discussion

In order to investigate how thermodynamic equilibrium might be controlling nitrogen partitioning, Aspen Plus software was used to calculate the equilibrium amounts of NH_3, HCN, and N_2 for the operating conditions featured in this study. A constant temperature of 750°C and a constant pressure of 1 atm were assumed. Equilibrium yields of NH_3 and HCN were found to be only 0.04% and 0.0003% yield of the FBN, respectively, which would be below the detection limits for our experimental apparatus. Simulations at 650 and 850°C produce similar nearly zero concentrations. Nearly all of the FBN was converted to N_2. Clearly, any measureable NH_3 and HCN concentrations for the gasification conditions studied here would indicate that non-equilibrium mass transfer and kinetic phenomena are determining nitrogen partitioning. No solid carbon was predicted by the equilibrium results, eliminating the possibility of char-N. No provisions for tar-N were included in the equilibrium calculations, but concentrations of C_2 hydrocarbons and propane were essentially zero, inferring that larger molecules were unlikely to be present at equilibrium.

The mass balances for the nine tests varied from 89% to 100%, with departure from 100% usually being caused by small gas leaks. One measurement each of HCN, char gravimetric yield, and char-N yield were not determined due to technical difficulties. These missed measurements did not have a significant impact on their associated overall mass balances since the products were minor compared to the total mass throughput.

Gravimetric char yields are reported on a percent moisture free biomass basis as a function of temperature in Figure 20. The char yields for all conditions tested were high compared to the yields reported by larger scale gasification studies where air was used as an oxidizing agent to support reactor temperature. The results reported by de Jong et al. [6, 7], Kurkela et al. [31], and van der Drift et al. [8] report char yields of approximately 2% and less. The relatively high yields of the present study may be due to the lack of oxygen provided to the reactor, hindering the carbon-oxygen reaction. The shape of the trend in char yield of the present study is unusual in that it has a parabolic shape, with a maximum yield of 22% (dry biomass basis) occurring at 750°C. This is contrary to theoretical expectations, which are that the char yields should continually decline with increasing temperatures, as chemical equilibrium is more closely approached at higher temperatures. Equilibrium results for all conditions tested in the present study demonstrate no solid carbon production. The parabolic trend in char yield may be a result of slightly parabolic superficial velocities in the reactor over the temperature range studied, which would lead to a similar trend in elutriation rate. While our operating conditions were designed to maintain constant superficial velocity for all temperatures, changes in syngas yield, gas makeup, and gas viscosity with temperature made it difficult to achieve perfect compensation. The parabolic-shaped trend in char yields may be due to a corresponding trend in superficial velocity.

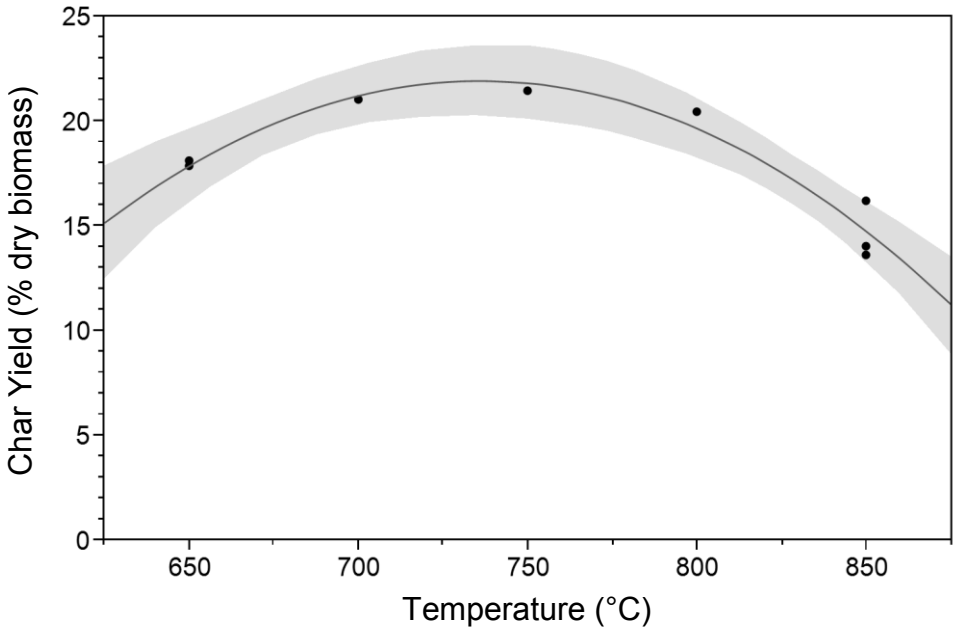

Figure 20. Char yield increased with temperature up to about 750°C before declining. The data have been fitted with a second order polynomial trend line; the shaded region represents a 95% confidence interval band. Reactor pressure and equivalence ratio for all tests were 1 atm and zero.

Tar yields as a function of operating temperature are shown in Figure 21. Tar yields were highest at 650°C (11% yield, moisture free biomass basis), declined steeply at first with increasing temperatures, and then moderated to about 2% yield at 850°C. This trend is consistent with expectations that tar yield should decline with increasing temperatures due to increasing rates of cracking, dry reforming, hydrocracking, and steam reforming reactions as described by de Jong et al. [6, 7] and Xu et al. [53].

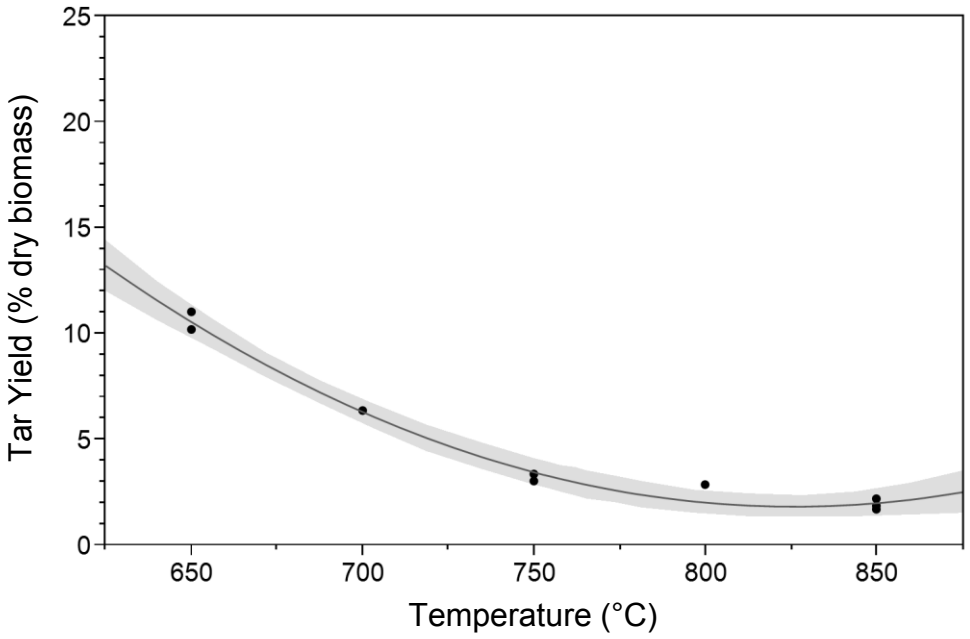

Figure 21. Tar yield decreased with temperature from about 11 wt% (dry biomass basis) at 650°C to about 2 wt% at 850°C. The data have been fitted with a second order polynomial trend line; the shaded region represents a 95% confidence interval band. Reactor pressure and equivalence ratio for all tests were 1 atm and zero.

Though experimental conditions were designed to reduce secondary gasification reactions, char and tar results suggest that this may not have been fully accomplished. A large fraction of char produced accumulated inside the reactor throughout its operation. The average char particle residence time probably far exceeded the gas residence time. The sensitivity of tar yield to reactor temperature may be evidence that secondary tar cracking is occurring at significant rates relative to the reactor residence time, though decreased yield of tar in the volatilization products at the higher temperatures could also be responsible.

Elemental analysis of the char and tar products uncovered the trends in char-N yield and tar-N yield that are shown in Figure 22 and Figure 23, respectively. Char-N represented 22-42% of the FBN over the range of operating temperatures explored in the present study. The response of char-N yield formed a parabolic

relationship with similar shape to the gravimetric yield of char itself. Tar-N yields were even higher than char-N yield for the lowest temperatures explored. At 650°C, tar-N amounted to nearly 60% of total FBN. The tar-N yield trend declined steeply with increasing temperatures at first, and then moderated to 16% at 850°C.

The sum of char-N and tar-N yields varied significantly with temperature, but remained significant for all temperatures tested. This suggests that an accurate kinetic model must simulate char and tar reactions that continue to release light nitrogen bearing gaseous species after devolatilization. None of the kinetic studies to date include tar-N chemistry [6, 7, 38, 39], and only Liu and Gibbs [13] have included secondary reactions for char-N.

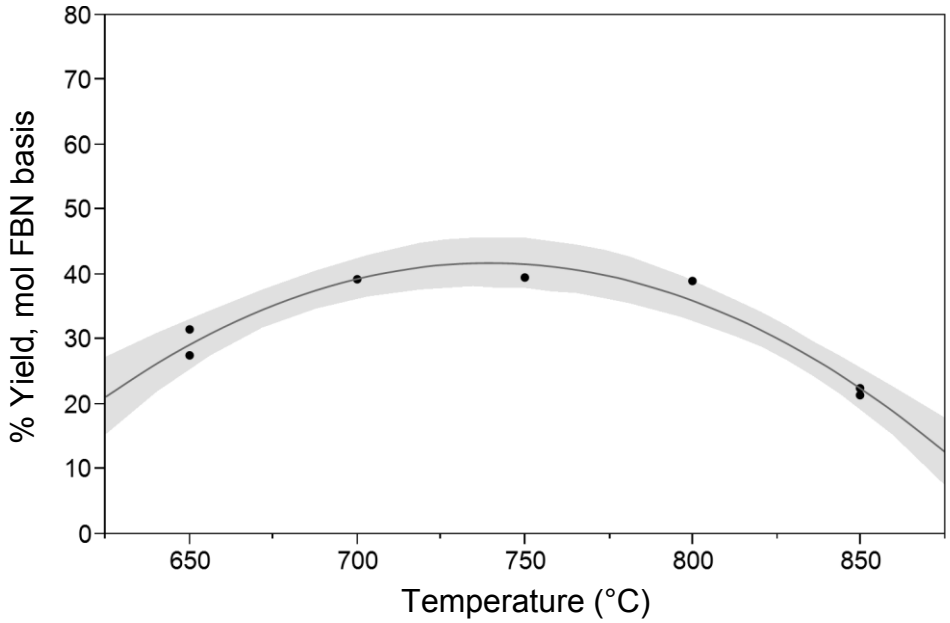

Figure 22. Yield of char-N increased with temperature up to a maximum of 42% (FBN basis) at about 750°C, before decreasing with further temperature increases. The data have been fitted with a second order polynomial trend line; the shaded region represents a 95% confidence interval band. Reactor pressure and equivalence ratio for all tests were 1 atm and zero.

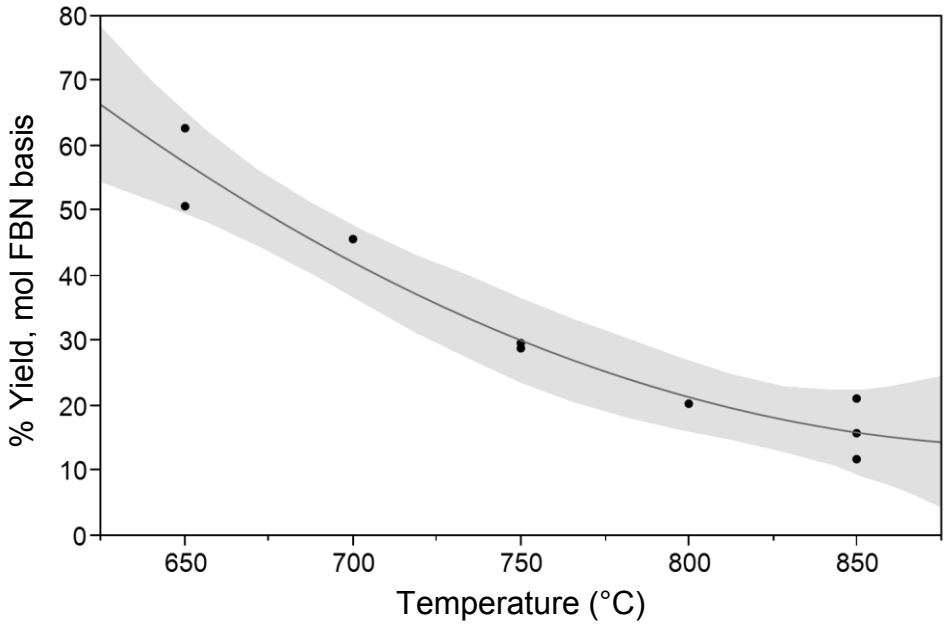

Figure 23. Yield of tar-N decreased from near 60% (FBN basis) to 16% as temperature increased from 650°C to 850°C. The data have been fitted with a second order polynomial trend line; the shaded region represents a 95% confidence interval band. Reactor pressure and equivalence ratio for all tests were 1 atm and zero.

A plot of the nitrogen concentration in the char is shown in Figure S1. The concentration did show statistically significant slope and curvature, but both slope and curvature effects were very small. There was also evidence of Lack of Fit ($p = 0.02$). The average concentration of nitrogen in the char over all tests, and its 95% confidence interval was 0.91 ± 0.05%. The concentration of nitrogen in the tar is shown in Figure S2, and did not demonstrate any statistically significant response to temperature. The mean and 95% confidence interval of the tar-N concentration was 4.0 ± 0.8% for the nine tests conducted.

Nitrogen was found in both the char and tar in higher concentrations than the original biomass. The lack of compelling trends in these two parameters leads to char-N and tar-N yields being more dependent on the gravimetric yields of char and tar rather than the concentrations of nitrogen in either of these products. It seems

effective to approximate the release of gaseous forms of nitrogen products from char and tar for a modeling effort by simply correlating nitrogen release rates to the rates of the secondary reactions that convert the overall mass of char and tar to permanent gas forms. This was in fact the strategy that was taken by Liu and Gibbs [39] for conversion of char-N.

The effect of reactor temperature on NH_3 yield from switchgrass gasified at an ER of zero is shown in Figure 24, and fitted with a linear regression. NH_3 yields were found to increase from about 2% to 15% yield of FBN as reactor temperature was increased from 650°C to 850°C. ANOVA demonstrates a statistically significant trend, though some scatter in the data was noted. Referencing the equilibrium results, we can see that non-equilibrium mass transfer and kinetic phenomena are important for determining NH_3 yields for all temperatures explored in the current study.

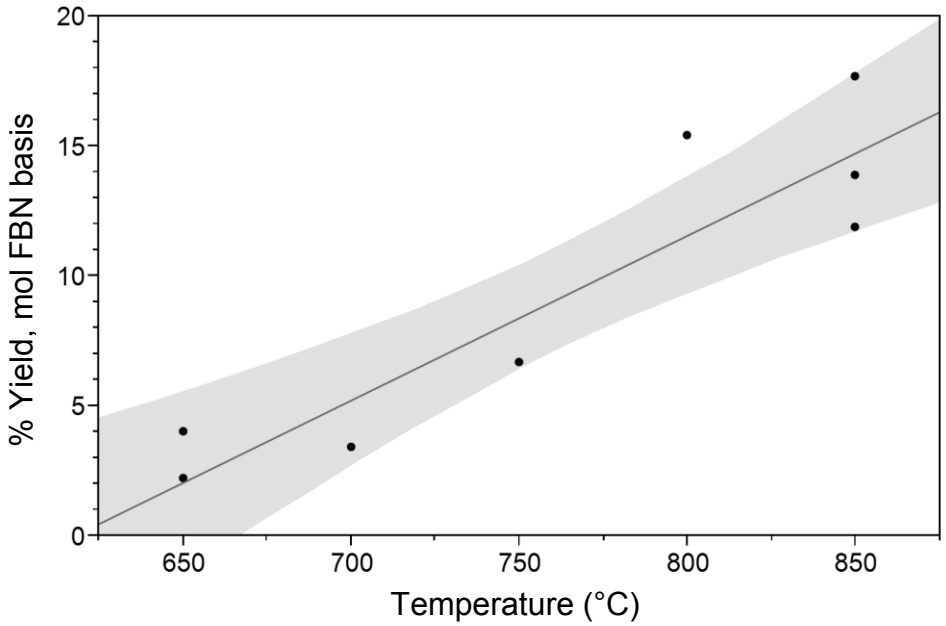

Figure 24. The yield of NH_3 (FBN basis) increased from 2% to 15% as temperature increased from 650 to 850°C. The data have been fitted with a linear trend line; the shaded region represents a 95% confidence interval band. Reactor pressure and equivalence ratio for all tests were 1 atm and zero.

The effect of temperature on HCN yield is shown in Figure 25, fitted with a second order polynomial regression. As the reactor temperature was increased from 650 to 850°C, HCN yield increased from about 4% to 11% with a slightly parabolic slope. ANOVA statistical analysis indicates both statistically significant slope and curvature. By comparing the range of HCN yields to the equilibrium results, we can see that non-equilibrium mass transfer and kinetic phenomena are also important for determining HCN yields for all temperatures explored.

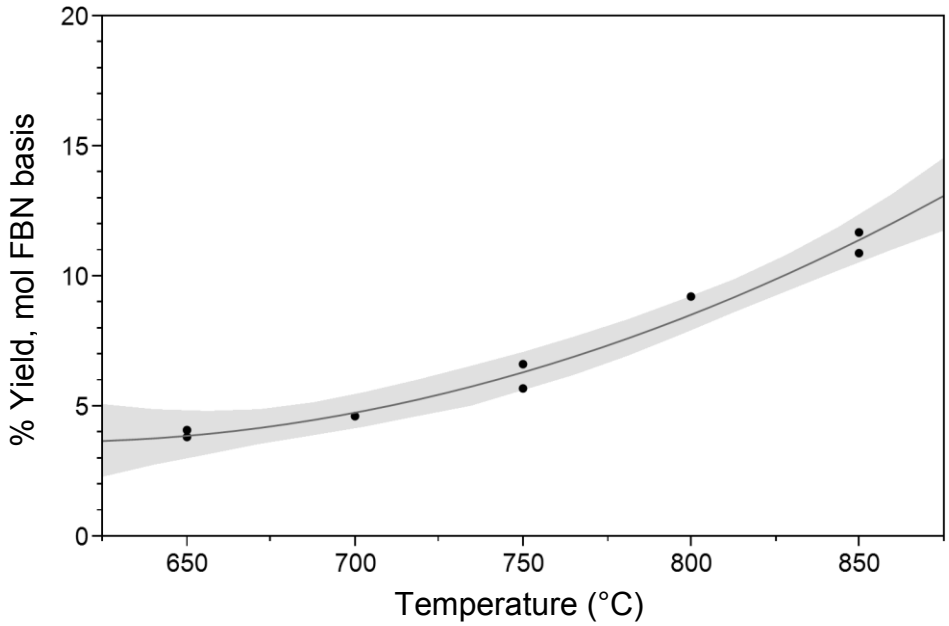

Figure 25. The yield of HCN (FBN basis) increased from about 4 to 11% as temperature increased from 650°C to 850°C. The data have been fitted with a second order polynomial trend line; the shaded region represents a 95% confidence interval band. Reactor pressure and equivalence ratio for all tests were 1 atm and zero.

By using the regression lines of the NH_3, HCN, char-N, and tar-N data together, it was possible to conduct a nitrogen elemental balance to estimate the yield of N_2 from the FBN. The results are shown as a stacked line graph in Figure 26. Yield of N_2 from FBN increased from only 7% at 650°C, up to 35% at 850°C. These increases demonstrate evidence of a slow, incomplete migration toward equilibrium as reactor temperature was increased over the range studied.

For all temperatures studied, a large portion of the FBN remained bound in the char and tar, though the sum of char-N and tar-N declined continuously with temperature. Meanwhile, the yields of NH_3 and HCN increased. The amount of N_2 produced (found by difference) became increasingly significant at the higher temperatures.

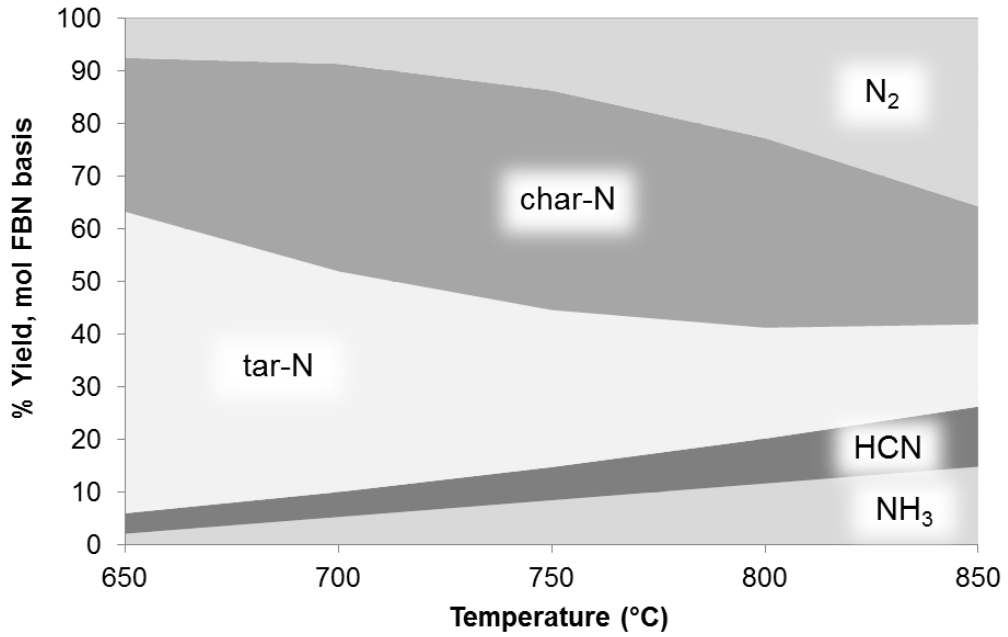

Figure 26. The char-N and tar-N were increasingly converted to the three gaseous forms of nitrogen (N_2, HCN, and NH_3) as temperature was increased from 650°C to 850°C. Reactor pressure and equivalence ratio for all tests were 1 atm and zero.

Our results demonstrate that attempts to model nitrogen chemistry during gasification have often misjudged the relative importance of the different nitrogen bearing compounds. For example, de Jong et al. [13] assumed in the earlier of their two modeling studies that devolatilization converts 100% of FBN to NH_3 whereas the present study found only 2-15% yield of NH_3 from FBN and a comparable yield (4-11%) of HCN. In a different model, Chen et al. [38] assumed that both tar-N and HCN were negligible nitrogenous products. In a third model, Liu and Gibbs [39] acknowledged that tar may contain significant tar-N, but that it is instantly converted to other gaseous nitrogen species. The importance of char-N and tar-N as sources of release of nitrogen gases may explain why many experimentalists have observed NH_3 to increase with temperature.

It is also interesting that significant amounts of N_2 appear for the higher temperature values tested. Diatomic nitrogen is predicted by thermodynamic equilibrium modeling to be the sole nitrogen product for the temperatures, pressures, and ER of zero employed in these experiments. The current study aimed to design these experiments to have short enough residence time to minimize secondary reactions, and therefore progress toward equilibrium nitrogen products. In the overview of gasification nitrogen reactions graphic presented by Abhela et al. [13], N_2 is depicted as only being a product of secondary reactions, not from the devolatilization process itself. The appearance of N_2 at the higher temperatures tested in the present study suggests that even a residence time as short as 1 s may be enough to allow secondary reactions to make significant progress.

Another significant unanswered question in the nitrogen modeling research field has been what determines the initial yields of HCN and NH_3 in the volatile products. By conducting calculations from the amino acid profile, it was determined that 60% of the FBN was accounted for as amino acids. The remaining nitrogen is presumably in other biomolecules. Within this protein based nitrogen, heterocyclic nitrogen was fairly rare – approximately 1% of the total FBN. As mentioned by Vriesman et al. [24], it is thought that HCN has a tendency to arise from nitrogen bound in the feedstock in heterocyclic rings, and $NH_3$from amine groups. The results of the current study found HCN yields of 4-11%, so apparently HCN can arise from other sources besides the heterocyclic rings in the protein. One explanation may be that it comes from other biomolecules such as chlorophyll, which also contains nitrogen in heterocyclic form [67]. Given the sensitivity of NH_3 and HCN yield to

temperature that was observed the present study, it appears that feedstock properties alone are not sufficient for predicting NH_3 and HCN yields.

Conclusions

The present study has documented partitioning of FBN into five major forms in syngas (NH_3, HCN, N_2, tar-N, and char-N). Significant amounts of nitrogen were found to not be immediately released as one of gaseous forms (NH_3, HCN, and N_2), and instead resided in the tar and char. This explains why other nitrogen partitioning studies have demonstrated increases in NH_3 yields as ER was increased, as this led to increased conversion of char and tar into gaseous form.

Our experimental findings demonstrate that in order for a gasification model to be effective in predicting the yields of nitrogenous products in the syngas, it is important that the release of nitrogen species from tar cracking and char gasification be included in the model. It was found that as increases in temperature increase char and tar conversion, the concentration of nitrogen in the char and tar remained approximately constant, suggesting that a simple way to approximate release of gaseous nitrogen compounds from the char and tar would be to directly correlate their release to char and tar conversion rates. It remains unclear however, how to effectively predict the ratio between the gaseous nitrogen products that are released.

CHAPTER 5

PARTITIONING OF NITROGEN DURING BIOMASS GASIFICATION: PART 2. THE EFFECT OF EQUIVALENCE RATIO

In preparation for submission to *Applied Energy*

Karl M. Broer[1], Robert C. Brown[2]

Introduction

Biomass gasification allows a wide variety of heterogeneous biological materials to be converted into syngas, a product that is energetic, gaseous, and relatively uniform in quality. Syngas can be utilized by direct combustion for either heat and power applications, or transformed into liquid fuels and chemicals via catalytic processes [16]. Gasification is also a promising option for removal and sequestration of CO_2 from the atmosphere via Bioenergy Carbon Capture and Storage (BECCS), as recently endorsed by the Intergovernmental Panel on Climate Change (IPCC) [1].

Most biomass gasification feedstocks contain small amounts of nitrogen. Much of this fuel bound nitrogen (FBN) originates from proteins. Nitrogen can also be present in woody and herbaceous feedstock as nitrates, ammonium, chlorophyll, and nucleic acids [67, 68]. Upon gasification, most of the FBN converts into five products - diatomic nitrogen (N_2), ammonia (NH_3), hydrogen cyanide (HCN), char

[1] Primary researcher and author
[2] Provided document editing assistance, serving as author for correspondence, and major professor

bound nitrogen (char-N) and tar bound nitrogen (tar-N). In addition to the five major nitrogen products, minor amounts of FBN can be converted to nitric oxide (NO), but usually at insignificant yields [26]. Isocyanic acid (HNCO) has also been reported by some authors, but for only small batch-fed reactors with slow heating rates [37]. When de Jong et al. [6] processed switchgrass in a pilot scale gasifier, no HNCO was detected. Because NO and HNCO are commonly included in combustion networks containing nitrogen reactions [64], it is possible that they play roles in evolution of nitrogen during gasification. Because most studies have not detected NO or HNCO, they were not measured in this study.

Of the five most significant nitrogen-bearing compounds, NH_3 and HCN are the most problematic as they are precursors to NO_X emissions during syngas combustion. They also can poison catalysts used to synthesize fuels and chemicals from syngas. For example, Einvall et al. [21] demonstrated that NH_3 interferes with water-gas shift catalysts. A better understanding of nitrogen partitioning would allow more accurate prediction of NH_3 and HCN in syngas, facilitating design of gas cleanup equipment.

A summary of past studies of the response of nitrogen partitioning to varying ER is presented in Table 12. Most of these studies had important shortcomings, as they monitored only a few nitrogen species, limiting their ability to determine nitrogen partitioning. None of these studies measured tar-N, which along with char-N has recently been shown to be important to nitrogen partitioning [69]. Finally, two of the studies that reported HCN had systematic errors in measurement of HCN, further limiting the usefulness of their data sets [24, 26, 63].

Table 12. A summary of continuous flow gasification studies measuring at least one nitrogen species while varying ER. All reactors are either bubbling fluidized bed or circulating fluidized bed. N_2 results are marked only when N_2 originating from FBN was measured, rather than from the fluidization gas. (ER/T – equivalence ratio and temperature varied together, ER – equivalence ratio varied while temperature was held constant)

Reference	Feedstock	Independent Variable	N_2	NH_3	HCN	char-N	tar-N	NO_X
Broer et al. [61]	Switchgrass	ER/T		X	X			
Berg et al. [54]	Miscanthus, Sawdust	ER		X				
Vriesman et al. [24]	Miscanthus	ER		X	X[1]	X		
Zhou et al. [26]	*Leucaena*	ER	X	X	X[1]	X		X
Zhang et al. [29]	Wood powder	ER/T		X				
de Jong et al. [6]	Wood pellets	ER/T		X	X	X[2]		
de Jong et al. [7]	Miscanthus	ER/T		X	X			

[1] HCN results should be interpreted with caution. Refer to a recent study by Broer et al. [63].

[2] Char-N was reported, but values of zero were reported for all test levels, due to a near absence of char production.

In the present study, ER will be varied while keeping experimental conditions as equivalent as possible to our previous study, which focused on the effects of temperature [69]. This will allow the effects of temperature documented in the previous study to be directly compared to the present study. The small size and design of the reactor employed for this study allows the ER and temperature to be varied independently.

Materials and Methods

The experimental equipment used, and procedures followed for this study are similar to those used in a previous study [69]. We will provide here a brief summary of our experimental methodology, noting the key changes that were made for the present study. Readers should refer to reference [69] for additional details.

Dry switchgrass was ground and sieved to produce 212-500 μm diameter particles. Wet basis moisture content, elemental analysis, and ash content were measured, and are listed in Table 13.

Table 13. Switchgrass fuel ultimate analysis, ash, and moisture content. Analysis reflects biomass as freshly processed. Uncertainties reflect a 95% confidence interval.

C	45.6 ± 0.5
H	5.27 ± 0.07
N	0.50 ± 0.04
O (by difference)	44.8
Ash	3.8 ± 0.4
Moisture	4.37 ± 0.11

The present study employed the same gasification reactor as our previous study [69]. The only configuration change was that 40/70 high purity silica sand

obtained from Badger Mining Corporation (409 South Church St., Berlin, WI USA) was used as a bed material. This sand was finer in order to allow bed fluidization to take place, promoting uniform temperatures as oxygen was added to the fluidizing gas to vary ER.

The minimum fluidization velocity of the sand bed was determined by conducting fluidization tests. The differential pressure over the sand bed was plotted while adjusting the flow of CO_2 supplied to the bed as the reactor was maintained at operating temperature. Fluidization testing was conducted using a clean sand bed before fuel feed was allowed. When gasification was underway, fuel was fed to the fluidized bed via a two auger feed system. The tip of the injection auger brought the fuel into the reactor at the resting height of the sand bed.

As in the previous study [69], particulates were removed from the syngas stream immediately after the reactor via a pair of gas cyclones installed in series configuration. An electrostatic precipitator (ESP) was then used to remove condensed tar aerosols from the gas stream. Following particulate and tar removal, glass impingers were installed, each containing 200 mL of 100 mM sodium hydroxide (NaOH) for collecting HCN or 5% hydrochloric acid (HCl) for collecting NH_3. These two nitrogen species were collected separately, with the basic and acidic impinger sets being placed inline in turns. A desiccant canister and final coalescing filter were used downstream of the impingers to act as final guard filters to protect downstream instruments. After all cleaning was complete, the gas stream was sent through a Ritter rotating drum-type gas flowmeter, and finally to a Varian CP-4900 micro gas chromatograph (mGC).

The temperatures of all syngas pipelines on the experimental setup were controlled at specific temperatures via computer controlled heat tracing underneath insulation, as described in our previous publication [69]. Tars that collected just upstream of and inside the ESP had condensation points above 110°C, and were considered to be "heavy tars." Tars that collected downstream of the ESP had condensation points less than 110°C, and were considered to be "light tars."

High purity CO_2 and O_2 (99.999% and 99.996% respectively) gases were used as gasifying agents for the present study. High purity gases were used with the intent of enabling direct measurement of the N_2 generated from the FBN; however, in practice it was found that the biomass fuel in the feed hopper contained significant amounts of N_2 in interstitial spaces. This N_2 tended to bleed slowly into the reactor throughout each test in amounts high enough that it was impossible to directly measure N_2 generated from FBN. Diatomic nitrogen was found instead by computing a nitrogen elemental balance which assumed that all FBN entering the reactor converted to either N_2, NH_3, HCN, char-N, or tar-N.

The reactor temperature set point for all experimental work in this study was 750°C. A total of fourteen test runs were completed. The char data from two runs was rejected, due to technical difficulties encountered in taking char measurements. Experimental trials were conducted at six different ER levels; exact gas flow rates used are shown in Table 14. The biomass feeder was calibrated beforehand and operated for an intended mass flowrate of 100 g/h for all tests. To more precisely determine exact feed rates, fuel in the feed hopper was weighed before and after each test, and total feeder operation time for each run was precisely recorded. This allowed for more exact ER values to be used for data reporting purposes.

The total volumetric flowrate to the fluidized bed was held constant at 3.0 SLPM for all tests, which provided 2.7 times the minimum fluidization velocity. ER was varied by trading specified flowrates of pure O_2 for equal volumetric flowrates of CO_2. In addition to the gas flow sent through the plenum and fluidized bed, the feed system hopper was purged with 1.0 SLPM of CO_2 for all tests. The flowrate of this purge gas and the flowrate of volatiles produced by the biomass were assumed not to contribute toward fluidization. The order of experiments at different ER levels was randomized unless technical obstacles prevented it. The reactor was operated at 1 atm for all tests.

Table 14. Experimental levels used for the fourteen test runs of this study. The reactor temperature setpoint was 750°C for all runs.

Target ER	Feed Hopper (SLPM CO_2)	Fluidized Bed (SLPM CO_2)	Fluidized Bed (SLPM O_2)
0.00	1.00	3.00	0.00
0.05	1.00	2.92	0.08
0.10	1.00	2.85	0.15
0.20	1.00	2.69	0.31
0.30	1.00	2.54	0.46
0.40	1.00	2.39	0.61

The reactor was preheated for one hour, and then fuel feed was operated for 20 minutes before data collection was permitted, just as was conducted for our previous study [69]. Two sessions of nitrogen species collection for analysis were conducted per experimental test, also as described previously [69]. After the two collection sessions were complete, the experiment was concluded by ceasing oxygen flow, biomass flow, and electrical heater power simultaneously. A small flowrate of CO_2 (0.6 SLPM) was used to cool the reactor after shutdown, minimizing further

char reactions. Of the fourteen tests documented in the present study, nine tests featured one NH_3 collection session and one HCN collection session. The order in which the two species were collected was randomized. Three tests were conducted in which two NH_3 collection sessions were conducted, and no HCN was collected. Two tests were conducted in which two HCN collection sessions were conducted, and no NH_3 was collected. These five cases where collection of the same species was conducted twice within a given test run served to compare variability of the data between test runs to that within test runs, and to focus efforts on collecting one species or the other at particular experimental levels where increased variability was encountered.

Each set of impingers was weighed before and after its collection session to measure the water content of the syngas. Gas meter readings were taken before and after the installation of each impinger set to monitor gas production rates. The permanent gas makeup of the syngas was analyzed using a micro gas chromatograph. Together these measurements were used to enable mass balances to be conducted for each experiment, allowing for any leaks or problems with flow controllers to be detected.

Upon conclusion of each test, the contents of each one of the six glass impingers was recovered and stored in preparation for analysis in a similar way to our previous study [69]. Analysis of the NH_3 and HCN samples was carried out within the same time frames as in our previous study [69]. In our previous study it was noted that the variance between replicate measurements of HCN samples was relatively small, so for the present study, three sample vials were prepared from each

HCN sample as before, but only two ion-chromatograph readings were taken per vial instead of three.

Char production from each run was measured in the same manner as previously [69]. Upon completion of a typical run, about 30-40% of the char was found in the reactor bed. Most (about 95%) of the char that left the reactor was trapped by the first cyclone, and essentially all remaining char by the second cyclone. The char from each run was analyzed for nitrogen content in the same way as previously [69]. The nitrogen content of the heavy tar was measured by following the same tar recovery procedure as in our previous study. Tars were washed off of the ESP and adjacent parts using acetone, the acetone was dried off, and then the composition of the remaining tar residue was analyzed.

From the experimental procedures, results were obtained for the percent yield of the NH_3, HCN, char-N and tar-N compared to the molar quantity of FBN that was fed into the reactor during each test. The yield of N_2 was found by difference. Overall char and tar yields on a moisture-free biomass basis were also determined. Regression lines were fitted to each set of data, and the significance of the slope and curvature were tested using ANOVA statistical techniques. Plots of the data with their trend lines were assigned 95% confidence interval bands to visually demonstrate the statistical quality of the data. Conclusions of significance were based on critical p-values of 0.05. Regression and ANOVA was conducted in two alternative ways for the NH_3 and HCN data. The first method utilized all individual NH_3 and HCN readings taken, including the ones from experimental trials where two measurements of NH_3 or HCN were taken. The second method found the mean of the pairs of NH_3 and HCN measurements, and plotted the averages. The first method

of plotting the data demonstrated slightly weaker statistical significance in the case of both the HCN and NH_3 data, and is featured here as the more statistically conservative option.

Results and Discussion

To investigate whether thermodynamic equilibrium influences nitrogen partitioning, Aspen Plus software was used to calculate the equilibrium amounts of NH_3, HCN, and N_2 corresponding to the bounds of the experimental conditions of the present study (750°C and 1 atm, ER of zero and 0.4). The predicted NH_3 and HCN yields were only 0.04% and 0.0003%, respectively, for ER of zero, and only 0.011% and 0.000093%, respectively, for ER of 0.4. Virtually all FBN was predicted to convert to N_2. Under these conditions, no solid carbon was predicted; thus, char-N would not be expected to be important to nitrogen partitioning. Neither are high molecular weight hydrocarbons predicted; thus tar-N would not be expected to be important. In fact, as described in the results below, all of these nitrogen species are important to nitrogen partitioning, indicating the importance of reaction kinetics in determining nitrogen species in syngas.

Mass balances for the fourteen tests varied from 93% to 103%. Departure from 100% was likely caused by small gas leaks, and small amounts of error related to gas flow control and measurement equipment. Of the fourteen tests reported, char gravimetric yield data and their accompanying char-N data were lost on two occasions, due to problems with recovering char from the reactor bed after the tests. Neither of these missed measurements had significant impact on their

corresponding mass balances, as char was a minor component of the total mass throughput.

The response of char yield to ER is plotted in Figure 27, and fitted with a second order polynomial regression. Statistical ANOVA was conducted, and revealed significant slope and curvature. The trend in char yield declined from about 19% to 7% as ER was increased, with the decline being steepest at the lower ER values. The consistently declining char yields were likely due to increases in oxygen availability, leading to increased progress of the carbon-oxidation reaction (Equation 7) [22]. The absence of oxygen in our previous study would have prevented this reaction.

$$C + \frac{1}{2}O_2 \rightarrow CO \qquad \text{Eq 7}$$

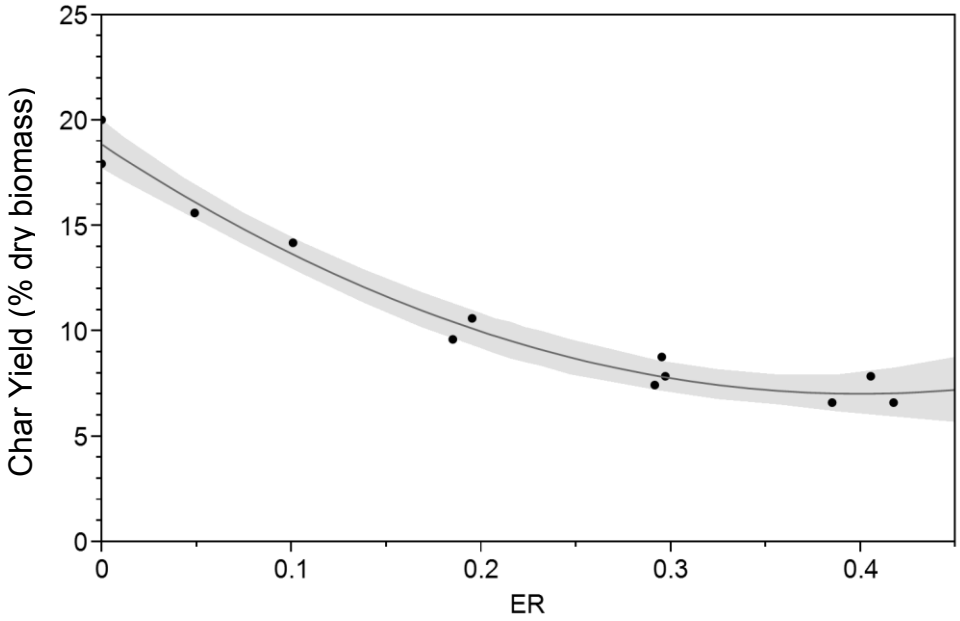

Figure 27. As ER was increased from 0 to 0.4, the char gravimetric yield declined steeply at first, and then moderated to about 7% at ER=0.4. The data have been fitted with a second order polynomial trend line; the shaded region represents a 95% confidence interval band. Reactor pressure and temperature for all tests were 1 atm and 750°C.

The response of tar yield on a dry biomass basis to ER is shown in Figure 28, and has been fitted with a linear regression. Tar yields declined from about 4.5% at an ER of zero to 1.9% at an ER of 0.4. Statistical ANOVA indicated significant slope. The trend and values in tar yields from an ER of zero to 0.4 in the present study are similar to the trend in tar yields documented in our previous study from 750°C to 850°C as ER was held at zero [69]. The declining yield of tar as ER is increased may be due to increased progress of the tar oxidation reaction.

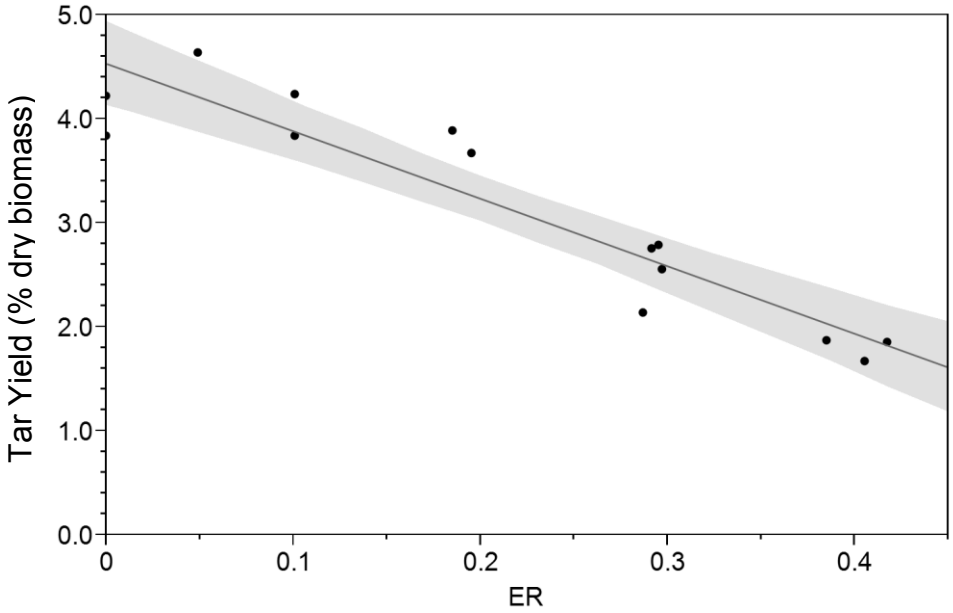

Figure 28. As ER was increased, the tar gravimetric yield declined linearly from 4.5% to 1.9%. The data have been fitted with a linear trend line; the shaded region represents a 95% confidence interval band. Reactor pressure and temperature for all tests were 1 atm and 750°C.

The responses of char-N and tar-N to changing ER are shown in Figure 29 and Figure 30, respectively. The yield of char-N from FBN declined from about 34% at ER=0 to about 11% at ER=0.4, with the most rapid decline occurring at low ER. Tar-N declined linearly from 38% yield to about 21% yield as FBN increased from zero to 0.4.

Both char-N and tar-N yields were significant for all ER levels. Even for ER of 0.4, where tar and char yields were only 1.9% and 7%, respectively, 24% of the FBN remained in these non-gaseous forms. The four published gasification models designed to predict nitrogen species (de Jong et al. [6, 7], Chen et al. [38], and Liu and Gibbs [39]) all failed to account for tar-N. Only the models by Chen et al. [38] and Liu and Gibbs [39] accounted for char-N, and the approaches taken by both studies were very simplified. In fact, Chen et al. [38] determined char-N yields strictly by assumption; no reaction mechanisms for char-N were proposed. The ability of these models to predict nitrogen partitioning could be improved if reactions of char-N and tar-N could be included.

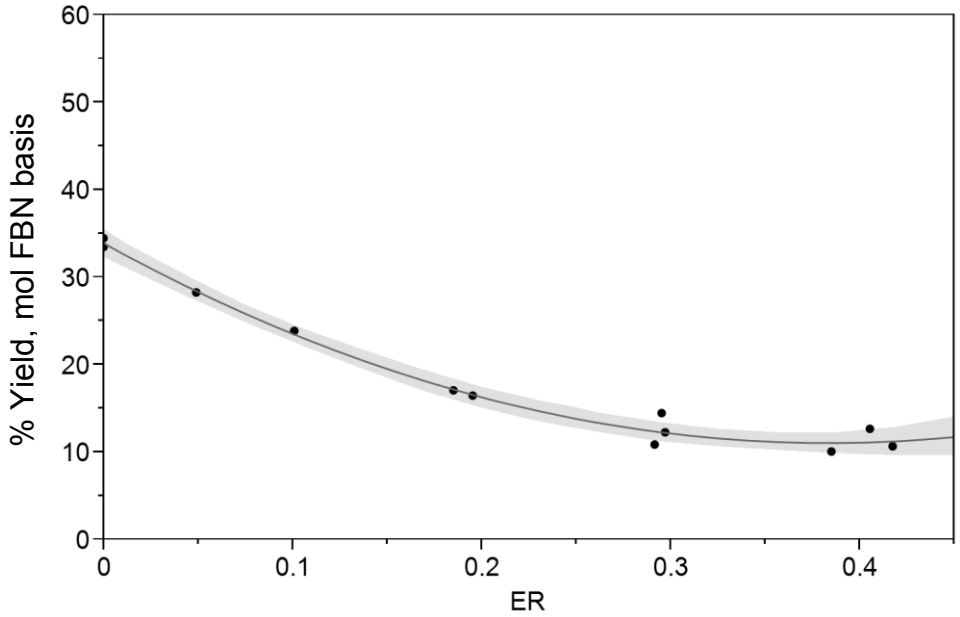

Figure 29. As ER was increased from 0 to 0.4, the yield of char-N from FBN declined steeply from 34%. Declines became more moderate at higher ERs, reaching 11% yield of the FBN at ER=0.4. The data have been fitted with a second order polynomial trend line; the shaded region represents a 95% confidence interval band. Reactor pressure and temperature for all tests were 1 atm and 750°C.

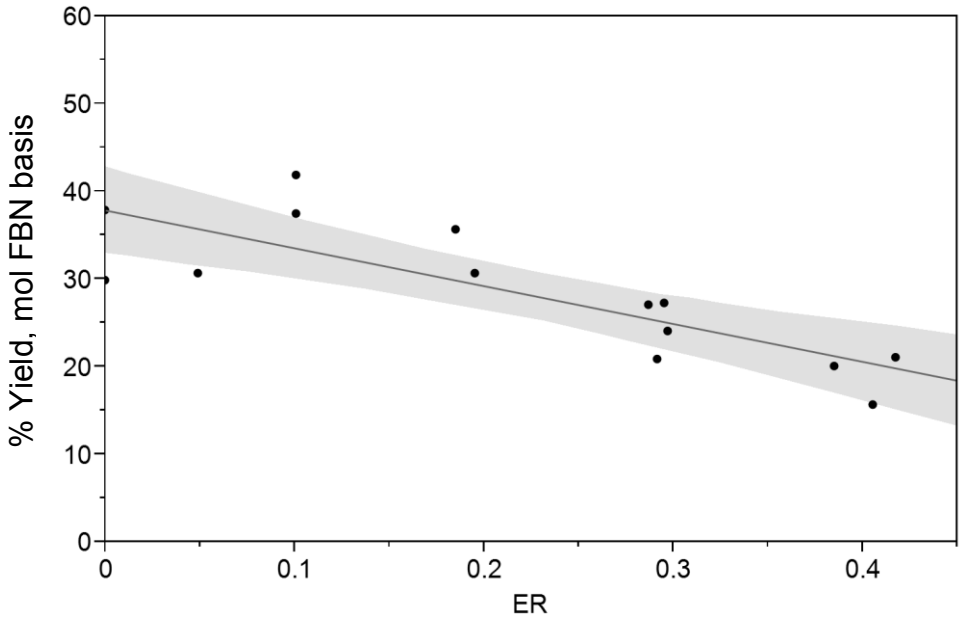

Figure 30. As ER was increased, the yield of tar-N decreased linearly from 38% to 21%. The data have been fitted with a linear trend line; the shaded region represents a 95% confidence interval band. Reactor pressure and temperature for all tests were 1 atm and 750°C.

The concentrations of nitrogen within the char and tar products were significantly higher than the biomass itself, and did not change very much in response to ER (Figure S3 and Figure S4). There was strong enrichment of nitrogen into the char and tar products compared to the original biomass. The concentration of nitrogen in the char and tar was almost twice, and almost ten times the concentration of the nitrogen in the biomass, respectively.

The response of NH_3 yield to increasing ER from zero to 0.4 is shown in Figure 31, fitted to a second order polynomial trend line. NH_3 yields increased as ER was increased, with the trend line rising from 6% yield at ER=0 to about 15% yield at ER=0.4. ANOVA analysis reveals that the slope and upward curvature are significant. From visual inspection of the NH_3 trend, it appears that NH_3 yield remained steady at about 6-7% from ER=0 to ER=0.2, increasing only after ER was increased beyond 0.2. Referencing the gaseous reaction mechanisms of nitrogen

species provided by Abhela et al. [13], it is unexpected that NH_3 should increase as ER is increased. The presence of O_2 should encourage reaction pathways that convert NH_3 to N_2 [13]. The residence time versus concentration results presented in the modeling study by de Jong et al. [7] also show modest declines in the amount of NH_3 when O_2 is introduced to a gasification environment. The large amounts of char-N and tar-N found at all ER levels tested, and their strong declines as ER was increased suggest an explanation. Increased conversion of char and tar and their associated nitrogen to gaseous form would easily provide enough nitrogen to account for the observed increases in NH_3 yields. The reaction network published by Abhela et al. [13] demonstrates that NH_3 can arise from char-N or from tar-N via HCN as an intermediate.

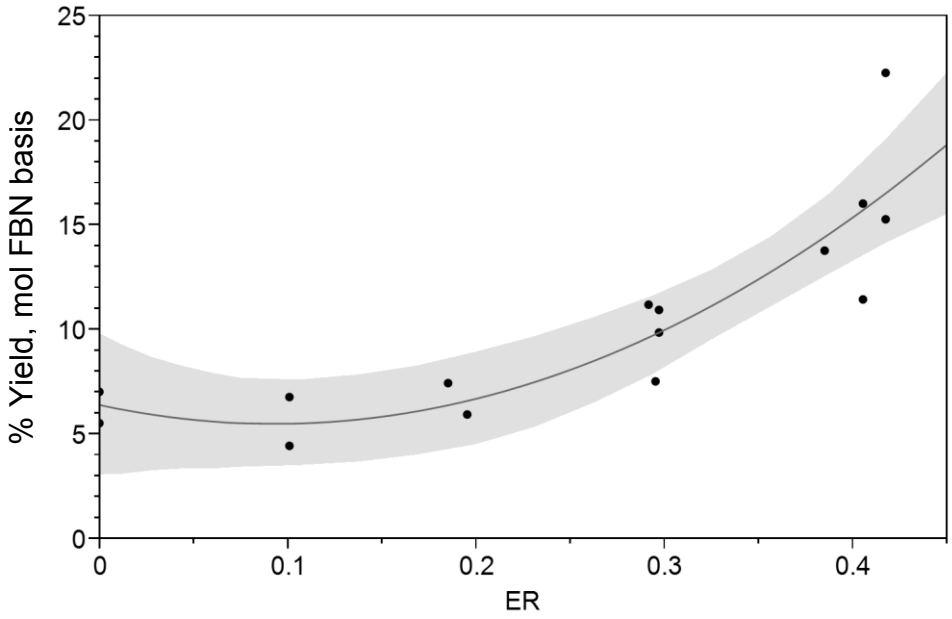

Figure 31. As ER was increased from zero to 0.2, NH_3 yields remained nearly the same (ca. 6-7%). As ER was increased beyond 0.2, the yield of NH_3 increased, reaching about 15% yield of the FBN at ER=0.4. The data have been fitted with a second order polynomial trend line; the shaded region represents a 95% confidence interval band. Reactor pressure and temperature for all tests were 1 atm and 750°C.

The response of HCN yield to reactor temperature is shown in Figure S5. Attempts at fitting both linear and polynomial trends to the data with statistical ANOVA found no significant response of HCN yield in response to ER. The average HCN yield and its 95% confidence interval across all tests conducted was 9.8 ± 1.0. According to the nitrogen reaction network presented by Abhela et al. [13], the addition of O_2 with increasing ER should increase conversion of HCN to other species such as N_2 and NH_3, but the lack of trend in the HCN yields provides no obvious evidence of these reaction pathways. As with NH_3, the large and declining yields of char-N and tar-N could provide a large potential source for HCN to be generated via the pathways outlined by Abhela et al. [13] as ER is increased. It seems possible that HCN might be simultaneous released in increasing amounts from char and tar, and increasingly converted to NH_3 and N_2 as ER is increased, resulting in the lack of trend.

Both NH_3 and HCN yields are several orders of magnitude higher than equilibrium calculations would predict for the operating conditions investigated. The concentrations of both were primarily controlled by kinetics and mass transfer.

A stacked line graph to summarize the relative amounts of the major forms of nitrogen was created based on the trend lines of NH_3, char-N, and tar-N, and is shown in Figure 32. Average yield of HCN was used in order to create the graph, as it did not demonstrate a statistically significant response to ER. Diatomic nitrogen was added to the chart based on the assumption that it comprised all remaining non-detected nitrogen. Char-N, tar-N and N_2 contained larger portions of the FBN than NH_3 and HCN for most ER levels. The increases in N_2 yield as ER was increased reflect partial approach toward thermodynamic equilibrium, which specified that all

FBN should eventually be converted to N_2. It is interesting that the increased yields of N_2 did not occur at the expense of NH_3 and HCN, when it is predicted that N_2 should be created from NH_3 and HCN, rather than directly from the volatiles and char [13]. The predictions of the model developed by de Jong et al. [7] also found that at least part of NH_3 should be converted to N_2 when exposed to O_2 in the fluidizing agents. It would seem that this should have produced declining HCN and NH_3 yields as ER was increased, when NH_3 yields increased instead. This could be easily explained by release of nitrogen from the char and tar. The models proposed by de Jong et al. [6, 7] ignored this possibility.

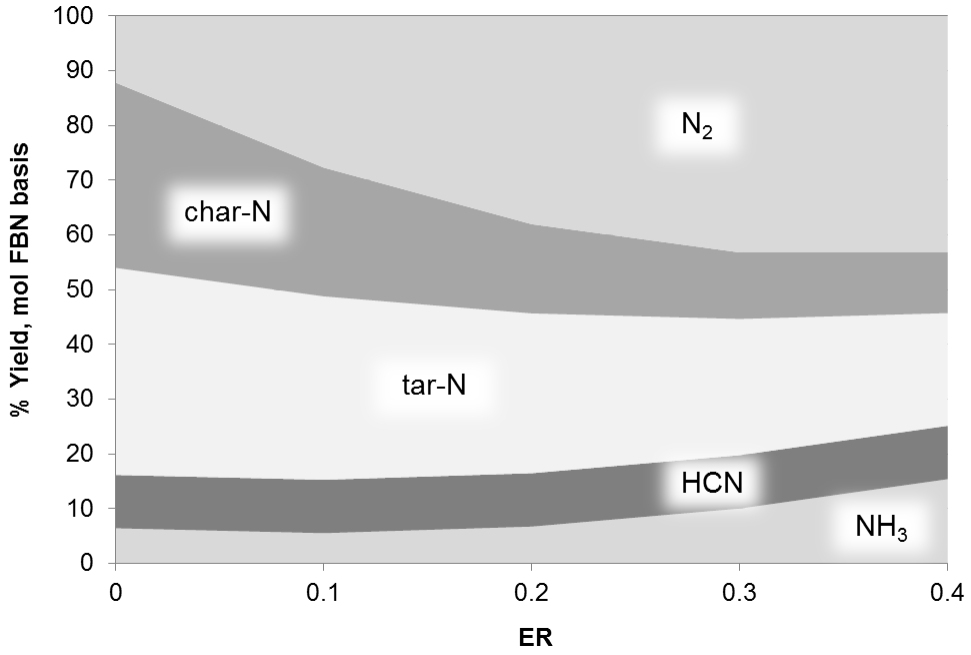

Figure 32. As ER was increased, yields of NH_3 and N_2 increased, HCN held steady, and char-N and tar-N yields both declined. Reactor pressure and temperature for all tests were 1 atm and 750°C.

Conclusions

For all levels of ER studied, significant amounts of the FBN failed to be released as gaseous forms of nitrogen (NH_3, HCN, and N_2), and instead resided in the tar and char.

As N_2 is essentially the only nitrogen species predicted by thermodynamic equilibrium, the experimentally observed increases in N_2 yield as ER was increased indicate a movement toward equilibrium yields. Nevertheless, diatomic nitrogen yields remained far short of equilibrium levels for all ERs studied. Significant nitrogen continued to reside in the char-N, tar-N, NH_3, and HCN forms. Available reaction networks for nitrogen species suggest that increased availability of O_2 should lead to increased conversion of NH_3 and HCN to N_2. Our NH_3 and HCN data failed to confirm this. The dramatic declines in char-N and tar-N that also occurred as ER was increased suggest a possible explanation that NH_3 and HCN might have simultaneously been created from char-N and tar-N as they were also being destroyed by O_2.

Experimental and modeling studies of nitrogen partitioning must consider nitrogen in char and tar. Large increases in gaseous nitrogen species can occur when char and tar are consumed as ER increases. Most proposed gasification models designed to predict nitrogen partitioning have not considered these effects [6, 7, 38, 39].

CHAPTER 6

CONCLUSIONS

We have documented among the first measurements of NH_3 and HCN for pilot scale steam and oxygen blown gasification using switchgrass fuel. The yields of both were found to decrease as ER was increased. HCN was produced at concentrations that were as much as an order of magnitude larger than reported in several previous biomass gasification studies. This has important implications for planning of syngas clean-up systems. The significant HCN yields are also important in regards to safe operation of gasifiers using feedstocks with high FBN content, as HCN is highly toxic.

In response to observing HCN yields that were one to two orders of magnitude higher than several other published studies, we traced the problem to instances where syngas was allowed to come into contact with aqueous solutions or solvents prior to the intentional removal of HCN for sampling. This unintentional removal can occur in acidic aqueous solutions used to remove NH_3 or in acetone solutions used to remove tar. Based on our results, we recommend that HCN be collected in impingers parallel to those used for NH_3 collection. If multiple sampling lines are not available, collection of NH_3 and HCN can also be carried out in turns, but they should never be collected together in series on the same sampling line. Polar solvents should not be used to remove tar upstream of HCN sampling. Instead a method of condensing the tars followed by tar aerosol knock out should be employed. Meticulous attention to temperature control in order to avoid water condensation in sample lines and components upstream of HCN sampling is also

important for accurate HCN analysis. Our measurements of HCN for a variety of gasification conditions on both a 25 kg/h pilot scale gasifier and a 100 g/h laboratory scale gasifier using careful sampling protocols found that HCN can be a significant product of the FBN. We have documented that for some operating conditions, HCN yields can be comparable or greater than NH_3 yields. This may have important safety implications, due to the highly toxic nature of HCN.

In addition to investigating partitioning of nitrogen in pilot scale gasification and studying HCN sampling techniques, two experimental studies were conducted to monitor all five of the major forms of nitrogen in syngas (NH_3, HCN, N_2, char-N, and tar-N). The first study varied reactor temperature from 650-850°C. The second study varied the ER of gasification from zero to 0.4. The results of both studies found that significant amounts of nitrogen failed to release as gaseous species, (NH_3, HCN, and N_2), and instead remained bound in the tar and char. Significant amounts of FBN remained in the char-N and tar-N forms for all temperature and ER experimental levels tested. These findings explain why many nitrogen partitioning studies have demonstrated increases in NH_3 and HCN yields as temperature and ER were increased. When temperature, ER, or both are increased, conversion of char and tar to gaseous species is more complete, and the nitrogen contained in the char and tar appears to release at nearly direct proportion to the extent of their conversion.

Our experimental findings demonstrate that in order for a gasification model to be effective in predicting the yields of nitrogenous products in the syngas, it is important that the nitrogen content of the char and tar products be included in the initial conditions. While available models feature many homogenous reactions for describing reactions in gas phase, relatively few reactions are included for reactions

in which the char and tar participate, especially for nitrogen bearing species. Char and tar reactions need to be included and more thoroughly developed in modeling efforts in order that the experimentally observed increases in NH_3 and HCN in response to increasing the temperature and ER can be successfully predicted by models. Accurate predictions of nitrogen bearing gasification products, particularly NH_3 and HCN, would facilitate the planning of future gasification products and syngas cleanup equipment.

In order to develop rate equations and mechanisms of nitrogen release from char and tar as they are converted, it would be helpful to conduct studies where residence time is varied and the partitioning of nitrogen into all of its five major products is monitored. This could be accomplished via either a gasifier with a freeboard made of detachable sections to allow it to be varied in height, or by extracting syngas samples for analysis at various freeboard heights. The second method was already employed by de Jong et al. [6], but only gaseous nitrogen species were measured, and the gasification conditions chosen (high temperature and ER) led to very little char and tar production. Similar work is needed, but with more moderate gasification conditions, and measurements of char-N and tar-N.

The importance of HNCO and NO in evolution of nitrogen compounds from biomass gasification remains unclear. Both experimental results in literature and our findings suggest that they are very minor final products of the FBN, but it seems that they could be important intermediates for nitrogen before it converts onwards to NH_3, HCN, and N_2. Continuous flow gasification experiments which vary residence time would allow insight into their importance if an appropriate time scale to study them could be determined and achieved in an experimental apparatus.

REFERENCES

[1] IPCC, "Climate Change 2014: Mitigation of Climate Change. Contribution of Working Group III to the Fifth Assessment Report of the Intergovernmental Panel on Climate Change," Cambridge University Press, Cambridge, United Kingdom and New York, NY, USA, 2014.

[2] Central Intelligence Agency, "The World Factbook," [Online]. Available: https://www.cia.gov/library/publications/the-world-factbook/geos/xx.html. [Accessed 15 August 2014].

[3] IPCC, "Climate Change 2014: Impacts, Adaptation, and Vulnerability. Contribution of Working Group II to the Fifth Assessment Report of the Intergovnermental Panel on Climate Change," Cambridge University Press, Cambridge, United Kingdom and New York, NY, USA, 2014.

[4] International Energy Agency, "World Energy Outlook 2012," International Energy Agency, Paris, France, 2012.

[5] B. Goldschmidt, N. Padban, M. Cannon, G. Kelsall, M. Neergaard, K. Stahl and I. Odenbrand, "Ammonia formation and NOX emissions with various biomass and waste fuels at the Varnamo 18 MWth IGCC plant," in *Progress in thermochemical biomass conversion Volume 1*, Osney Mead, Blackwell Science Ltd, 2001, pp. 524-535.

[6] W. de Jong, Ö. Ünal, J. Andries, K. R. G. Hein and H. Spliethoff, "Thermochemical conversion of brown coal and biomass in a pressurise fluidised bed gasifier with hot gas filtration using ceramic channel filters: measurements and gasifier modelling," *Applied Energy,* vol. 74, pp. 425-437, 2003.

[7] W. de Jong, Ö. Ünal, J. Andries, K. R. G. Hein and H. Spliethoff, "Biomass and fossil fuel conversion by pressurised fluidised bed gasification using hot gas ceramic filters as gas cleaning," *Biomass & Bioenergy,* vol. 25, pp. 59-83, 2003.

[8] A. van der Drift, J. van Doorn and J. W. Vermeulen, "Ten residual biomass fuels for circulating fluidized-bed gasification," *Biomass & Bioenergy,* vol. 20, pp. 45-56, 2001.

[9] P. Garcia-Ibanez, A. Cabanillas and J. M. Sanchez, "Gasification of leached orujillo (olive oil waste) in a pilot plant circulating fluidised bed reactor. Preliminary results.," *Biomass & Bioenergy,* vol. 27, pp. 183-194, 2004.

[10] F. Pinto, R. N. André, H. Lopes, C. Franco, C. Carolino, M. Galhetas, M. Miranda and I. Gulyurtlu, "Comparison of a pilot scale gasification installation performance when air or oxygen is used as gasification medium 2. Sulfur and nitrogen compounds abatement," *Fuel,* vol. 97, pp. 770-782, 2012.

[11] X. Meng, W. de Jong, N. Fu and A. H. Verbooijen, "Biomass gasification in a 100kWth steam-oxygen blown fluidized bed gasifier: Effects of operational conditions on product gas distribution and tar formation," *Biomass and Bioenergy,* vol. 35, pp. 2910-2924, 2011.

[12] F. Pinto, H. Lopes, R. N. André, M. Dias, I. Gulyartlu and I. Cabrita, "Effect of Experimental Conditions on Gas Quality and Solids Produced by Sewage Sludge Cogasification. 1. Sewage sludge mixed with coal," *Energy & Fuels,* vol. 21, pp. 2737-2745, 2007.

[13] P. Abelha, I. Gulyurtlu and I. Cabrita, "Release of nitrogen precursors from coal and biomass residues in a bubbling fluidized bed," *Energy & Fuels,* vol. 22, pp. 363-371, 2008.

[14] R. L. Bain and K. Broer, "Gasification," in *Thermochemical Processing of Biomass*, R. C. Brown, Ed., Chichester, John Wiley & Sons, Ltd, 2011, pp. 47-77.

[15] T. B. Reed, Biomass Gasification: Principles and Technology, Park Ridge: Noyes Data Corporation, 1981.

[16] P. Spath and D. Dayton, "Preliminary Screening — Technical and Economic Assessment of Synthesis Gas to Fuels and Chemicals with Emphasis on the Potential for Biomass-Dervied Syngas," *NREL Technical Report,* no. NREL/TP-510-34929, 2003.

[17] American Physical Society, "Direct Air Capture of CO2 with Chemicals: A Technology Assessment for the APS Panel on Public Affairs," APS Physics, College Park, MD, United States, 2011.

[18] R. C. Brown, Thermochemical Processing of Biomass, Chichester, West Sussex, United Kingdom: John Wiley and Sons, 2011.

[19] P. J. Woolcock and R. C. Brown, "A review of cleaning technologies for biomass-derived syngas," *Biomass and Bioenergy,* vol. 52, pp. 54-84, 2013.

[20] C. Van Huynh and S.-C. Kong, "Performance characteristics of a pilot-scale biomass gasifier using oxygen-enriched air and steam," *Fuel,* vol. 103, pp. 987-996, 2013.

[21] J. Einvall, C. Parsland, P. Benito, F. Basile and J. Brandin, "High temperature water-gas shift step in the production of clean hydrogen rich synthesis gas from gasified biomass," *Biomass and Bioenergy,* vol. 35, pp. S123-S131, 2011.

[22] T. R. Brown and R. C. Brown, Biorenewable Resources: Engineering New Products from Agriculture, 2nd Edition, Ames: Wiley-Blackwell, 2014, p. 149.

[23] P. Abelha, C. Franco, F. Pinto, H. Lopes, I. Gulyurtlu, J. Gominho, A. Lourenço and H. Pereira, "Thermal conversion of cynara cardunculus L. and mixtures with eucalyptus globulus by fluidized-bed combustion and gasification," *Energy & Fuels,* vol. 27, pp. 6725-6737, 2013.

[24] P. Vriesman, E. Heginuz and K. Sjöström, "Biomass gasification in a laboratory-scale AFBG: influence of the location of the feeding point on the fuel-N conversion," *Fuel,* vol. 79, pp. 1371-1378, 2000.

[25] M. Aznar, M. San Anselmo, J. J. Manyá and M. B. Murillo, "Experimental study examining the evolution of nitrogen compounds during the gasification of dried sewage sludge," *Energy & Fuels,* vol. 23, pp. 3236-3245, 2009.

[26] J. Zhou, S. M. Masutani, D. M. Ishimura, S. Q. Turn and C. M. Kinoshita, "Release of Fuel-Bound Nitrogen during Biomass Gasification," *Ind. Eng. Chem. Res.,* vol. 39, pp. 626-634, 2000.

[27] S. H. Aljbour and K. Kawamoto, "Bench-scale gasification of cedar wood - Part II: Effect of Operational conditions on contaminant release," *Chemosphere,* vol. 90, pp. 1501-1507, 2013.

[28] M. Xu, R. C. Brown, G. Norton and J. Smeenk, "Comparison of a Solvent-Free Tar Quantification Method to the International Energy Agency's Tar Measurement Protocol," *Energy & Fuels,* pp. p 2509-2513, 2005.

[29] W. Zhang, X. Dai, U. Söderlind, C. Wu and X. Luo, "A preliminary test on an industrial biomass CFB gasifier.," in *Proceedings of the 12th European Biomass Conference "Biomass for Energy, Industry, and Climate Protection*, Amsterdam, 2002.

[30] J. Leppalahti and E. Kurkela, "Behaviour of nitrogen compounds and tars in fluidized bed air gasification of peat," *Fuel,* vol. 70, pp. 491-497, 1991.

[31] E. Kurkela, J. Laatikainen-Luntama, P. Ståhlberg and A. Moilanen, "Pressurised fluidised-bed gasification experiments with biomass, peat and coal at VTT in 1991-1994: Part 3. Gasification of Danish wheat straw and coal," *VTT Publications,* 1996.

[32] T. Pröll, I. G. Siefert, A. Friedl and H. Hofbauer, "Removal of NH3 from biomass gasification producer gas by water condensing in an organic solvent scrubber," *Ind. Eng. Chem. Res.,* vol. 44, pp. 1576-1584, 2005.

[33] P. Ståhlberg, M. Lappi, E. Kurkela, P. Simell, P. Oesch and M. Nieminen, "Sampling of contaminents from product gases of biomass gasifiers," Technical Research Centre of Finland, Espoo, Finland, 1998.

[34] Agilent Technologies, Inc., "Nitrogen Chemiluminescence Detector," 31 December 2006. [Online]. Available: http://www.chem.agilent.com/Library/brochures/5989-6102EN.pdf. [Accessed 4 April 2014].

[35] National Institute for Occupational Safety and Health, "Hydrogen Cyanide," May 1994. [Online]. Available: http://www.cdc.gov/niosh/idlh/74908.html. [Accessed 7 April 2014].

[36] Q.-Z. Yu, C. Brage, G.-X. Chen and K. Sjöström, "The fate of fuel-nitrogen during gasification of biomass in a pressurised fluidised bed gasifier," *Fuel,* vol. 86, pp. 611-618, 2007.

[37] W. de Jong, A. Pirone and M. A. Wójtowicz, "Pyrolysis of Miscanthus Giganteus and wood pellets: TG-FTIR analysis and reaction kinetics," *Fuel,* vol. 82, pp. 1139-1147, 2003.

[38] G. Chen, B. Yan and G. Li, "Circulating fluidised bed gasification of biomass: Modelling of fuel-bound nitrogen evolution," in *ASME Turbo Expo 2006: Power for Land, Sea and Air*, Barcelona, 2006.

[39] H. Liu and B. M. Gibbs, "Modeling NH3 and HCN emissions from biomass circulating fluidized bed gasifiers," *Fuel,* vol. 82, pp. 1591-1604, 2003.

[40] International Energy Agency, "Key World Energy Statistics," International Energy Agency, Paris, 2013.

[41] J. Gil, M. P. Aznar, M. A. Cabellero, E. Frances and J. Corella, "Biomass gasfication in fluidized bed at pilot scale with steam-oxygen mixtures. Product distribution for very different operating conditions.," *Energy & Fuels,* vol. 11, no. 6, pp. 1109-1118, 1997.

[42] F. Pinto, R. N. André, C. Franco, C. Carolino, R. Costa, M. Miranda and I. Gulyurtlu, "Comparison of a pilot scale gasification installation performance when air or oxygen is used as gasification medium 1. Tars and gaseous hydrocarbons formation," *Fuel,* vol. 101, pp. 102-114, 2012.

[43] M. Campoy, A. Gomez-Barea, F. B. Vidal and P. Ollero, "Air-steam gasification of biomass in a fluidised bed: Process optimized by enriched air," *Fuel Processing Technology,* vol. 90, pp. 677-685, 2009.

[44] M. Siedlecki and W. de Jong, "Biomass gasification as the first hot step in clean gas production process - gas quality optimization and primary tar reduction measures in a 100 kW thermal input steam-oxygen blown CFB gasifier," *Biomass and Bioenergy,* vol. 35, pp. S40-S62, 2011.

[45] S. Turn, C. Kinoshita, Z. Zhang, D. Ishimura and J. Zhou, "An experimental investigation of hydrogen production from biomass generation," *International Journal of Hydrogen Energy,* vol. 23, no. 8, pp. 641-648, 1998.

[46] C. Stairmand, "The role of the cyclone in reducing atmospheric pollution," *Chemistry & Industry,* vol. 42, pp. 1324-1330, 1955.

[47] P. J. Woolcock, "Development and application of a rapid sampling technique for identification and quantification of compounds in high temperature process gas streams produced from biomass gasification and pyrolysis.," *PhD Dissertation, Iowa State University,* 2013.

[48] S. Q. Turn, C. M. Kinoshita, D. M. Ishimura and J. Zhou, "The fate of inorganic constituents of biomass in fluidized bed gasification," *Fuel,* vol. 77, no. 3, pp. 135-146, 1998.

[49] P. Basu, Combustion and Gasification in Fluidized Beds, Boca Raton, FL U.S.A.: CRC Press, 2006.

[50] P. J. Woolcock, J. A. Koziel, P. A. Johnston and R. C. Brown, "Analysis of trace contaminents in hot gas streams using time-weighted average solid-phase microextraction: Proof of concept.," *Journal of Chromatography,* vol. 1281, no. 1, 2013.

[51] The Standard Methods Organization, "4500-NH3 Nitrogen (Ammonia)," 2006. [Online]. Available: http://www.standardmethods.org/Store/ProductView.cfm?ProductID=191. [Accessed 11 June 2014].

[52] N. Padban, "PFB Air gasification of biomass, investigation of product formation and problematic issues related to ammonia, tar and alkali," *PhD Thesis, Lund University, Department of Chemical Engineering II, Sweden,* 2000.

[53] C. C. Xu, J. Donald, E. Byambajav and Y. Ohtsuka, "Recent advances in catalysts for hot-gas removal of tar and NH3 from biomass gasification," *Fuel,* vol. 89, pp. 1784-1795, 2010.

[54] M. Berg, P. Vriesman, E. Heginuz, K. Sjöström and B.-G. Espenäs, "Fuel-bound nitrogen conversion: results from gasification of biomass in two different small scale fluidized beds," in *Progress in Thermochemical Biomass Conversion*, Seefeld, Austria, Blackwell Science Ltd, 2001, pp. 322-332.

[55] J. Leppälahti and T. Koljonen, "Nitrogen evolution from coal, peat and wood during gasification: Literature review," *Fuel Processing Technology,* vol. 43, pp. 1-45, 1995.

[56] L. L. Tan and C.-Z. Li, "Formation of NOX and SOX precursors during the pyrolysis of coal and biomass. Part I. Effects of reactor configuration on the determined yields of HCN and NH3 during pyrolysis," *Fuel,* vol. 79, pp. 1883-1889, 2000.

[57] R. W. R. Zwart, A. van der Drift, A. Bos, H. J. M. Visser, M. K. Cieplik and H. W. J. Könemann, "Oil-Based Gas Washing - Flexible Tar Removal for High-Efficient Production of Clean Heat and Power as Well as Sustainable Fuels and Chemicals," *Environmental Progress & Sustainable Energy,* vol. 28, no. 3, pp. 324-335, 2009.

[58] B. S. Turk, T. Merkel, A. Lopez-Ortiz, R. P. Gupta, J. W. Portzer, G. N. Krishnan, B. D. Freeman and G. K. Fleming, "Novel Technologies for Gaseous Contaminants Control," *DOE Report,* Vols. DE-AC26-99FT40675, 2001.

[59] National Institute for Occupational Safety and Health, "Carbon Monoxide," May 1994. [Online]. Available: http://www.cdc.gov/niosh/idlh/630080.html. [Accessed 7 April 2014].

[60] L. L. Tan, J. F. Mathews and C.-Z. Li, "Formation of HCN, NH3 and H2S during the pyrolysis of coal," in *Prospects for Coal Science in the 21st Century*, 1999.

[61] K. M. Broer, P. J. Woolcock, P. A. Johnston and R. C. Brown, "Steam/oxygen gasification system for the production of clean syngas from switchgrass," *Fuel,* vol. 140, pp. 282-292, 2015.

[62] C. Rosén, "Fundamentals of pressurized gasification of biomass," *Developments in thermochemical biomass conversion,* vol. 2, pp. 817-827, 1997.

[63] K. M. Broer, P. A. Johnston, A. Haag and R. C. Brown, "Resolving inconsistencies in measurements of hydrogen cyanide in syngas," *Fuel,* vol. 140, pp. 97-101, 2015.

[64] E. C. Zabetta, P. Kilpinen, M. Hupa, K. Ståhl, J. Leppälahti, M. Cannon and J. Nieminen, "Kinetic modeling study on the potential of staged combustion in gas turbines for the reduction of nitrogen oxide emissions from biomass IGCC plants," *Energy & Fuels,* pp. 751-761, 2000.

[65] W. P. Jones and R. P. Lindstedt, "Global reaction schemes for hydrocarbon combustion," *Combustion and Flame,* vol. 73, pp. 233-249, 1988.

[66] A. Gomez-Barea and B. Leckner, "Modeling of biomass gasification in fluidized bed," *Progress in Energy and Combustion Science,* vol. 36, pp. 444-509, 2010.

[67] J. M. Berg, J. L. Tymoczko and L. Stryer, Biochemistry, 6th ed., New York: W.H. Freeman and Company, 2007.

[68] R. J. Haynes, K. C. Cameron, K. M. Goh and R. R. Sherlock, Mineral nitrogen in the plant-soil system, London: Academic Press Inc., 1986.

[69] K. M. Broer and R. C. Brown, "Partitioning of nitrogen during biomass gasification: Part I. The effect of temperature," *Submitted for publication,* 2014.

APPENDIX

SUPPLEMENTARY FIGURES

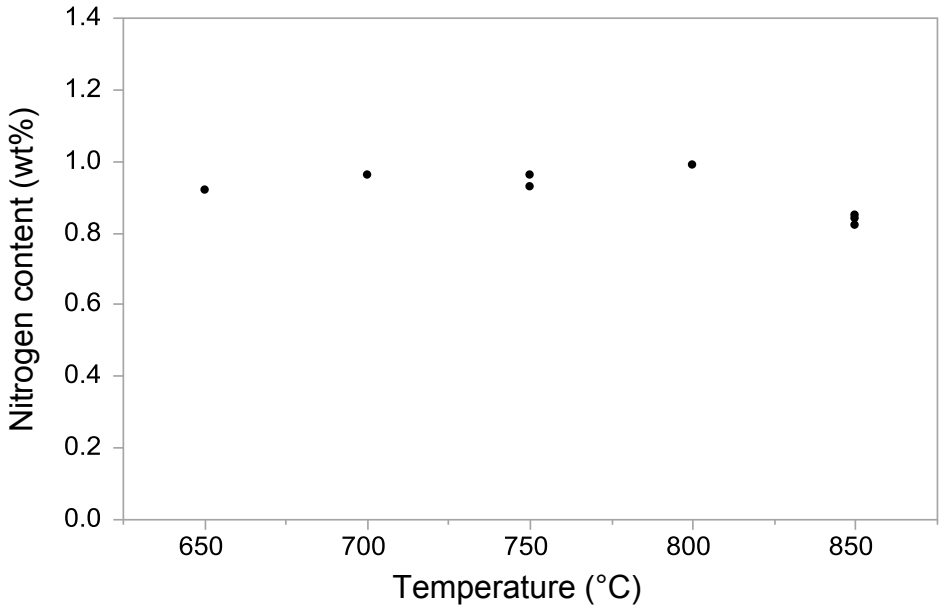

Figure S1. The concentration of nitrogen in the char changed very little as temperature was increased from 650°C to 850°C. An attempt to fit a second order polynomial regression resulted in slope and curvature terms that were statistically significant, but very small. Statistical Lack of Fit was also noted (p=0.02). Reactor pressure and equivalence ratio for all tests were 1 atm and zero.

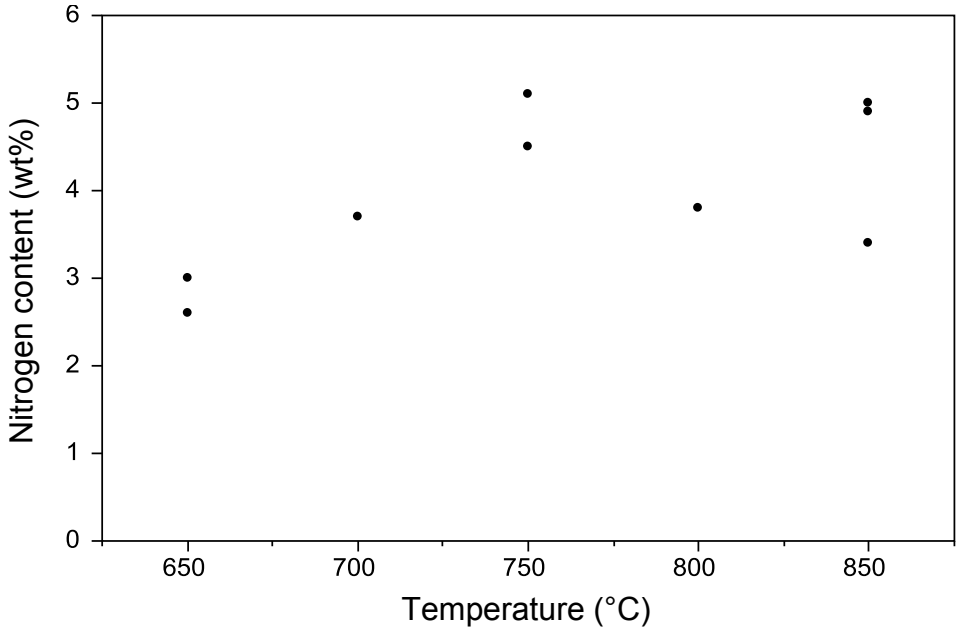

Figure S2. As reactor temperature was increased from 650°C to 850°C, the concentration of nitrogen in the tar seemed to rise at lower temperatures, reach a maximum at 750°C, and then fall again, but attempts to fit a polynomial trend line found no statistically significant trend. Reactor pressure and equivalence ratio for all tests were 1 atm and zero.

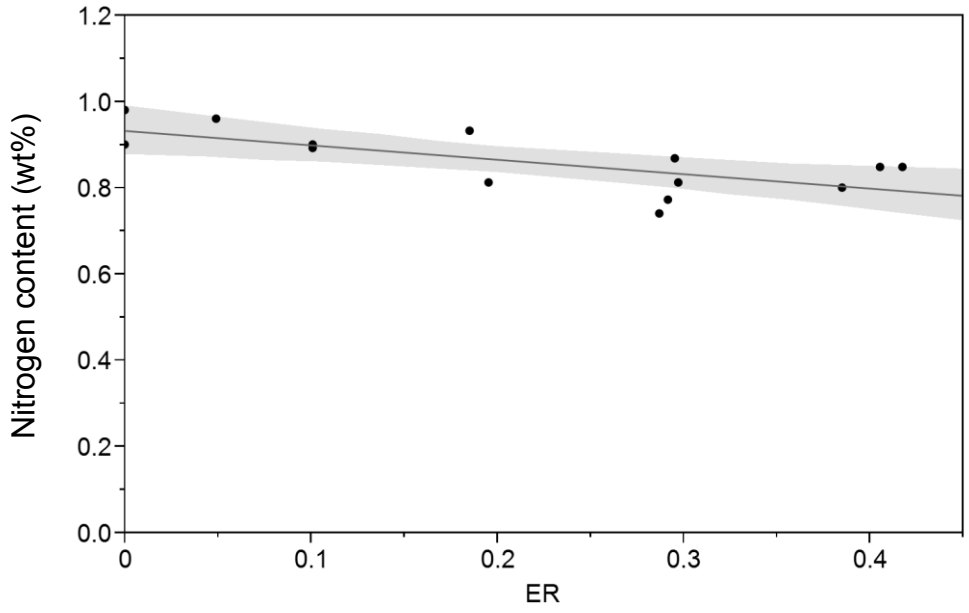

Figure S3. As ER was increased, there was a statistically significant, but small decline in the concentration of nitrogen in the char. The data have been fitted with a linear trend line; the shaded region represents a 95% confidence interval band. Reactor pressure and temperature for all tests were 1 atm and 750°C.

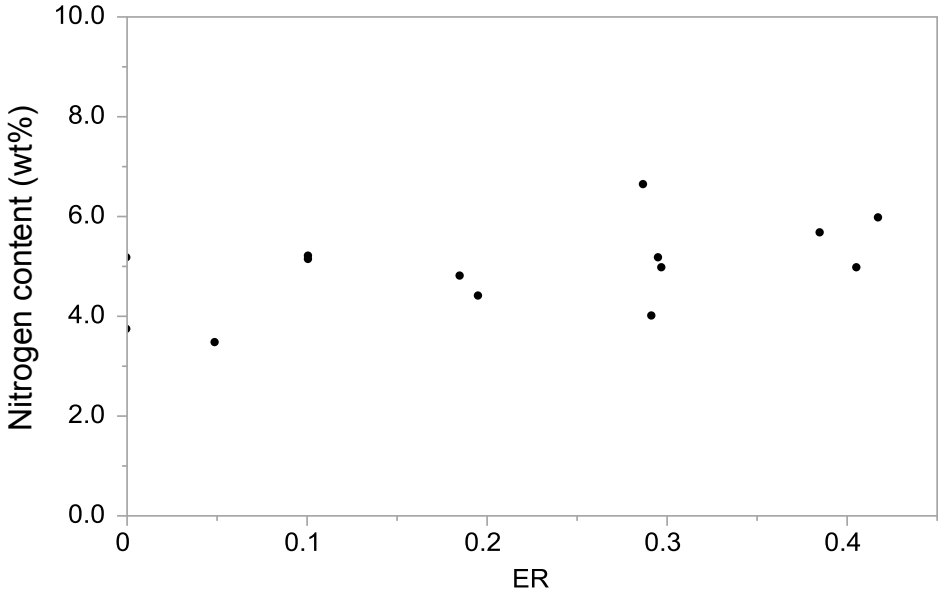

Figure S4. As ER was increased, there was no statistically significant response in the concentration of nitrogen in the tar. Reactor pressure and temperature for all tests were 1 atm and 750°C.

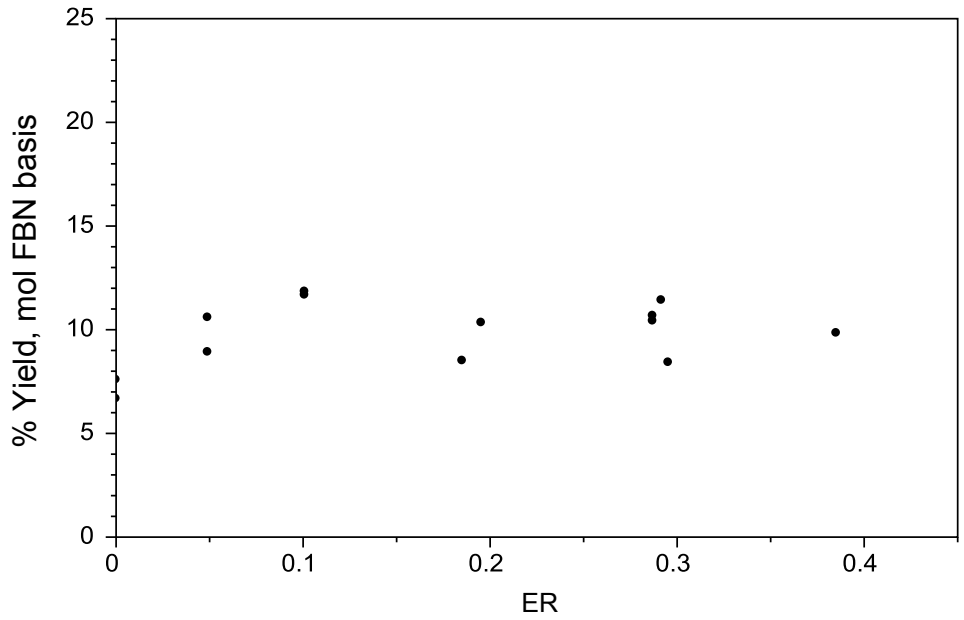

Figure S5. As ER was increased, there was no significant response in the yield of HCN from the FBN. Reactor pressure and temperature for all tests were 1 atm and 750°C.